The Structure of Many-body Entanglement

by

Brian Gordon Swingle

B.S., Georgia Institute of Technology (2005)

Submitted to the Department of Physics
in partial fulfillment of the requirements for the degree of

Doctor of Philosophy

at the

MASSACHUSETTS INSTITUTE OF TECHNOLOGY

September 2011

Author . . . .
Department of Physics
August 30, 2011

Certified by . . . .
Xiao-Gang Wen
Professor of Physics
Thesis Supervisor

Accepted by . . . .
Krishna Rajagopal
Professor of Physics
Associate Department Head for Education

The Structure of Many-body Entanglement

by

Brian Gordon Swingle

Abstract

In this thesis we discuss the general spatial structure of quantum entanglement in local many-body systems. A central theme is the organizing power of the renormalization group for thinking about many-body entanglement. We argue that the coarse structure of entanglement across of wide variety of systems, from gapped topological phases to gapless Fermi liquids in a variety of dimensions, can all be understood within a unified framework. We discuss tensor network states inspired by entanglement considerations, probe the limits of the boundary law for entanglement entropy, speculate about connections between entanglement renormalization and holography, and develop the formalism of mutual information in quantum field theory. We proceed from general considerations about entanglement in lattice models of many-body physics to specific attempts to isolate the low energy structure of entanglement in quantum field theories. We conclude by describing some major open questions in the subject of many-body entanglement that we find particularly interesting.

Thesis Supervisor: Xiao-Gang Wen
Title: Professor of Physics

Acknowledgments

This thesis is dedicated to my beautiful wife, Louise Helen Jones, who has given me so much. Thank you, Louise, I love you! I would also never be here without my parents, John and Amy Swingle. Thanks and love for always answering my questions. Thanks to my brother, Daniel, for many many hours of laughter. Thanks to my advisor Xiao-Gang Wen, who first got me interested in entanglement and who gave me the freedom to follow my own path. Xiao-Gang, your creativity and careful exploration of the unknown inspires me. Thanks to John McGreevy for a large N number of conversations about everything (he gets it). John, I found in you a fellow scientist whose breadth of interest matched my own. Thanks to Wolfgang for helpful comments on my thesis. Finally, thanks to all my friends and collaborators: Maissam, Nan, Vijay, Tarun, Senthil, Patrick, Tom, Evelyn, Eric, Nabil, David M., Rahul, Drew, Dave G., Jimmy, Zheng-Cheng, Xie, Michael, T.-K., Teppo, Ky-Anh, Roman, Allan, Hong, Wati, Krishna, Frank, and many others too numerous to mention. It's been a lot of fun!

Contents

Chapter 1

Quantum Many-body Physics

1.1 Introduction

In this thesis we will explore the physics of many interacting quantum objects. From its first clear appearance in the spectra of atoms over one hundred years ago, the quantum physics of few degrees of freedom is by now relatively well understood. Nevertheless, we have long known that the transition to many degrees of freedom represents a conceptual leap to a new realm of quantum physics, a realm we are aware exists but which we are not yet fully able to understand. There is a richness in the physics of many interacting quantum particles that rivals that of the great ecosystems of the world, each phase of matter a unique form of life, suited to its own environment, with its own unique dynamics. Like the theory of evolution, we seek to know the principles that underlie the formidable complexity of quantum many-body physics.

Like the great catalogs of living forms, we too have many forms of matter to study and the promise of many more not yet imagined. Insulators like diamond and metals like sodium were some of the first phases of matter from this catalog to be understood. These materials illustrate well the concepts of quantum many-body physics from the first one hundred years [1]. More recently, physicists have been interested in the layered copper oxide materials better known as high temperature superconductors. These materials display an incredible diversity manifesting essentially every kind of

symmetry breaking order imaginable, and there are even hints of exotic fractionalized degrees of freedom. The physics here is totally unlike that of a superconductor like aluminum, for in the cuprates superconductivity emerges from an insulating state of effectively two dimensional electrons [2]. If we take these same electrons confined in two dimensions, perhaps in a semiconductor device, and apply a strong magnetic field, we discover a new kind of quantum organization known as the fractional quantum hall effect [3]. In such a phase of quantum matter, electrons literally break apart into fractionally charged pieces and a new kind of topological robustness appears. Analogous to the deconfinement that occurs in electronic quantum hall systems, we can consider many-body systems like the strongly interacting quark gluon plasma. This plasma was last seen thirteen billion years ago until it was recreated recently by colliding ultra-relativistic nuclei [4]. Here the problem is to understand the quantum dynamics of thermally liberated quarks and gluons.

These examples represent only the tiniest fraction of the catalog quantum phases, but it should already be clear that providing a common framework to organize the physics of these various systems is a mammoth task. Indeed, an entirely new kind of inquiry is available, a way of thinking where we are more focused on understanding the space of possibilities than on any particular example. In this way of thinking we might seek to explain why certain phases of matter are common experimentally while others seem never to occur. We can also ask about the limits of nature, trying to understand what are the most extreme possibilities for electrons in a solid. Related to all these questions is the need for a general method for determining the macroscopic physics of a collection of quantum objects in terms of their microscopic properties. In this thesis we will explore some of these issues by asking about the general structure of quantum correlation or entanglement in large quantum systems. To begin our journey, let us first recall the physics of small quantum systems.

A key feature of finite quantum systems is their linearity: all physical properties of interest can be obtained from the diagonalization of finite dimensional matrices. From the computation of energy levels to exact time evolution, everything is computable in terms of a few simple ingredients with the aid of a modern (classical) computer.

These theoretical advances are mirrored by an increasingly precise agreement with experimental probes of relatively simple quantum systems. But while this beautiful theory is supremely successful for small quantum systems, already at the size of small molecules we begin to discover the complexity of many-body quantum physics.

The formal complexity of simulating a quantum mechanical system with a D dimensional Hilbert space grows only polynomial in the dimension D. In other words, the behavior of the system can be fully specified to any desired accuracy with resources - space, time, etc. - that grow only polynomially in D. For example, to store the Hamiltonian of a D dimensional quantum system we need only remember roughly D^2 numbers. But now the thorn: the dimension D of a many-body systems grows *exponentially* with the number of constituents in that system. For example, a system of N electrons sitting at fixed positions in space has $D = 2^N$ because each electron can be either spin up or spin down. Thus the formal complexity of simulating or describing a quantum many-body system grow exponentially with the number of components and physical size.

In truth, the 2^N dimensional Hilbert space of a many-body system is a convenient illusion. Most of the states in this space are never realized in nature. They would take a time longer than the age of the universe to prepare even for a modest number like $N \sim 100$ spins! Similarly, it would take more space than the Hubble volume of our universe to store classically the quantum state of $N \sim 100$ spins. We might have dared to say that many-body quantum mechanics is trivial, after all we just have to diagonalize a big matrix, but this is totally wrong. Because the many-body Hilbert space is an illusion we never truly face the linear problem of matrix diagonalization. Instead, we are faced with the *nonlinear* problem of motion within a tiny constrained corner of the massive many-body Hilbert space. Whether we ask for the ground state or quantum dynamics, we must try to optimize over or move within the space of physical states. This nonlinear problem is the basic challenge of many-body quantum physics.

This problem is an old one and much is known about it. For example, we know how to find the ground state of bosons interacting via two body interactions because we

understand the space of physical states well enough to solve the nonlinear problem and give a simple physical picture for the possible phases of matter and their dynamics. These simple pictures are then augmented by powerful numerical techniques like quantum Monte Carlo that permit us to answer many questions both qualitatively and quantitatively.

However, most many-body quantum problems are not of this type. Some kinds of dynamical questions about our bosons above cannot be answered. Similarly, if the bosons have more complicated interactions then we have little room to maneuver. Replacing the bosons by fermions, like the electrons that are responsible for chemical bonds, takes the problem beyond our abilities. This is not to say that we understand nothing about such systems, only that our knowledge is fragmented and incomplete.

Both the defining feature of our endeavor and our greatest resource is the availability of experimental data. Experiments have shown us the ubiquity of quantum many-body physics, helped us add innumerable examples to the catalog of quantum phases, and given us a wealth of non-perturbative information about interacting quantum systems. However, experiments also need an interpretative framework, so the development of quantum many-body physics inescapably binds theory and experiment. At the level of theoretical abstraction we contemplate here, the single most important experimental fact is the diversity of quantum many-body systems. We wish to provide a theoretical framework for this diversity as a first step towards developing universal computational tools, and an understanding of quantum entanglement is a necessary part of this framework.

These then are the problems of quantum many-body physics: to enumerate the general principles that govern the quantum diversity of such systems, to characterize the physical space of quantum states, to map the landscape of possible phases of quantum matter, to develop qualitative pictures for the dynamics of complex quantum systems, and to back it all up with general computational and experimental techniques. This thesis is a small step towards realizing this dream.

1.2 Quantum many-body physics

1.2.1 Locality and renormalization

We are interested in quantum systems of many degrees of freedom, but we do not study completely generic $2^N \times 2^N$ matrices. Our many-body quantum system will be made of many simple pieces interacting locally with one another. We speak generically of spins or qubits, elementary quantum degrees of freedom from which more complex systems can be built. The qubit is the simplest quantum system, a two level system, described by the Hilbert space $\mathbb{C}^2$. Experimentally, a qubit could be an electron spin sitting on a a crystal defect or it could be a two level atomic system. We will usually abstract away the details of the qubit, so we are free to imagine whatever particular two level physical system we like as forming the qubit. We can always build more complicated systems out of multiple qubits, or more formally, we can efficiently simulate the dynamics of any other quantum system using a collection of qubits [5, 6]. Thus thinking in terms of qubits as the basic building blocks is sufficient. We will meet a wide variety of specific physical systems - Fermi liquids, large N critical gauge theories, topological liquids, and conventional magnetic critical points, but the reader is encouraged to think in terms of their own favorite quantum many-body system.

Having defined the basic ingredients, we now turn to a description of their local organization. Locality in its most primitive form means that the Hamiltonian of the system is a sum of many terms, the number of terms growing with the number of qubits, but with each term coupling a bounded number of qubits together. For example, the Heisenberg interaction $\vec{S}_1 \cdot \vec{S}_2$ between spins 1 and 2 is local but the interaction $\prod_{i=1}^{N} S_i^z$ between N spins is not. If every spin or qubit interacts directly with every other via local interactions then the system is naturally regarded as an infinite dimensional system or a lattice system on a complete graph.

In fact, we want an even stronger kind of locality, geometric locality, where qubits are arranged in a more or less regular way in space of a given dimensionality. For example, we might arrange qubits on a hyper-cubic lattice in d dimensions or a kagome lattice in 2 dimensions. Thus for us locality means qubits arranged in space

of a given dimensionality interacting with a bounded number of other qubits in their general vicinity. We are interested exclusively in quantum systems of this type in this thesis. A few comments are in order. Systems with long range interactions do occur in nature, and we can sometimes consider them without seriously modifying the structure of the theory. We can also always regard them as lower dimensional systems. For example, a one dimensional qubit chain with long range interactions can just be thought of as a qubit system on the complete graph. Also, although we required that the qubits be arranged in a semi-regular way, we do not necessarily require translation invariance. Disorder as well as confining potentials and other non-translation invariant features can be accommodated. Henceforth, we should have in mind the picture of a large array of spins arranged in a space of fixed dimension interacting locally. This is our basic theoretical model of electrons in a solid, atoms in optical traps, quarks in the quark-gluon plasma, quantum gravity (via holographic duality), and basically any other local quantum system defined in the continuum or on a lattice.

Within the context of local many-body physics we can ask many questions of the system. Since all systems eventually behave classically at sufficiently high temperature, we are often interested in the low temperature (relative to a typical energy scale in the quantum Hamiltonian) or zero temperature physics of local many-body systems. Here we will focus exclusively on zero temperature quantum many-body physics and adjacent low temperature quantum thermal physics. Thus we focus on the long wavelength and low energy parts of the many-body spectrum in order to describe physics associated with the quantum ground state. The low energy physics of quantum many-body systems displays many universal features independent of the precise details of the microscopic theory, be it electrons hopping on a lattice, cold atoms in an optical lattice, or quarks in a neutron star. We are interested in all these systems, but to be concrete we will usually choose to imagine that the low energy physics we are interested in comes from some lattice model at high energy. The resulting low energy physics is inevitably described by an effective quantum field theory with a given microscopic cutoff where it is "completed" into a regulated microscopic

theory.

Thus we want to separate the non-universal aspects of the high energy regulator from the universal aspects of the low energy physics. Let us emphasize that we are not saying that the high energy physics is uninteresting, only that we want to extract the universal features of the low energy physics for our purposes here. The process of flowing from a given high energy microscopic theory to a low energy effective theory is known as renormalization. The concepts and techniques of renormalization will play an essential role in this thesis. We always try to understand the physics of our many-body system "scale by scale", that is, by building up the low energy physics by successively integrating high energy degrees of freedom. We will recall the detailed theory of renormalization as we need it.

1.2.2   Quantum ground states

At last we come to our main interest in this thesis, namely, ground states of quantum many-body systems. Gazing out at the enormously rich spectrum of quantum phases, we see everything from traditional symmetry breaking phases, through gapless metallic states, to exotic topological liquids that support fractionalized excitations. Given this quantum diversity, we want to understand the general rules that guide these systems and the arena on which quantum many-body physics unfolds. Of course, quantum ground states are only a part of the story, but they play a very important role. Although formally the ground state is only a single eigenstate of the many-body Hamiltonian, it typically displays a pattern that governs the low energy physics as well. A few examples follow. In a system with Lorentz invariance, equal time correlators computed from the ground state also tell us about unequal time correlators and hence dynamics. The presence of localization in the ground state signals insulating charge dynamics. A ground state that breaks a continuous symmetry also signals information about collective dynamical modes via the presence of Goldstone bosons. Even more interesting is the recent idea that the spectrum of the reduced density matrix for a sub-region in the bulk is actually related to the spectrum of a thermal state of a real boundary. This connection provides information about non-trivial ex-

citations in topological phases and much more just from a knowledge of the ground state wavefunction.

Although ground states are not the whole story by any means, the patterns present in these states often tell us a great deal about the dynamics of the many-body system. There is no better illustration of this idea than Kitaev's construction of a quantum ground state that encodes the result of an arbitrary local time evolution (time evolution under a local Hamiltonian). These states, called history states, are ground states of local Hamiltonians that encode the entire dynamical history of a quantum system in a series of superpositions [7]. Ultimately we are also interested in thermal properties and dynamics of excited states, but the ground state problem is already so rich that it deserves its own exposition. In this thesis we focus on the properties of quantum ground states.

1.2.3 Aims of this work

We are primarily aiming to establish a broad theoretical framework for thinking about entanglement in quantum many-body systems. More than the simple confrontation of experimental data with theoretical calculations, our purpose is to understand the physical systems we study. Suppose we were given a black box that could produce the answer to any experimental probe, would we be satisfied? We would still ask how the box itself produces the answers, why the answers are what they are, and what patterns exist among the answers. We want a physical picture of quantum many-body entanglement because there is one overwhelming experimental fact that we must contend with: we live in a quantum many-body world, and we do not yet understand the richness of that world. For example, there exist phases of matter, experimentally realized in electronic quantum hall systems, that are defined by the existence of long range entanglement. Until we have a physical picture of quantum entanglement, we cannot truly understand such a phase of matter. Alternatively, consider the quest to build a quantum computer, a device not unlike the black box mentioned above. Such a computer could, in principle, efficiently simulate the result of any experiment we could carry out so long as the world is a quantum many-

body system, but to understand how the computer itself works, we must understand quantum entanglement.

We consider ourselves explorers struggling to understand the structure of entanglement in the still unfamiliar land of many-body quantum physics. We will not generally be computing neutron scattering cross sections, or RF spectra, or I-V curves, although some of our results could be directly measured. However, one of the major long term goals of the study we are undertaking is the development of theoretical machinery to perform just such calculations in a controlled way. As we said above, experiment plays the role of understated muse. We draw our inspiration from the wide diversity of phenomena displayed by quantum many-body systems. The work described in this thesis makes also contact with numerical approaches to many-body systems. Whether we deal with experimental data or numerical data, we seek to answer the exquisitely complex question of how a given low energy phase of matter arises from some particular microscopic ingredients. This question is especially challenging for more exotic quantum phases that have been discovered in recent years, as exemplified by the fractional quantum hall effect [3], because the low energy degrees of freedom in these systems do not resemble the microscopic variables e.g. electrons. By studying the structure of many-body entanglement, we hope to better understand the space of physical states. This understanding will in turn lead to new numerical and heuristic approaches for theoretical calculation of experimentally relevant quantities.

There is hope that we will succeed. We have experienced a revolution in our understanding of the physics of one dimensional quantum systems thanks in part to a revolution in our understanding of quantum entanglement in one dimension. Although history did not unfold this way, the powerful method of density matrix renormalization group (DMRG) [8] and its many time dependent variations [9] can be viewed as part of the larger entanglement based effort to understand the physics of quantum many-body systems. These methods work exceedingly well in one dimension and have also contributed much to the study of higher dimensional systems. In fact, they work so well that we can regard DMRG as essentially like the black box we described above. We would also emphasize that entanglement is not the end of the

story, for example at finite temperature quantum and classical correlations are both important, but it does seem to be the right place to start in one dimension. Our goal is to achieve a similar level of understanding of entanglement in higher dimensional quantum many-body systems and to develop the powerful calculational tools that would inevitable accompany such an understanding.

What does the future hold for this program of research? An increasingly cooperative effort involving researchers from quantum information science and quantum many-body physics. An increased emphasis on understanding the functioning and capabilities of quantum computers. Perhaps even contact with holographic ideas originating in quantum gravity and string theory. Most importantly, a growing contact with laboratory experiments, giving us new calculational tools to address the full spectrum of strongly interacting quantum many-body systems, from ground states to finite temperature dynamics.

1.3 Outline and results

1.3.1 Overview of results

Let us now give an overview of the main results in this thesis. This section contains a brief description of the model systems we will consider as well as our principle results. The next section describes in more detail the structure of the thesis. We wish to emphasize that this section functions as an overview, we will not try (yet) to convey in any detail the deeper connections and importance of these results. In addition to the unique renormalization based perspective we take on the traditional aspects of many-body entanglement, our core results include:

- a tensor network description of non-chiral topological phases,

- a preliminary method to extract topological properties from tensor network states,

- an intuitive picture of entanglement in Fermi liquids for which no analytic cal-

culation exists,

- a physical justification of the (mathematically unproven) Widom conjecture,

- a complete characterization of the leading contribution to mutual information in Fermi liquids,

- a proposal connecting "holographic" tensor network states to holographic models of quantum gravity,

- and an elucidation of the universal physics contained in the mutual information in quantum field theories.

The material in this thesis is largely adapted from work reported in [10, 11, 12, 13, 14, 15, 16, 17], as well as considerable additional unpublished work.

By the end of this thesis, we will have a comprehensive picture of entanglement in local quantum systems. This picture is not the end of the story, but we will argue that the renormalization group perspective is the right rough guide for further investigations of many-body entanglement. As we make future refinements of the rough outline of quantum entanglement presented here, as we understand the microstructure of quantum entanglement, we should gain in computational power and continue to realize some of hopes expressed above for experimental contact.

1.3.2 Guide to the thesis

The logical structure of the thesis is as follows. First, we describe the basic context and goals of quantum many-body physics in Chapter 1. Second, we introduce the basic structure of many-body entanglement, including the boundary law, from a renormalization group perspective in Chapter 2. In Chapter 3, we discuss a very general class of variational states that flow from the basic existence of a boundary law. Fourth, we explore the limits of the boundary law for entanglement entropy in Chapter 4. Having explored the general physics of the boundary law and its limitations, we enrich the description in Chapter 5 by making a connection between entanglement

renormalization and holography. In Chapter 6, we try to further refine and isolate the low energy features of entanglement in quantum field theory, the coarse grained description of any many-body system. We conclude in Chapter 7 with a summary and a dream for the future.

The presentation will not be completely general, and the interested reader can consult the original literature for details. Instead, we want to convey a unified vision of many-body entanglement that we have helped develop in the last few years. Although there is plenty of room for doubt about the usefulness of new entanglement based approaches to many-body physics, this thesis is fundamentally optimistic about the future. Throughout we try to give an informal assessment of the prospects and problems facing the field as we see them.

Chapter 2

Many-body Entanglement

2.1 Overview

In this chapter we introduce the context surrounding entanglement in many-body systems. The development will be in keeping with a point of view emphasizing the role of renormalization. We begin by formalizing some of the structures described in Chapter 1. We will also discuss entanglement in ground states, give numerous perspectives on the boundary law for entanglement entropy, and give a scaling argument that encapsulates the basic structure of many-body entanglement.

2.2 What is entanglement?

As we said in Chapter 1, quantum many-body systems are defined as local aggregates of many small quantum systems. To introduce the idea of entanglement formally, we group those local degrees of freedom into two clusters. Thus consider a quantum system that is composed of two subsystems, $\mathcal{H}_A$ and $\mathcal{H}_B$, so that the full Hilbert space is $\mathcal{H}_{AB} = \mathcal{H}_A \otimes \mathcal{H}_B$. A basis for $\mathcal{H}_{12}$ is provided by the states $\{|n\rangle_A \otimes |m\rangle_B\}$ where $|n\rangle_A$ and $|m\rangle_B$ are basis states for $\mathcal{H}_A$ and $\mathcal{H}_B$. However, a general state in $\mathcal{H}_{AB}$ cannot be written as a product $|\phi\rangle_A \otimes |\psi\rangle_B$ of states in $\mathcal{H}_A$ and $\mathcal{H}_B$. Whenever no product decomposition exists we say that systems $\mathcal{H}_A$ and $\mathcal{H}_B$ are entangled. Loosely speaking, systems are entangled when neither component has its own independent

state, that is when the states are two subsystems are tied together.

Entanglement is a consequence of the superposition principle of quantum physics because we can superpose product states in $\mathcal{H}_{AB}$ to produce states that are entangled. As a quantum effect, entanglement can be viewed as a quantum resource. It enables us to engage in quantum communication, perform quantum computations, and is the raw material from which quantum many-body systems are built. We want to quantify and understand the role of this resource in local quantum systems.

2.2.1 Quantum ground states

We may measure the entanglement of quantum ground states in many ways. In this thesis we focus on entanglement between two spatial partitions in a many-body system. This kind of partitioning is particularly natural given the local structure of many-body systems, but other kinds of partitions are certainly possible e.g. momentum space partitions. Thus we consider a total system in its ground state $|\Omega\rangle$ and bipartition the system into two pieces that we call A and B. The entanglement entropy of A is $S(A) = -\mathrm{tr}(\rho_A \log \rho_A)$, and it is equal to $S(B)$ since the total system is in a pure state. Other measures are also possible, specifically the Renyi entropies $S_n(A) = \frac{1}{1-n} \log \mathrm{tr}(\rho_A^n)$ which generalize the von Neumann or entanglement entropy. We would like to just mention that the assumption that $|\Omega\rangle$ is pure is important because the characterization of entanglement in mixed states is a much more subtle endeavor.

What should we expect from the entanglement entopy? If the full quantum state factorizes into $|\Omega\rangle_A \otimes |\Omega\rangle_B$ then $S(A) = 0$. On the other hand, if we select a state at random (with respect to the Haar measure) from the many-body Hilbert space, then we typically find $S(A) \approx \log \dim(V_A)$ with V_A the Hilbert space of the A subregion [18]. In a local many-body system the log of the dimension of this space scales as the volume of the region, and we say the entanglement entropy satisfies a "volume law". Indeed, $\log \dim(V_A)$ is a sharp upper bound for $S(A)$ and hence we may say that random many-body states are nearly maximally entangled. We shall see that random many-body states are actually far from what we want to describe ground

states. Another place where such a volume law for entanglement appears comes by considering highly excited energy eigenstates of a many-body system. Following the logic of eigenstate thermalization, for any region A occupying less than half the system size, $S(A)$ will look thermal with a temperature set by the average energy density determined from the energy eigenstate in question. Here again we find a volume law since thermal entropy is extensive, but there is no thermal ensemble, instead entanglement along with the typicality of energy eigenstates produces thermal physics locally.

2.2.2 Measuring entanglement

There is currently no universal way to measure entanglement experimentally, although there have been many isolated proposals. For certain kinds of non-interacting systems it has been shown that number fluctuations, of electrons, say, are related in a definite way to entanglement entropy [19]. It is possible to compute entanglement numerically in some cases, for example, in one dimensional critical systems using density matrix renormalization group and in some higher dimensional systems without a sign problem using quantum Monte Carlo. We have experimental procedures to determine if entanglement is present at all, a kind of yes-no question, but it is currently not known how to measure entanglement precisely in many-body systems and whether such a measurement is even feasible. Indeed, given that entanglement entropy is such a non-local quantity, it might be quite hard to measure experimentally or even numerically in the general case.

If we had a quantum computer that could, given some local Hamiltonian H, reliably prepare ground states of that Hamiltonian, then we can give a procedure to measure entanglement in one dimensional systems using a quantum computer. We proceed as follows. To measure the second Renyi entropy $S_2(A) = -\log \text{tr}(\rho_A^2)$ we prepare two copies of the ground state restricted to region A and introduce an auxiliary qubit initialized in the state $|0\rangle + |1\rangle$. Next we apply a controlled swap operation in region A to the two copies of the ground state. This operation can be understood as a transformation on three inputs. Conditioned on the value of one of the inputs

25

we swap the states of the other two inputs. If we now look at the state of the control qubit, it has become mixed since the circuit implemented a coherent superposition of swapping and not swapping thus entanglement the control qubit with the other inputs. In fact, the reduced density matrix for the qubit has the form

$$\rho_{\text{qubit}} = \frac{1}{2} \left(|0\rangle\langle 0| + |1\rangle\langle 1| + \text{tr}(\rho_A^2)|0\rangle\langle 1| + \text{tr}(\rho_A^2)|1\rangle\langle 0| \right)$$

and measurements in the $|\pm\rangle = |0\rangle \pm |1\rangle$ basis give $+$ with probability $(1 + \text{tr}(\rho_A^2))/2$ and $-$ with probability $(1 - \text{tr}(\rho_A^2))/2$.

This means we have access to a biased coin that encodes $\text{tr}(\rho_A^2)$, and by flipping that coin enough times, we can learn the bias as precisely as desired. There is one very important subtlety, namely that $\text{tr}(\rho_A^2)$ can be quite small for gapless systems, going like an inverse power of system size. Thus we may need to flip the coin many times to see the bias clearly, but the procedure given here is sensible in the formal sense that it wouldn't take longer than a time that grows polynomial with system size. However, this subtlety is more serious in higher dimensions where we expect $\text{tr}(\rho_A^2)$ to be exponentially small. In this case, the method presented here would take a time that grows exponentially with system size and hence is formally inefficient. It is important to note that these formal statements don't preclude the possibility of applying this procedure successfully for smaller system sizes in higher dimensions. We merely state that the procedure is not efficient in a formal asymptotic sense. As an additional complication, one must also face potential errors in the preparation of our state so that the coin bias may fluctuate slightly from trial to trial.

Thus it remains an open question to provide efficient methods to measure or compute the entanglement Renyi entropies for a generic many-body system. We believe this problem may be hard even for a quantum computer in the worst case, on the other hand, it seems that sensible one dimensional ground states are within reach. Similarly, recent calculations of the Renyi entropy using quantum Monte Carlo seem to suggest that accurate calculations may be possible for a restricted class of problems (those that have all negative off diagonal elements of the Hamiltonian in some basis)

[20, 21]. However, we note that one still has to contend with the exponentially small nature of $\text{tr}(\rho_A^2)$. The power of a quantum computer to compute entropies of ground states of more general Hamiltonians is simply not known. There are a few scattered proposals to measure entanglement using fluctuations of various conserved quantities [19] or via quantum quenches [22], but here again we have very little information. Especially outside of one dimension, entanglement entropy remains poorly connected to numerics and experiment.

2.2.3   Basic structure of entanglement in local quantum systems

The basic behavior of entanglement entropy in ground states of many-body systems is encapsulated in the boundary law [23]. The boundary law states that the entanglement entropy of a region of linear size L in d dimensions scales as L^{d-1} like the boundary of the spatial region considered. There are several exceptions to this scaling including critical or gapless systems in one dimension, infinite randomness fixed points in one dimension, and Fermi liquids in higher dimensions with a codimension one Fermi surface. In all these cases the boundary law is weakly violated with a logarithmic correction going like $L^{d-1} \log L$. There are additional constructions in the context of quantum information science that have higher entanglement, for example, one dimensional systems with entanglement scaling like L^α with $\alpha < 1$. However, these constructions are typically pathological or unnatural from the point of view of generic local systems. These pathologies include long range interactions, highly fine tuned couplings, many nearly degenerate ground states, and so forth.

The boundary law for entanglement entropy is a nearly universal feature of quantum ground state. It can be translated into an extremely general and useful class of variation states known collectively as tensor network states. However, it should also be emphasized that the value of the entanglement entropy is not itself universal. For example, two systems with different microscopic Hamiltonians which nevertheless exist in the same phase may have different values of entanglement entropy. In the

language of quantum field theory, entanglement entropy is a divergent quantity that is sensitive to the details of the high energy regulator. On the other hand, there are subleading in L terms in the entanglement entropy that are believed to be universal. In one dimension such terms can even dominate the boundary law contribution as in conformal field theories where there exists a logarithmic correction with a coefficient given by the central charge.

2.3 Understanding the boundary law for entanglement entropy

Because the boundary law for entanglement entropy is of foundational importance, we now review a large number of points of view justifying the boundary law. Very little of what we will say constitutes a complete proof, but we can amass a large amount of physical intuition concerning the origin of the boundary law. Following these notes we will present a very general and simple set of ideas we have developed based on the renormalization group that correctly capture all known forms of entanglement in sensible many-body ground states.

2.3.1 Model calculations

The most elementary evidence comes from calculations in model systems. Free gapless bosons in more than one spatial dimension obey a boundary law as do free fermions without a Fermi surface. As we have mentioned, gapless bosons or fermions in one dimension and Fermi surfaces in higher dimensions are all associated with weak universal violations of the boundary law. Model calculations for free gapped bosons and fermions indicate a boundary law in all dimensions. Various model wavefunctions for topological phases can be shown, either numerically or analytically, to satisfy a boundary law for entanglement entropy. There is also recent numerical evidence for the boundary law in non-trivial interacting theories via sophisticated quantum Monte Carlo calculations. So we have some evidence that both gapless and gapped phases

of matter satisfy a boundary law with some notable (but understood) logarithmic corrections. How general can this conclusion be?

2.3.2 Gapped phases

Gapped phases of matter with a finite correlation length ξ might be expected to obey an boundary law because of the short range nature of correlations in such a phase. We might expect that the entanglement entropy could be no more than a constant times ξL^{d-1} since regions more than ξ away from each other are essentially uncorrelated. Hence we should enclose the boundary of our region of interest with a shell of thickness ξ. If the region of interest and the shell are in a combined pure state, then the entanglement entropy of the region of interest is equal to the entanglement entropy of the shell, but the latter is boundary above by log dim. shell Hilbert space $\sim \xi L^{d-1}$. We note also that in one dimension it can be rigorously proven that a gap implies the boundary law [24], but rather such a result is true in higher dimensions is not yet known, although we believe it is true.

2.3.3 Imaginary time evolution

Another way to approach the boundary law is to imagine preparing the quantum ground state of interest by imaginary time evolution. Suppose we take as our initial state an unentangled state $\psi_0\rangle$. As long as this state has some overlap with the true ground state, we know that $\lim_{\beta \to \infty} e^{-beta H} |psi_0\rangle$ will be proportional to the ground state of H. To understand the boundary law from this point of view we need to understand how big β needs to be in practice and how much entanglement imaginary time evolution can generate. Once again, if the true ground state has a gap to all excitations then we might expect that for $\beta \gg 1/\Delta$ the imaginary time evolution of the product state will produce a state in the same universality class as the true ground state. For example, if the first excited state consists of a single spin flip that can occur at any one of N sites, then take $\beta \sim 1/\Delta \log N$ will provide a very good approximation to the ground state (the log accounts for the degeneracy associated

with the first excited state). More generally, we would like to argue to that $\beta \gg 1/\Delta$ independent of system size produces a wavefunction in the same phase as the true ground state of H. If this is so, then so long as $e^{-\beta H}$ doesn't generate too much entanglement, the boundary law will follow. In the same way that ordinary time evolution cannot establish correlations between arbitrarily distant regions arbitrarily fast (a result known as the Lieb-Robinson bound), imaginary time evolution for a finite imaginary time (i.e. not growing with system size) can be expected to correlate regions up to a given finite distance ℓ away where $\ell \sim v_{LR}\beta \sim v_{LR}/\Delta \sim \xi$. Thus we recover the intuition of the previous paragraph for gapped phases. Although imaginary time evolution can also often be fruitfully applied to produce approximate gapless ground states, we cannot with the same degree of confidence use this method to assert a boundary law for such states.

2.3.4 Twist fields

Still another perspective comes from the technology of twist fields. We will have much more to say about these objects later in the thesis. For now, let us say that they are operators defined so that their expectation values give various of powers of a reduced density matrix: $\langle K_n[R] \rangle = \text{tr}_R(\rho_R^n)$. The important property of these operators for our current purposes is that they are extended, like Wilson lines in gauge theory. In particular, they are extended along the boundary of the region of interest, here called R. In addition, they sit at a particular point in time, the time at which we would like to compute the trace. For example, in one spatial dimension they are point like operators and in two spatial dimensions they are line operators. Taking the case of two dimensions as an example, analogous to the physics of Wilson lines in gauge theory, the expectation of these operators will depend on certain geometrical features of the region R in question. The boundary law corresponds to the statement that $\langle K_n[R] \rangle \sim e^{f(n)|\partial R|}$. This is a very natural result if the different local "sections" of the twist field along ∂R have decaying correlations with each other (either sufficiently fast power law or exponential decay). In other words, we would like to claim the boundary law is essentially a consequence of locality. We will see that this is so later

on.

2.3.5 Gluing of regions

We can also form the state of the full system by "gluing" the regions together using the interaction Hamiltonian. Write the Hamiltonian as $H = H_A + H_B + V_{AB}$ where V_{AB} is localized along the boundary between A and B. Importantly, this operator acts on a Hilbert space of dimension roughly $\exp c|\partial A|$ where c is some constant and $|\partial A|$ is the size of the boundary of A (and also of B). Even more importantly, this does not imply that the entropy due to the coupling induced by V_{AB} is bounded by $|\partial A|$. One dimensional critical systems are an exception, as are fermion systems with a Fermi surface. Nevertheless, the boundary law is the statement that this intuition is often correct. The important question is, how far does the influence of V_{AB} penetrate into the bulk of A and B when we restrict to low lying states of H_A and H_B?

If the spectra of H_A and H_B are gapped, or more generally, if the gapless states in the spectrum are restricted to the boundary (to allow for edge states), then we expect that the influence of V_{AB} doesn't propagate too far into the bulk and the resulting entanglement entropy obeys a boundary law. In the case of a gapless bulk spectrum, the influence of V_{AB} obviously extends into the bulk, but this does not imply that the boundary law is violated. We must balance the entangling power of V_{AB} on low lying states with its decaying influence in the bulk. In fact, the renormalization group argument given below makes this tradeoff explicit.

2.3.6 Adiabatic continuity

We have already seen that some free theories, both gapless and gapped, may be shown to have a boundary law. Assuming the qualitative structure of entanglement doesn't change as various interactions are turned on (free theories already seem to show most entanglement phenomena), then we should expect any phase that is adiabatically connected to a non-interacting phase to have a boundary law. This applies to both gapless and gapped phases. We should caution, however, that is important that the

31

free theory be "generic in some sense". As an example of the danger is provided by the Mott insulating phase of the Bose Hubbard model. If we consider bosons at integer filling and turn the hopping matrix element completely off, then the resulting state is unentangled and is adiabatically connected the finite hopping Mott insulating phase which does have an boundary law scaling for its entanglement entropy. Thus we must insure that the solvable point we consider has generic entanglement behavior in order to draw conclusions about the whole phase. Statements of adiabatic continuity can be checked using perturbation theory for the entanglement entropy or more generally for the Renyi entropies.

2.3.7   Conformal mapping

For a class of gapless systems known as conformal field theories that typically describe critical points, a non-perturbative mapping of the entanglement entropy of a d dimensional ball to the thermal entropy of a d dimensional hyperbolic space guarantees that at least the ball satisfies a boundary law [25]. This is because the curved geometry of hyperbolic space insures that "areas" and "volumes" scale the same way. Thus the thermal entropy on the hyperbolic space, which is extensive and scales as the volume, also scales as the area. This in turn implies that the entanglement entropy satisfies a boundary law in the flat geometry. This argument is powerful despite its restricted applicability because it gives us complete confidence in the boundary law for certain gapless phases in more than one dimension.

2.3.8   Holographic calculations

Along these lines, the powerful technology of holographic duality can be used to compute the entanglement entropy in certain very special theories, for example, large N (number of colors) non-Abelian gauge theories. These model systems are not easily found in the laboratory, but we can nevertheless determine that they satisfy a boundary law using the tools of holographic duality. We emphasize that this is a non-trivial class of gapped and gapless theories that demonstrably have boundary law

scaling of entanglement. Along the lines of the adiabatic continuity argument given earlier, if any of the exotic models are in the same phase as a more realistic model, we expect those realistic models to share the same leading scaling for entanglement entropy.

2.3.9 Finite T mutual information

A quantity we shall consider in much greater detail later is the quantum mutual information $\mathcal{I}(A,B) = S(A) + S(B) - S(AB)$ between two regions A and B. If AB is a pure, then $S(AB) = 0$ and $\mathcal{I}(A,B) = 2S(A) = 2S(B)$. Thus if the mutual information obeys a boundary law then so does the entanglement entropy, at least we the total system is pure. We can generalize this construction to finite temperature where the subtraction in the definition of the mutual information removes the extensive part of the entropy. As a result, one can prove quite rigorously that the mutual information obeys a boundary law at finite temperature [26]. To the extent that this behavior persists to zero temperature, the entanglement entropy also obeys a boundary law. However, we are only able to prove that the mutual information at finite temperature obeys a boundary law with a coefficient that diverges as $T \to 0$, so boundary law violations are still possible at zero temperature. Nevertheless, there is often a deep connection between thermal entropy and entanglement entropy since the same low energy degrees of freedom are responsible for both.

2.3.10 Limitations

Despite all these heuristic arguments, there are known limitations to the boundary law. Gapless states in one dimension are known violate the boundary law logarithmically [27, 28]. Random systems in one dimension are also known the violate the boundary law. Here the violation comes from the presence of long range singlets in the ground state of the random system. Fermi liquids with a codimension one Fermi surface also violate the boundary law for entanglement entropy in more than dimension. Another way to violate the boundary law for entanglement entropy is to study

quantum systems on curved spaces. Hyperbolic space has the property that areas and volumes scale in the same way with linear size, hence although the entanglement entropy of a region may still be proportional to the area of the region, the area and the volume may be indistinguishable in terms of scaling. Many of these seeming anomalies are actually perfectly sensible once we understand the renormalization group perspective on entanglement in local quantum systems.

2.4   Entanglement and renormalization

There is a simple scaling picture which captures much of the variety of possible entanglement behavior. Consider a local lattice model or quantum field theory in d space dimensions. We wish to analyze the behavior of entanglement as a function of energy scale. To this end, let us introduce a variable r which encodes the length scale of interest. $r = \epsilon$ corresponds to the high energy cutoff where the field theory is superseded by some high energy completion, perhaps a lattice model. $r \to \infty$ corresponds to the low energy limit of the quantum field theory, and if the field theory is gapped then this limit gives a trivial theory. As in standard renormalization group treatments, r changes as we move along the renormalization group flow, and the appropriate measure for changes in r is the logarithmic measure dr/r.

We wish to make a hypothesis about the entanglement at a scale r in order to recover the familiar boundary law scaling of entanglement entropy. To motivate the coming assumption, consider the coarse grained Hamiltonian $H(r)$ as a function of r. At each scale r, this Hamiltonian is local at scales longer than r, for example, the microscopic Hamiltonian $H(\epsilon)$ is local at the lattice scale. Thus, considering a region of size L and its complement, the coarse grained Hamiltonian at scale r only entangles the region with its environment along the boundary of the region. Now, the rough number of degrees of freedom at the boundary of the region of size L at scale r is $\left(\frac{L}{r}\right)^{d-1}$ in d space dimensions. If we assume that each degree of freedom contributes roughly one "ebit" to the entanglement entropy, then the contribution to

the entanglement entropy at scale r is

$$dS(r) = \left(\frac{L}{r}\right)^{d-1} \frac{dr}{r}.$$ (2.1)

To obtain the full entanglement entropy we simply integrate this contribution from the high energy cutoff down to an appropriate low energy cutoff:

$$S = \int_{r_{UV}}^{r_{IR}} \left(\frac{L}{r}\right)^{d-1} \frac{dr}{r}.$$ (2.2)

The high energy or UV cutoff is simply $r_{UV} = \epsilon$, but the low energy or infrared cutoff depends on the nature of the theory. For a conformal field theory, the only scale is the region size L, so the infrared cutoff is the region size $r_{IR} = L$. This naturally reproduces the boundary law in dimension $d > 1$ and the logarithmic violation in $d = 1$. This scaling ansatz also shows that corners in a conformal field theory can be associated with logarithmic corrections because corners can contribute a fixed amount of entanglement at every scale giving $\int dr/r \sim \log L$. Keeping subleading terms in L/r gives rise to subleading corrections to the boundary law for smooth regions including some universal logarithmic terms in odd spatial dimensions. On the other hand, if the theory has a finite correlation length, then the infrared cutoff is given by $r_{IR} = \min(L, \xi)$ where ξ is the correlation length. In this case one always obtains a boundary law for sufficiently large L. Note that the "entanglement per scale" in the one dimensional conformal case is a quantity of some interest, namely the central charge of the conformal field theory. We would like to say that in any conformal field theory in any dimension, the notion of "entanglement per scale" is a well defined and universal quantity. However, the entanglement entropy as it stands is bound up with non-universal cutoff scale physics and cannot provide a clean definition of "entanglement per scale".

35

2.5　Summary of results: Chapter 2

We have shown in this chapter that we can summarize and encode the diversity of many-body entanglement, including the leading behavior and the structure of sub-leading terms, into a simple scaling form. We have also reviewed the basic structure of many-body entanglement and given several heuristic justifications for the boundary law. Based on the renormalization group argument, any violations of the boundary law must be due to low energy degrees of freedom, and in general we should look to low energy degrees of freedom for universal contributions to entanglement. Ultimately, we believe the renormalization group perspective is the most general and powerful, and in later chapters we will explore in more detail this scaling picture.

Chapter 3

Tensor Network States

3.1   Overview

This chapter focuses on tensor network states for many-body simulation. First, we describe how these states arise naturally from the considerations in Chapter 2. Then we show that a large variety of interesting quantum states can be cast in this framework. Then we discuss some of the physical properties that can be extracted from tensor network states. Finally, we address in broad terms the challenges and prospects for this method.

3.2   The physical corner of Hilbert space

As we have already described, the physical region of Hilbert is a complicated nonlinearly defined region within a much larger many-body Hilbert space. One useful definition of this space is the following: give a quantum computer acting with arbitrary local operations (gates) on a many-body quantum system, the states such a computer could reach in time polynomial in the system size are physical. More simply, if a quantum computer can prepare a state in a reasonable amount of time then that state is physical. This definition is useful, but given our limited understanding of quantum computers at this time, we would like to have an alternative way to characterize this space of physical states.

The area law for entanglement entropy that we encountered in the last chapter is precisely such a principle. Since ground states of local Hamiltonians often satisfy a boundary law, we should on very general grounds look for parameterizations of the physical space that naturally encode this feature. Tensor network states satisfy this purpose.

3.3 Tensor network states

Tensor network states are a class of variational states that are defined in terms of a network of auxillary degrees of freedom and linear mappings (the tensors). Let us begin by imagining a linear chain of spins. We would like to give a recipe for computing the amplitude $\psi(m_1, m_2, ..., m_N)$ for N spins to have the values $\{m_1, ..., m_N\}$. Knowledge of all the amplitudes requires 2^N complex numbers (modulo a trivial overall normalization), but we want to express this complicated set of data in terms of a smaller number of physical parameters. This leads to matrix product states for one dimensional spin chains. In the simplest case we pick two matrices A^m ($m = 0, 1$ or up and down) of size $D \times D$ and write the amplitude as

$$\psi(m_1, ..., m_N) = \text{tr}(A^{m_1}...A^{m_N}).$$

For example, if we want to know the amplitude of 001 for an $N = 3$ chain, we simply take two of the $m = 0$ matrices A^0 and one of the $m = 1$ matrices and compute the trace $\text{tr}(A^0 A^0 A^1)$. We should not confuse the m-label on A^m as powers of a single matrix A.

Matrix product states are useful for a number of purposes. First, they underlie the functioning of the density matrix renormalization group algorithm which has had a profound impact on physics in one dimension [8]. Second, they are known to accurately represent quantum ground states of gapped Hamiltonians [24]. Thus the problem we outlined in the introduction, of characterizing the space of physical states, has largely been achieved for gapped phases of matter in one spatial dimension.
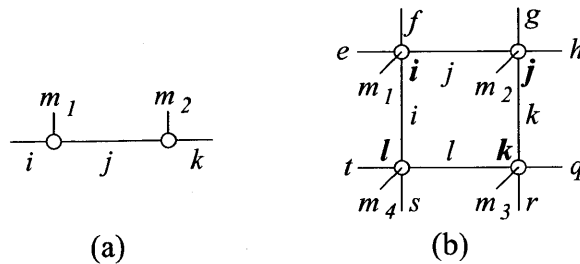
Figure 3-1: A schematic illustration of matrix product states for a one dimensional spin chain and tensor network states for a two dimensional square lattice.

Third, these variational states are useful for studying dynamics of one dimensional systems [9].

Tensor network states represent a broad class of variational states for quantum many-body systems that generalize the ideas of matrix product states to higher dimensions. Imagine now a square lattice instead of a spin chain. Now instead of associating matrices A^m with each site we will associate tensors T^m to each site. Where the matrix had two indices or "legs" (one for each neighbor) that were contracted in the spin chain, the tensor will have more indices (each running from 1 to D) that we will contact together in one large network. In principle, we calculate amplitudes in a precisely analagous fashion. Namely, for a given configuration of spins, we contract together a particular choice of N tensors in a way specified by the lattice geometry. This is illustrated in Fig. 3.3 Note that any state in the Hilbert space can be represented as a tensor network state as long as we take D of order $\exp(N)$, but in practice we want to capture the universal physics of phases of matter using an internal dimension D of order one.

3.3.1 Examples

The simplest example of a tensor network state is any mean field state. In such a mean field state, the quantum state factorizes in real space into a pure state on each lattice site. The tensors in the tensor network representation may then be chosen with $D = 1$ yielding a simple number T^m for each choice m. The contraction is trivial and T^m is simply the amplitude for state m on a given site. Thus all of mean field

theory fits within the framework of tensor network states, at least as long as we allow general tensors, for example, relaxing translation invariance to describe spontaneous symmetry breaking.

The simplest non-trivial tensor network state (and indeed the origin of the concept) may the AKLT state of an $s = 1$ spin chain [29]. This state is the exact solution of a certain deformation of the antiferromagnetic Heisenberg chain that describes a gapped ground state with interesting edge states. Indeed, at each end of a finite chain there is a dangling $s = 1/2$ spin. Since we are describing the spin chain our tensors will have one physical index and two internal indices (for the two neighbors of each site) and thus may be described as matrices as above. Labeling each site by eigenstates of $S_z = \pm 1, 0$ we have three matrices: $A^{+1} = \sigma^+$, $A^0 = \sigma^z$, and $A^{-1} = \sigma^-$. We we contract together a long chain of these matrices and perform a final trace we obtain the amplitudes for the AKLT state on a circle. This representation also reproduces in a simple way well known features of the AKLT states, for example, that we can never have two adjacent sites with $S_z = 1$. Here this follows because $(\sigma^+)^2 = 0$.

Recent efforts at classification of phases in one dimension have led to a belief that such matrix product states are a completely general description of gapped phases of matter [30, 31]. In fact, it has been rigorously proven that matrix product states can accurately approximate gapped ground states in one dimension [24]. In higher dimensions the situation is less clear. We can still certainly capture symmetry breaking phases of matter as well as short range entangled phases of matter such as generalizations of AKLT. We can even described critical points in some cases in higher dimensions, although the analogous construction in one dimension requires a mild extension of matrix product states [?]. We will return to this point later. For the moment, we wish to focus on a particularly interesting class of phases in two dimensions, namely those phases that are described by topological order.

3.3.2 Topological Phases

Topological order describes gapped phases of matter in two (or more) dimensions which possess interesting properties related to the topology of space [32, 33]. For

example, a system on a sphere will have a unique ground state, but the same system on a torus will have a ground state degeneracy. Furthermore, this degeneracy is not protected by any symmetry, it has its origin in the topology of the underlying space. Such phases of matter also possess interesting quasiparticle excitations known as anyons that generalize the notion of fermions and bosons and can even be non-abelian. Non-abelian anyons have the property that to a given configuration of anyons we assign a space of states, and motions of the anyons can realize unitary transformations on this space. Like ground state degeneracy on a torus, these braiding operations have a topological character and are insensitive to local perturbations. For these reasons, topological phases of matter have been proposed as a useful substrate for doing quantum computation, a scheme known as topological quantum computation [34, 35].

Here we show that a large class of such topologically ordered phases can be written exactly as tensor network states at a special point in their parameter space. Hence tensor network states can capture the physics of topological order, a feat that is beyond conventional mean field theory. We can also use the tensor network representation to calculate physical properties of a given topological phase. However, we also face some challenges that will be described below.

The simplest example of a topologically ordered phase is provided by Kitaev's toric code [34]. We will work on the honeycomb lattice. The Hilbert space consists of a spin half degree of freedom on each edge of the honeycomb lattice. We focus on two kinds of structure: stars s which include the three spins adjacent to a site and plaquettes p which include the six spins in one hexagon of the honeycomb lattice. The toric code Hamiltonian is

$$H = -U \sum_s \prod_{i \in s} \sigma_i^x - K \sum_p \prod_{i \in p} \sigma_i^z.$$

Every term commutes with every other and hence the toric code is exactly solvable. If we interpret the the state $\sigma^x = -1$ as an empty link and the state $\sigma^x = 1$ as string, then the ground state may be described as a superposition of all closed string

41

configurations. The first term in the Hamiltonian enforces the closed string constraint at each vertex, and the second term forces us to sum over all closed string states (it creates elementary closed string states around plaquettes).

On the plane the above Hamiltonian has a unique ground state, but the same Hamiltonian on a torus has a ground state degeneracy. The four degenerate states are topologically protected, hence the description topological order, and are robust to any local perturbation. The ground state wavefunction on the plane possesses long range entanglement as quantified by the topological entanglement entropy which is here $\log 2$. Any gapped phase of matter adiabatically connected to a product state always has zero topological entanglement entropy, hence product states cannot capture even qualitatively the physics of topological phases. Now we show that tensor network states can capture such phases.

We introduce two kinds of tensors, T_{abc} living on the sites of the sites of the honeycomb lattice and G_{ab}^m living on the links of the honeycomb lattice. $a, b, \ldots$ are internal indices running from $0, 1, \ldots, D-1$ while m is a physical index running over $0, 1$ corresponding to the absence/presence of strings (eigenvalue of $(1 + \sigma^x)/2$). We will only need $D = 2$ for an exact representation. Set $G_{ab}^m = \delta_a^m \delta_{ab}$ and $T_{abc} = (a + b + c) \bmod 2$. Then the tensor contraction the honeycomb network formed from G and T give exactly the ground state wavefunction of the toric code. This is because G maps the physical index directly into the internal index and then T simply expresses the closed string constraint. When we sum over internal indices we recover a superposition of all closed string states.

This construction can be generalized to a large class of topologically ordered states known as string-net models [11, 36]. These are exactly solvable lattice models of non-chiral topological phases primarily in two dimensions. Exact representations of string-net states are always possible using an internal dimension $D = N^3$ where N is the number of string types. $N = 2$ in the toric code (no string and string). The construction is algebraically cumbersome, but the basic intuition is the same as for the toric code. We map the physical index onto the internal index via a "triple line construction" and implement a certain set of constraints. We can also extract

42

topological data from the tensors defining the tensor network representation of a topologically ordered phase.

3.4 Challenges and prospects

There remain many challenges going forward with tensor network states. While the contraction of tensor networks in one dimension is an efficient process, contraction of higher dimensional tensor networks require approximations. Even with these approximations, the numerical cost of tensor network algorithms in higher dimensions typically scale as a high power of D. Unlike in one dimension where one can easily achieve $D \sim 10^3$, $D \sim 10$ is already challenging in higher dimensions. Because D is the naive refinement parameter of the tensor network class of states, we are somewhat limited at the present time in higher dimensions. However, this limitation is not fundamental, instead we must understand better the detailed structure of entanglement in such states to make better use of our limited resources.

Part of the reason why the detailed structure of entanglement is murky in tensor network states is that these states suffer from an ambiguity known as gauge symmetry. Gauge symmetry or gauge redundancy means many tensors give the same physical wavefunction. For example, along any tensor contraction insert identity as $1 = MM^{-1}$ for any invertible matrix M. Now absorb M and M^{-1} into the adjacent tensors being contracted to define new tensors. These new tensors give the same state by construction, but they can appear quite different. Thus characterizing what is physical about a given tensor is non-trivial, just as extracting the physics of a gauge field requires one to look for gauge invariant observables. There are two immediate consequences of this gauge redundancy. First, symmetries present in the physical wavefunction need not appear at the level of the tensors because we can always jumble these tensors up with gauge artifacts. Second, attempts to minimize the energy of a system as a function of the tensors may encounter many flat or gauge directions in the energy landscape that complicate numerical efforts.

Besides using tensor network states as variational states for local Hamiltonians,

we can also find local a local Hamiltonian for which a given tensor network state is the exact ground state. This procedure is possible because the Schmidt rank of the reduced density of a subregion of linear size L in d dimensions is bounded by cL^{d-1} where c depends only on the internal dimension and connectivity. Thus the reduced density matrix of a sufficiently large block always has a non-trivial null space since the dimension of the block Hilbert space scales as L^d. By summing many such projectors onto null spaces of large blocks, we can build a non-trivial Hamiltonian that is guaranteed to have the tensor network state as an exact ground state. Furthermore, while projectors for overlapping blocks may not commute in general, the tensor network state is nevertheless a frustration free ground state of this parent Hamiltonian. This means that it is separately a ground state of every local term in the Hamiltonian (the ground state space of a projector is simply the set of of states annihilated by the projector). The non-trivial fact about this Hamiltonian that we cannot guarantee in general is the presence of a gap, in other words, the Hamiltonian may have many degenerate ground states or low lying states. Of course, if we want to represent gapless phases using a tensor network state we certainly should not be able to prove a gap, nevertheless, we should keep in mind that the parent Hamiltonian coming from a tensor network state may be very fine tuned or singular.

If we believe that every phase of matter satisfying a boundary law for entanglement can be captured by a tensor network state, then every phase of matter has a frustration free Hamiltonian with a ground state that captures the qualitative low energy properties of the phase. This is by no means certain, and as we will explore in the next chapter, there are also states that explicitly violate the boundary law. However, there are many interesting gapped phases that are known to be ground states of Hamiltonians that are sums of non-commuting projectors. These include string net models as well as ideal Hamiltonians for fractional quantum hall states. However, it is also appropriate to mention a danger of the parent Hamiltonian approach. It is possible to make small changes in the tensors forming a tensor network state that drastically change the parent Hamiltonian. For example, the toric code is provably

absolutely stable to all local perturbations, nevertheless, we can easily introduce a string breaking term in the tensor T defined above that immediately causes us to flow out of the topological phase under renormalization. Thus the parent Hamiltonian for this string breaking tensor network must be drastically different from that of the true topological phase. By requiring certain symmetries to be present, these unphysical modifications can be avoided [37], but there is still much to understand here.

We mention one final point of confusion regarding tensor network states and the boundary law. While matrix product states and density matrix renormalization group in one dimension seem to capture the physics of one dimensional phases very well, we can be sure there is more to the story in higher dimensions beyond the boundary law. This follows from the simple observation that systems we consider computationally "easy", like the bosonic Hubbard model, and systems we consider computationally "hard", like the fermionic Hubbard model, may both have satisfy a boundary law for entanglement entropy. What exactly we mean by computational hardness is not clear, but one candidate is the viability of using quantum Monte Carlo, and of course the fermionic system may have a Fermi surface in which it would be more highly entangled. But the general point remains that the boundary law is too universal or too coarse a measure and hence there must be additional structure, perhaps in the finer details of entanglement, that distinguish easy from hard. Of course, we would also hope that some problems that appear hard for quantum Monte Carlo would actually be easier for tensor network based approaches, but we do not yet have a good idea about how entanglement cuts through the space of hard problems.

Let us end on a point of optimism by noting that tensor network states in one dimension have revolutionized the study of one dimensional phases of matter. They have been used to find ground states, to simualate dynamics, and to classify phases of matter. There are tantalizing hints that tensor network states will open up new vistas in higher dimensional systems as well. They are already playing an important role in quantum information studies of Hamiltonian complexity and in description of topological phases of matter. We are at an early stage and tensor network states have yet to prove their worth in higher dimensions, but we believe the future is promising.

3.5   Summary of results: Chapter 3

In this chapter we have focused on the leading boundary law term in the entanglement entropy of spatial regions. We have reviewed how the existence of the boundary law leads to a suggestive class of variational states that automatically incorporate boundary law scaling for entanglement entropy. Our main results here include an exact tensor network description of a variety of interesting topological phases [11] as well as an approach to extracting universal topological data from tensor networks [12]. The tensor network approach to general many-body quantum systems is still in its infancy, but building on the success of DMRG in one dimension and other recent results in higher dimensions, we believe it will mature into a useful tool for local quantum physics. Tensor network states are certainly part of the broader theoretical picture we are trying to develop for quantum many-body systems.

Chapter 4

Boundary Law Violations

4.1 Overview

In Chapter 3 we described a class of variational states suited to simulation of many-body systems with a boundary law. In this chapter, to probe the limits of this formalism, we develop an understanding of systems known to violate the boundary law in more than one dimension. This includes the Fermi gas, Fermi liquids, exotic spin liquids, and much more. The unifying theme is the existence of an effectively one dimensional description of the gapless excitations in the system.

4.2 One dimension and beyond

Recall that one dimensional gapless systems are known to violate the boundary law for entanglement entropy [27, 28]. Conformal field theories describe a special subset of these theories where the low energy scale and Lorentz symmetry is enhanced to the full $1 + 1$ dimensional conformal group. These theories are partially characterized by a central charge c which controls many important properties including thermal entropy, density of states, the trace anomaly, and most important for our purposes, the leading behavior of entanglement entropy. In a conformal field theory with central

charge c the entanglement entropy of a region of linear size L is

$$S(L) = \frac{c}{3} \ln \left(\frac{L}{\epsilon} \right)$$

with ϵ an ultraviolet cutoff. The simplest example of such a CFT is given by the interacting electron gas in one dimension, the Luttinger liquid, which has $c = 1$. However, while these one dimensional theories violate the boundary law, we argue that they are not actually anomalous in the sense that they conform to the basic scaling intuition outlined at the end of Chapter 2.

There are systems in higher spatial dimensions that also violate the boundary law, but here the scaling intuition is not adequate to explain the anomaly. In fact, we will show that the solution to all known anomalies of this type actually stems from the physics of one dimension. That is, all systems that violate the boundary law for entanglement entropy actually contain many gapless one dimensional degrees of freedom. This leads to the general expectation that they will have an additional logarithmic term in their entanglement entropy, an expectation we will clarify and refine now.

4.3 Free fermion gas

Consider spinless fermions hopping on a square lattice in two dimensions. The lattice provides an ultraviolet regulator for the theory. It is possible to add spin and consider more generic lattices in different dimensions without any serious difficulties. The physics is completely specified by giving the fermion dispersion relation ϵ_k as a function of the pseudomomentum k lying in the 1st Brillouin zone. In particular, the ground state is a Fermi sea where all states with energy less than the chemical potential μ are filled. For fermions at half filling there is one fermion per two lattice sites and hence the Fermi sea will occupy half the Brillouin zone. Generic filling fractions and dispersion relations lead to a Fermi surface with codimension 1. This means that the surface separating occupied and unoccupied regions in momentum space is a $d-1$

dimensional subspace of the the d dimensional Brillouin zone. The generic presence of a finite density of states at the Fermi surface is responsible for many of the unusual properties of the Fermi gas.

As an example of such an unusual property, the Fermi gas has a heat capacity linear in T in any dimension d. This result may be contrasted with the strongly dimension dependent result for superfluid bosons $C \sim T^d$. My interest here is in the anomalous entanglement entropy of the Fermi gas. Many bosonic and gapped fermionic systems in $d > 1$ spatial dimensions have an entanglement entropy scaling as L^{d-1} for a region of size L, but free fermions with a codimension 1 Fermi surface have the anomalous scaling $L^{d-1} \ln L$. Remarkably, a precise formula for the logarithmic term in the entropy was conjectured and verified numerically [38, 39, 40]. This formula reads

$$S = \frac{L^{d-1}}{(2\pi)^{d-1}} \frac{\log L}{12} \int \int |n_x \cdot n_k| dA_x \, dA_k, \qquad (4.1)$$

where n_x and n_k are unit normals for the real space boundary and the Fermi surface respectively. The integrals are over a scaled version of the real space boundary (hence the overall L^{d-1} factor) and the Fermi surface, and the whole expression is written in units where the volume of the Fermi sea is one. I would like to understand how this anomaly arises from the presence of the Fermi surface.

Because of the finite density of states at the Fermi surface it is useful to reinterpret the low energy modes in terms of a large number of decoupled "radial" excitations. The word radial is used because the Fermi velocity $v_k = \nabla_k \epsilon_k$ is normal to the Fermi surface. Thus we can assign to each point on the Fermi surface a radial fermionic mode with approximately linear dispersion and velocity given by the local Fermi velocity. These modes are effectively relativistic and $1 + 1$ dimensional traveling in the local radial direction as a function of time. They are also chiral because the direction of propagation is fixed by the local Fermi velocity. Modes traveling in the opposite direction are typically on the other side of the Fermi surface. Chirality is equivalent to the statement that there are no holes above the Fermi surface. This kind of patching procedure is the first step towards a higher dimensional analog of

49

bosonization, but we will not need anything more than the heuristic picture of many chiral excitations. This point of view is also visible in various renormalization group treatments of Fermi liquid systems [41, 42, 43].

4.3.1 Entanglement entropy

The presence of a large number of chiral one-dimensional excitations at low energy strongly suggests a violation of the boundary law. To make this precise we need some way to count the effective number of such chiral modes. This counting can be performed using some intuition from the study of entanglement entropy, namely that the imaginary partitions introduced to compute the entanglement entropy behave very much like real physical boundaries. Tracing out degrees of freedom outside a region of characteristic size L should coarse grain the Fermi surface into patches of typical size $1/L^{d-1}$ exactly as in a finite size system. Each patch contributes a factor of $\log L$ to the entanglement entropy because of the presence of a gapless one dimensional mode. The total contribution from the Fermi surface should therefore scale as $L^{d-1} \log L$ with the Fermi momentum making up the units where necessary. This simple argument is made more precise below, but it already captures the basic intuition behind the violation of the boundary law.

Consider the case of half filling with dispersion $\epsilon_k = -2\epsilon_0 \cos k_y a$ arising from a strongly anisotropic lattice model where fermions are unable to hop in the x direction. The Fermi surface is nested and has two disconnected components given by the lines $k_y = \pi/2a$ and $k_y = -\pi/2a$ where a is the lattice spacing. Let the subsystem of interest be a box-like region of dimensions $L \times L$ aligned with the x and y axes. The mode density on the Fermi surface is $L/2\pi$ and the length of the Fermi surface is $2\pi/a + 2\pi/a = 4\pi/a$ for a total of $2L/a$ modes. Each mode is chiral with left and right central charges given by $c_L = 1$ and $c_R = 0$. Left and right are defined locally on each patch relative to Fermi velocity, but the important point is only that one of the central charges is one while the other is zero. The entanglement entropy of a one dimensional conformal field theory on an interval of length L is $\frac{c_L + c_R}{6} \log (L/\epsilon)$ [27, 28]. Putting everything together I find a total entropy of $\frac{L}{3a} \log L$. In order to

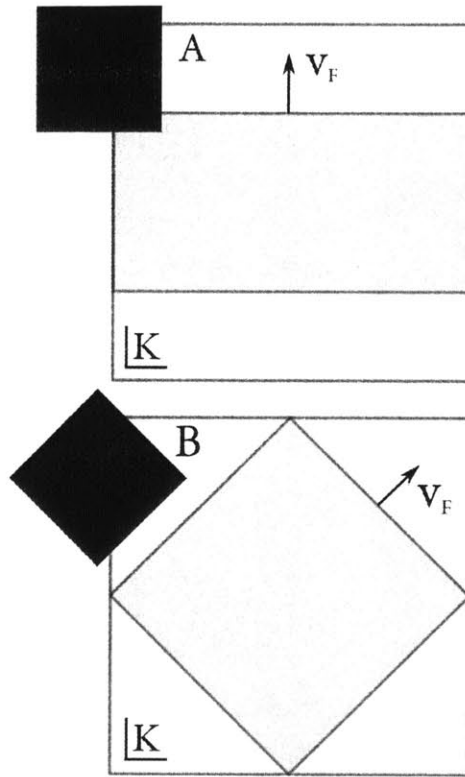Figure 4-1: A sketch of the two model systems considered. Box A shows the Fermi sea (in gray) of the strongly anisotropic model. The relative orientation of the Fermi velocity and the chosen real space region (in black) is shown. Box B shows the Fermi sea (in gray) at half filling for a fermion hopping on a square lattice. Again, the relative orientation of the Fermi velocity and the chosen real space region (in black) is shown.

compare with previous work I use units where the volume of the Fermi sea is one. This requirement is $4\pi^2/(2a^2) = 1$ (the 2 is for half filling) giving $a = \sqrt{2}\pi$. I find a total entropy of $S = \frac{1}{3\sqrt{2}\pi} L \log L$ in agreement with the Widom formula.

Another simple situation is the case of equal hopping with dispersion $\epsilon_k = -2\epsilon_0 \cos k_x a - 2\epsilon_0 \cos k_y a$. At half filling the Fermi surface consists of a square rotated by 45 degrees occupying half the Brillouin zone. To again make things simple consider an $L \times L$ region rotated by 45 degrees so that it is oriented identically to the Fermi surface. Similar mode counting arguments now give $2\sqrt{2}L/a$ modes. Using units where $a = \sqrt{2}\pi$, I find a total entropy of $S = \frac{1}{3\pi} L \log L$ again in agreement with the Widom formula.

After these examples an understanding of the general Widom formula can be obtained by breaking the real space boundary into small segments. We focus on the two dimensional case to make the notation as simple as possible. Consider a segment ΔA_x of the real space boundary and a segment ΔA_k of the Fermi surface. With a mode density of $\Delta A_x/2\pi$ the patch ΔA_k contributes

$$\frac{\Delta A_x \Delta A_k |n_x \cdot n_k|}{2\pi} \tag{4.2}$$

modes. The flux factor $|n_x \cdot n_k|$ counts the number of modes perpendicular to the real space boundary. In d dimensions the above formula is modified by replacing 2π with $(2\pi)^{d-1}$ since ΔS_x is now a general $d-1$ dimensional surface element. Each of these modes is chiral and contributes

$$\Delta S \sim \frac{c_L + c_R}{6} \log L_x = \frac{1}{6} \log L \tag{4.3}$$

to the entanglement entropy on an interval of length L. Note that the precise choice of linear size L in the logarithm is not critical as differences can be absorbed into the non-universal boundary law piece of the entanglement entropy.

The total entanglement entropy is given by integrating the contributions from all patches of the real space boundary and the Fermi surface. This result must be multiplied by an additional factor of 1/2 because intervals are double counted in the
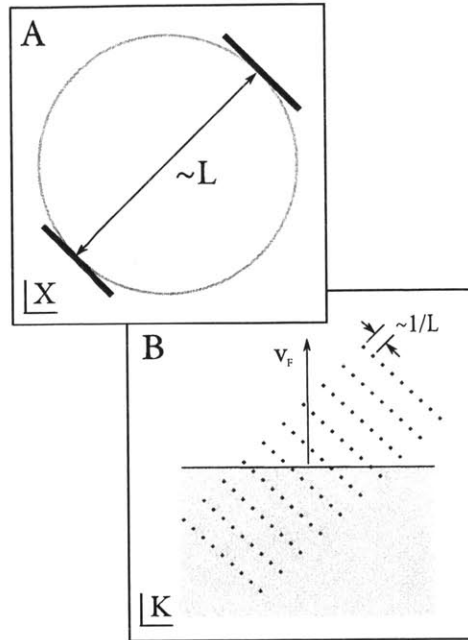
Figure 4-2: Box A shows a spherical real space region of linear size L along with a chosen real space patch on the boundary. The size of the patch (bold black bar) has been exaggerated for clarity. Box B shows a local piece of the Fermi sea with filled states in gray. The dots are an exaggerated representation of the effective mode quantization coming from the real space patch. The relative orientation of the Fermi velocity $\propto n_k$ and the real space patch normal n_x is the origin of the "flux factor" $|n_x \cdot n_k|$ counting the effective number of modes that propagate perpendicular to the real space patch normal n_x. Here the angle between n_x and n_k is $\pi/4$.

integration. Equivalently, each end of a one dimensional interval can be thought of as contributing $\frac{c_L + c_R}{12} \log\left(L/\epsilon\right)$ to the entropy [28]. The full result is

$$S \sim \frac{\log L}{6} \frac{1}{2} \int \int \frac{dA_x dA_k}{(2\pi)^{d-1}} |n_x \cdot n_k|, \tag{4.4}$$

and this is the Widom formula before rescaling the real space integral.

We have shown in some simple cases that the entanglement entropy for free fermions can be obtained using counting arguments and intuition from one dimensional systems. We also argued that an explicit formula based on the Widom conjecture is the correct generalization to arbitrary Fermi surface shape and region geometry. These arguments naturally reproduce the fully one dimensional case exactly. It is remarkable that the central charges of the chiral fermion are just right to make the Widom formula true. Nevertheless, the value of the present point of view is not that it provides a rigorous derivation but that it gives intuition to search for other violations of the boundary law.

The theory described here predicts a violation of the boundary law in any system with a large number of gapless $1 + 1$d modes. Fermi liquids certainly qualify. The recently proposed d-wave Bose liquid phase should also violate the boundary law [44]. Similarly, non-Fermi liquids with a sharp Fermi surface but no Landau quasiparticle should violate the boundary law [45]. Gauge/gravity duality has recently provided an interesting example of such a strongly correlated non-Fermi liquid phase [46]. Frustrated quantum magnets where the low energy description is in terms of deconfined spinons with a Fermi surface should also violate the boundary law [47]. In fact, this violation may be a useful numerical test for the existence of such a spinon phase. This is because the logarithmic correction to the boundary law is a low energy phenomenon that grows faster with region size than the non-universal boundary law term.

4.4 Other highly entangled systems

Recall again that many systems, gapless or not, satisfy a boundary law for entanglement entropy in higher dimensions [23]. This boundary law means that the entanglement entropy of a region of linear size L in d spatial dimensions scales as L^{d-1}. The simplest exception in more than one dimension is provided by free fermions which violate the boundary with an extra logarithmic correction [48, 38, 39, 49, 40]. It can also be argued that Fermi liquids violate the boundary law in a universal way [14]. This argument is a refinement of the connection we just made between the boundary law violation of free fermions and the gapless one dimensional nature of excitations on the Fermi surface[13]. We will return to it later in this chapter.

For the moment we want to use similar intuition to argue for boundary law violations in a variety of systems in higher dimensions. We will compute the entanglement entropy for three systems: a Weyl fermion in a magnetic field, a holographic system of many interacting Weyl fermions in a magnetic field [50], and some topological insulators with finite dislocation density [51, 52, 53, 54, 55, 56, 57]. These systems all share a common feature which unifies the discussion, namely the appearance of a large number of gapless one dimensional modes at low energies. It is these one dimensional modes which are responsible for the violations of the boundary law.

4.4.1 Weyl fermion in a magnetic field

Consider a single Weyl fermion ψ charged under a gauge field A with charge q in $3+1$ dimensions. The equation of motion for this fermion is $\gamma^\mu D_\mu \psi = 0$ with $\gamma^5 \psi = -\psi$ where $D_\mu = \partial_\mu - iqA_\mu$ is the covariant derivative. Let there be a finite magnetic field, say in the z direction: $F_{12} = \partial_1 A_2 - \partial_2 A_1 = B$. The magnetic field defines a length scale called the magnetic length $\ell_B^2 = 1/B$ (the units are made up by the flux quantum). On length scales much less than ℓ_B the theory looks like a $3+1$ dimensional conformal field theory. On length scales much bigger than ℓ_B the theory becomes effectively $1+1$ dimensional. Indeed, the Weyl fermion is special because it possesses zero modes that avoid being gapped by the magnetic field.

Let us take the gamma matrices to satisfy $\{\gamma^\mu, \gamma^\nu\} = 2\eta^{\mu\nu}$ with $\eta^{\mu\nu}$ mostly minus. The chiral gamma matrix is defined to be $\gamma^5 = i\gamma^0\gamma^1\gamma^2\gamma^3$ and we work in the chiral basis where Dirac spinors decompose as $\psi^T = \begin{pmatrix} \psi_L & \psi_R \end{pmatrix}^T$ with

$$\gamma^5 = \begin{pmatrix} -1_2 & 0 \\ 0 & 1_2 \end{pmatrix}. \tag{4.5}$$

The Weyl equation for a left handed spinor is

$$(i\partial_t - i\sigma^i D_i)\psi_L = 0, \tag{4.6}$$

with σ^i the usual Pauli matrices. The vector potential in Landau gauge is $A_y = Bx$ for a constant magnetic field B in the z direction. Most solutions of the Weyl equation in a finite magnetic field have a gap coming from the cyclotron motion, but there are also zero mode solutions. These solutions may be heuristically understood as arising from a balance between the Zeeman energy and the orbital cyclotron energy.

Zero mode solutions may be found by putting $\partial_t\psi_L = \partial_z\psi_L = 0$ to obtain

$$\sigma^x\partial_x\psi_L + \sigma^y(\partial_y - iqBx)\psi_L = 0. \tag{4.7}$$

Landau gauge maintains translation invariance in the y direction, so I try a solution of the form $\psi_L(x, y) = \psi_L(x)e^{iky}$. The Weyl equation reduces to

$$\partial_x\psi_L = -\sigma^z(qBx - k)\psi_L \tag{4.8}$$

with solution

$$\psi_L(x) = \exp\left(-\frac{qB}{2}\left(x - \frac{k}{qB}\right)^2 \sigma^z\right)\psi_L(0). \tag{4.9}$$

In order for this solution to be normalizable we must have $\sigma^z\psi_L(0) = \psi_L(0)$ (assuming $qB > 0$) leaving only one degree of freedom. The spacing of k is determined by the length of the system in the y direction to be $\Delta k = \frac{2\pi}{L_y}$. We have one zero for each value of k such that $\psi_L(x)$ sits inside the system in the x direction. The degeneracy g

of zero modes is thus $g = \frac{qBL_x}{\Delta k} = \frac{qBL_xL_y}{2\pi}$. More generally, these zero modes and their degeneracy are protected by an index theorem relating the number of zero modes to the magnetic flux penetrating the system: $N_{\text{zero modes}} = \frac{q}{2\pi} \int F_{12} dx dy$.

So far we have ignored the z direction, but these zero modes actually disperse in the z direction. Assuming a more general solution of the form $\psi_L(x, y, z, t) = e^{ip_zz + ip_yy - iEt}\psi_L(x)$ the full Weyl equation becomes

$$E\psi_L - p_z\sigma^z\psi_L - i(\sigma^x\partial_x + \sigma^y(\partial_y - iqBx))\psi_L = 0. \qquad (4.10)$$

The second half of this equation is solved with the same zero mode profile as above. The first half reduces to the equation $E = p_z$ using the fact that $\sigma^z\psi_L = \psi_L$ following from the normalization condition. Thus each zero mode is actually relativistic chiral fermion in one spatial dimension. The low energy physics is controlled entirely by these zero modes as all other modes are gapped by the cyclotron motion.

Using the one dimensional structure we can compute the entanglement entropy of the Weyl fermion. Consider a box of linear size L. The entanglement entropy S_L is defined as the von Neumann entropy of the reduced density matrix corresponding to the box: $S_L = -\text{Tr}(\rho_L \ln \rho_L)$. For one dimensional conformal field theories the entanglement entropy is known to have the form

$$S_L = \frac{c_L + c_R}{6} \ln \left(\frac{L}{\epsilon}\right), \qquad (4.11)$$

where c_L and c_R are the left and right central charges and ϵ is an ultraviolet cutoff [28]. Weyl fermions in a magnetic field may be described by a large number of one dimensional gapless modes, and these modes are each equivalent to a chiral $1 + 1$ dimensional conformal field theory, the dimensions being z and t. Each chiral fermion mode has $c_L = 1$ and $c_R = 0$ and hence contributes $(1/6)\ln L$ to the entanglement entropy. For a cube of side length L aligned with the z direction we have $qBL^2/(2\pi)$

zero modes for a total entanglement entropy

$$S_L = \left(\frac{qBL^2}{2\pi}\right) \frac{1}{6} \ln \left(\frac{L}{\epsilon}\right). \tag{4.12}$$

This formula may be checked using the generalization of one dimensional entanglement entropy to finite temperature

$$S_L = \frac{c_L + c_R}{6} \ln \left(\frac{\beta}{\pi\epsilon} \sinh \frac{\pi L}{\beta}\right). \tag{4.13}$$

The thermal entropy of these zero modes in a cube of size L is thus

$$S = \left(\frac{qBL^2}{2\pi}\right) \frac{\pi LT}{6} \tag{4.14}$$

which agrees with the direct thermodynamic calculation.

Before moving on, let us note that a single charged Weyl fermion does not give a consistent quantum theory. This is due to the presence of a gauge anomaly proportional to $\text{Tr}(Q^3)$ where Q is the charge matrix. There is also a gravitational anomaly proportional to $\text{Tr}(Q)$. Both of these anomalies must vanish for a completely well defined chiral gauge theory, but this can be accomplished by adding Weyl fermions with compensating charges. The boundary law violating behavior remains, and thus there are consistent configurations of Weyl fermions that violate the boundary law for entanglement entropy.

4.4.2 Holographic generalization

We have computed the entanglement entropy for a single free Weyl fermion and found a term that violates the boundary law for entanglement entropy. A useful choice for incorporating interactions is $\mathcal{N} = 4$ SU(N) Yang-Mills theory which includes $4N^2$ Weyl fermions as part of the field content. These fermions sit in the adjoint of the non-Abelian gauge group SU(N), while the magnetic field B corresponds to a weakly gauged U(1) subgroup of the R-symmetry. In zero magnetic field this theory is conformal at all values of the t'Hooft coupling $\lambda = g_{YM}^2 N$, but it is particularly

amenable to study at strong coupling because of holographic duality. This duality relates the $\mathcal{N} = 4$ theory to a theory of quantum gravity, IIB string theory, in an asymptotically five dimensional anti-de-Sitter spacetime (AdS$_5$). The limit $\lambda \to \infty$ and $N \to \infty$ in the field theory gives classical supergravity in anti-de-Sitter space on the gravity side.

In this strong coupling limit, configurations of the super Yang-Mills theory have an emergent geometric interpretation in terms of classical gravitational field configurations. The ground state of the field theory is dual to pure anti-de-Sitter space, and the field theory at finite temperature is accessed via a bulk black hole. The field theory in a background magnetic field at zero temperature is obtained from a magnetically charged extremal black hole in the bulk. Given the bulk geometric configuration, the leading large N contribution to the entanglement entropy can be determined holographically by computing the area of certain minimal surfaces in the bulk [58, 59].

Consider extremal magnetic brane solutions in Einstein-Maxwell theory with negative cosmological constant in five dimensions [50]. These solutions interpolate between an asymptotically AdS$_5$ region and a near horizon AdS$_3 \times$ T^2 region (assuming the xy plane is compactified). The asymptotic AdS$_5$ region corresponds to the unperturbed $\mathcal{N} = 4$ theory at high energies. The near horizon region appears as a result of turning on a magnetic field in the gauge theory. The radial evolotion represents a renormalization group flow from a $3 + 1$ dimensional conformal field theory at high energies to an effectively $1 + 1$ dimensional conformal field theory at low energies. This is qualitatively similar to the physics of free Weyl fermions, and even at strong coupling the cross-over scale is determined by the magnetic length. At zero temperature the metric may be written in the form

$$ds^2 = -U(r)\,dt^2 + \frac{dr^2}{U(r)} + U(r)\,dz^2 + e^{2V}(dx^2 + dy^2), \qquad (4.15)$$

with r the radial coordinate ($r \to \infty$ is the boundary) and z the direction of the magnetic field on the boundary [50]. We use bulk units with the AdS radius set to

one. In addition to the metric, the gauge field has a profile given by $F = B\, dx \wedge dy$. The asymptotic AdS_5 region is described by $U = e^{2V} = r^2$ while the near horizon $AdS_3 \times T^2$ region corresponds to $U = 3r^2$ and $e^{2V} = B/3$. Notice that in the near horizon region the xy plane has decoupled from the radial coordinate and has fixed size given by the magnetic length.

The entanglement entropy of a region in the dual field theory is determined by the area of the minimal surface in the bulk that terminates on the boundary of the region in the field theory. The entanglement entropy is just this minimal area divided by $4G_N^{(5)}$. I will focus on the entanglement entropy of a rectangular region in boundary theory of size $L \times L \times L_z$. Assuming $L \gg L_z$ gives approximate translation invariance in the xy plane. The minimal surface calculation reduces to a two dimensional problem involving only the variables z and r. The zero temperature geometry is only known numerically, and the minimal surface calculation can also only be done numerically. However, the important physics can be extracted without the numerical details. For cubic regions with all dimensions less than the magnetic length, the minimal surface only probes the AdS_5 region and gives the usual ultraviolet divergent boundary law for entanglement entropy.

For boundary regions of linear size much larger than the magnetic length, the minimal surface passes right through the asymptotic AdS_5 region towards the near horizon region. Once in the near horizon region, the x and y directions freeze out, and the minimal surface behaves exactly as in AdS_3. In particular, we find the characteristic $\ln(L_z/\ell)$ dependence familiar from $1+1$ dimensional conformal field theory with the magnetic length providing the cutoff. The entanglement entropy thus consists of two pieces, a non-universal boundary law contribution from the asymptotically AdS_5 region and a universal low energy piece $S_L \sim N^2 B L^2 \ln(L_z/\ell_B)$. The appearance of the magnetic field can be understood because the effective $1 + 1$ dimensional central charge is related to $1/G_N^{(3)}$ which is enhanced relative to $1/G_N^{(5)}$ by a factor of BL^2 from the freeze out of the xy plane. This strong coupling version of the free Weyl fermion system thus also violates the boundary law for entanglement entropy at low energies.

4.4.3 Topological insulators

In both the cases considered above, the appearance of many gapless one dimensional modes was responsible for the highly entangled nature of the quantum state. This intuition can be applied to more experimentally relevant systems known as strong topological insulators. These systems are time reversal invariant electronic band insulators that are not smoothly connected to trivial band insulators. In particular, they possess interesting topological structure that gives rise to protected edge modes. These edge modes are robust so long as time reversal invariance is preserved [51, 53, 57]. Topological insulators in three spatial dimensions have gapless surface states living in two spatial dimensions, but these modes do not lead to a violation of the boundary law for entanglement entropy. Similarly, the bulk of a topological insulator is gapped in a perfect crystal and certainly satisfies a boundary law for entanglement entropy.

However, experimentally realized topological insulators are not perfect crystals, they possess topological defects including dislocations in the crystalline bulk. Remarkably, for certain kinds of topological insulators and dislocation types, the dislocations have been shown to support gapless fermionic modes [60]. These effectively one dimensional modes make the dislocations into gapless quantum wires threading the otherwise gapped bulk. The one dimensional modes in the quantum wires are analogous to the Weyl zero modes considered above, with the dislocations playing the role of magnetic field lines. In the presence of a finite density of dislocations supporting gapless modes, the bulk of a strong topological insulator violates the boundary law for entanglement entropy.

To estimate the size of the violation, consider the artificial situation of a dilute array of topologically non-trivial dislocations all aligned. Let these dislocations have an areal density ρ (a typical value of ρ might be $10^{12}\,\mathrm{m}^{-2}$ [60]). A region in the bulk of size $L \times L \times L_z$, with the z axis chosen parallel to the dislocations, effectively contains ρL^2 gapless one dimensional fermionic modes. These modes should each contribute roughly $\ln\left(L_z/\epsilon\right)$ to the entanglement entropy. The boundary law violating compo-

61

nent of the entanglement entropy is thus of order $S_L \sim \rho L^2 \ln (L_z/\epsilon)$. This estimate is crude, but it should suffice for a reasonably uniform and collimated set of dislocations. Note that despite the enhanced L dependence relative to the usual boundary law, this term may be much smaller than the boundary law term for experimentally accessible system sizes and dislocation densities. We also wish to emphasize that this is a statement about the zero temperature quantum state. The helical modes modes are protected from elastic scattering (such scattering might otherwise localize a one dimensional gapless mode), but at finite temperature or in the presence of inelastic processes, the boundary law violating behavior will be disrupted.

4.5   Beyond entanglement entropy

We have been discussing a variety of systems in higher dimensions that violate the boundary law for the entanglement entropy. This class includes free fermions [48, 38, 39, 49, 40, 61, 13], Fermi liquids [14], Weyl fermions in a magnetic field [15], and more exotic systems including critical Fermi surfaces and Bose metals. The apparent unifying theme is the existence of many gapless one dimensional degrees of freedom in all these systems. Fermi liquids with a codimension one Fermi surface have long been known to be equivalent to a set of nearly decoupled one dimensional gapless modes [43, 42, 41].

We now return to this case to to compute Rényi entropies, defined again below, for a free Fermi gas and for interacting fermions in a Fermi liquid state. These quantities are interesting because they give in principle complete knowledge of the spectrum of the reduced density matrix, although we will only compute them in the low energy limit. We also describe the form of the entanglement entropy of more general regions (non-convex or even disjoint) using the same one dimensional formulation. This permits a calculation of the mutual information between two distant regions in a Fermi liquid. All of these information theoretic quantities turn out to provide direct access to the geometry of the interacting Fermi surface. They are universal in the sense that they depend only on the geometry of the interacting Fermi surface and not on any

other details of the Fermi liquid fixed point. Additionally, we compute the fermion number fluctuations in a region of size L in a Fermi liquid and give general finite temperature crossover forms for both the entropy and the number fluctuations. Together these results provide a very complete characterization of the quantum information theoretic content of Fermi liquids in terms of the geometry of low energy excitations.

4.5.1 One dimensional framework

The low energy physics of a system of free fermions is given in terms of the geometry of the free Fermi surface. For example, the heat capacity of such a free fermion system is simply proportional to the density of states times temperature, and the density of states may be written as an integral of $1/v_F$ over the Fermi surface. Each patch of the Fermi surface contributes to physical quantities like a chiral $1 + 1$ dimensional free fermion.

Including interactions is possible at the free Fermi fixed point because phase space restrictions reduce the effects of interactions to certain forward scattering terms labeled by an infinite set of Landau parameters. Each Landau parameter corresponds to a single exactly marginal deformation of the free Fermi fixed point which preserves all scaling dimensions. These forward scattering interactions preserve the fermion number on each patch of the Fermi surface, and the Fermi liquid has a very large symmetry group: $U(1)^\infty$ [62, 63]. This one dimensional framework permits computation of the usual physical observables of Fermi liquids, observables like heat capacity and compressibility. In addition, it provides simple access to many of the anomalous entanglement and fluctuation properties of Fermi liquids.

These anomalous properties characterize the reduced density matrix of a region of linear size L inside the Fermi liquid, and they represent non-traditional global observables as opposed to local correlations functions. These observables include entanglement entropy, defined as the von Neumann entropy of the reduced density matrix of the region, and fermion number fluctuations, defined as the variance of the fermion density integrated over the region. The entanglement entropy can be

generalized to the Rényi entropy defined as

$$S_\alpha = \frac{1}{1-\alpha} \ln\left(\text{tr}(\rho_L^\alpha)\right). \tag{4.16}$$

The von Neumann entropy $S_{\text{vN}} = -\text{tr}(\rho_L \ln \rho_L)$ is recovered from S_α in the limit $\alpha \to 1$. Fermionic systems without a codimension one Fermi surface and most bosonic systems have a Rényi entropy which scales with the boundary L^{d-1} of the region considered. This leading scaling behavior is sensitive to the cutoff of the low energy effective theory and does not define a universal low energy observable. Other sub-leading terms in the entanglement entropy may provide universal numbers characterizing different phases, but these terms are in general hard to calculate and interpret.

Fluctuations of conserved quantities also behave similarly to the entanglement entropy. Consider a system of fermions with a conserved fermion number obtained by integrating the density $n(x)$ over the entire system. Given access to only a subregion of linear size L we may ask about the observable $N_L = \int_{x \in L^d} n(x)$. The average $\langle N_L \rangle = \text{tr}(\rho_L N_L)$ is simply the average density times the volume of the subregion for a translation invariant system. The fluctuations $\Delta N_L^2 = \langle (N_L - \langle N_L \rangle)^2 \rangle = \text{tr}(\rho_L (N_L - \langle N_L \rangle)^2)$ are generically non-zero and typically scale as the boundary of the subregion. However, there are exceptions to this scaling, for example, it receives a logarithmic correction, like the entanglement entropy, for critical one dimensional systems. Also, symmetry breaking states have fluctuations in conserved quantities that scale as the volume of the subregion; these fluctuations are due to the zero mode of the order parameter.

Note that the presence of fluctuations in fermion number within a subregion is not in conflict with a fixed total fermion number for the entire system as we always study small subsystems of a larger system. Like the entanglement entropy of Fermi liquids, the number fluctuations in a metal with codimension one Fermi surface are anomalously large. One finds that $\Delta N_A^2 \sim L^{d-1} \ln L$ with a multiplicative logarithmic correction [64, 38, 65, 14]. We will later determine the precise form of this leading logarithmic term.

These results are not restricted to zero temperature; indeed, there are universal crossover functions that determine how the entanglement entropy and ground state number fluctuations go over into the corresponding thermal quantities as the temperature is raised. For example, consider a circular region in a two dimensional spherically symmetric Fermi liquid. The reduced density matrix for this region displays crossover behavior at finite temperature from the zero temperature anomalous entanglement regime to the finite temperature thermal regime. This crossover is captured by a universal scaling function

$$S(L, T) = \frac{1}{2\pi} \frac{1}{12} \int_k \int_x dA_k dA_x |n_x \cdot n_k| \ln \left(\frac{\beta v_F}{\pi \epsilon} \sinh \left(\frac{\pi L_{\text{eff}}}{\beta v_F} \right) \right), \qquad (4.17)$$

where L_{eff} is the chordal distance across the circle. This crossover function depends only on the geometry of the Fermi surface and the real space region; the physical Fermi velocity v_F appears simply as a unit conversion. It is the only trace of interactions in this remarkably universal formula. We will discuss and generalize this formula later in the paper. A similar formula exists for the number fluctuations which we will derive below.

4.5.2 Rényi entropy

We turn first to the calculation of the Rényi entropy of the Fermi liquid. Like the entanglement entropy, the Rényi entropy is a cutoff sensitive quantity. It typically satisfies a boundary law, but we will find that Fermi liquids have a universal boundary law violating piece tied to the geometry of the Fermi surface. The Rényi entropy is of interest for several reasons. It is often easier to compute, both in field theory and numerically, for example, by quantum Monte Carlo [66]. It can also be used to characterize phases of matter, for example in topological phases, conformal field theories, and holographic theories [67, 28, 68]. From a quantum information perspective, the notion of single copy entanglement [69], given by the limit $\alpha \to \infty$ of S_α, determines the maximal deterministically distillable entanglement from the bipartition of

a single copy of a quantum state. The entanglement entropy only gives the distillable entanglement in the unphysical limit of many copies of the quantum state. I find that the single copy entanglement is, for large L, simply one half the entanglement entropy, similar to the one dimensional conformal result [70]. We will now use the one dimensional framework to compute the Rényi entropy of a Fermi liquid.

Restricting first to the non-interacting case, each patch on the Fermi surface is equivalent to the chiral half of one dimensional free fermion. The Rényi entropy S_α of such a one dimensional chiral fermion is known from conformal field theory. In fact, it is simply proportional to the entanglement entropy with an α dependent prefactor. The precise result is

$$S_{\alpha(1+1)} = \frac{1}{2}\left(1 + \frac{1}{\alpha}\right)\frac{c_L + c_R}{6}\ln\left(\frac{L}{\epsilon}\right), \tag{4.18}$$

where L is the length of the one dimensional interval and ϵ is a short distance cutoff. Returning to the Fermi surface problem, each patch contributes such a term to the entanglement entropy with $c_L = 1$ and $c_R = 0$. The resulting Rényi entropy of the Fermi liquid is remarkably simple; the universal part controlled by the low energy theory is simply

$$S_\alpha = \frac{1}{2}\left(1 + \frac{1}{\alpha}\right)S_1, \tag{4.19}$$

where again, S_1 is the usual entanglement entropy in two dimensions given by

$$S_1 = S = \frac{1}{2\pi}\frac{1}{12}\int_k \int_x dA_k dA_x |n_x \cdot n_k| \ln\left(\frac{L}{\epsilon}\right). \tag{4.20}$$

This isn't the end of the story. Using the finite temperature crossover form for the von Neumann entropy of the reduced density matrix we obtain a finite temperature crossover form for the Rényi entropy. The result for two dimensions is

$$S_\alpha = \frac{1}{2}\left(1 + \frac{1}{\alpha}\right)S(L, T), \tag{4.21}$$

and in any spatial dimension with a codimension one Fermi surface

$$S_\alpha = \frac{1}{2}\left(1 + \frac{1}{\alpha}\right)\frac{1}{(2\pi)^{d-1}}\frac{1}{12}\int_k\int_x dA_k dA_x |n_x \cdot n_k| \ln\left(\frac{\beta v_F}{\pi\epsilon}\sinh\left(\frac{\pi L_{\text{eff}}}{\beta v_F}\right)\right). \quad (4.22)$$

We want to note that since the Fermi surface system has a cutoff, this formula cannot truly be valid for all α. For example, the $\alpha \to 0$ limit of the Rényi entropy always produces the Schmidt rank of the reduced density matrix under study. However, the $\alpha \to 0$ limit of the conformal field theory result diverges corresponding to the statement that a theory which is truly conformal to arbitrarily high energy must have an infinite number of local degrees of freedom. At finite temperature we must keep $T/\alpha < T_F$ or $\alpha > T/T_F$ in order not to probe high energy physics, and similarly, at zero temperature we must keep $\alpha > 1/(k_F L)$ to avoid the influence of non-universal physics away from the Fermi surface.

Now at last restoring the interactions, the complete finite temperature crossover function remains correct even in the presence of interactions because of the nature of the Fermi liquid fixed point (more properly, fixed manifold). The counting of low energy degrees of freedom remains the same. There are two possible modifications of this formula when including interactions. First, the interactions may change the geometry of the low energy Fermi surface. Spherical symmetry can prevent such a modification, but in a solid state metal the crystal lattice breaks the rotational symmetry. Nevertheless, the interacting Fermi surface in this less symmetric systems continues to control the Rényi entropy. Second, the Fermi velocity must be replaced by the renormalized physical Fermi velocity.

There are several checks of this formula. First, it correctly reproduces the one dimensional result that must occur for non-interacting systems with nested Fermi surfaces. Second, it reproduces the finite temperature Rényi entropy of the free Fermi gas; this follows by a direct computation. Third, it reproduces the thermal Rényi entropy of an interacting Fermi liquid. At finite temperature the Rényi entropy is

$$S_\alpha = \frac{1}{1-\alpha}\ln\left(\text{tr}\left(\rho(T)^\alpha\right)\right) = \frac{1}{1-\alpha}\ln\left(\frac{Z(\alpha\beta)}{Z(\beta)^\alpha}\right) \quad (4.23)$$

where $Z(\beta)$ is the partition function. The partition function of the Fermi liquid is $-\ln Z \sim T$ for small T compared to E_F, and this permits us to write $Z(\alpha\beta) = Z(\beta)^{1/\alpha}$. The final result is that the Rényi entropy for an interacting Fermi liquid is the same universal function of α times the thermal entropy as predicted by the formula above.

4.5.3 Entanglement entropy of disjoint regions

Having described in detail the leading behavior of the Rényi entropy for a single convex region, we now turn to the problem of describing the entanglement entropy for more complicated subregion geometries. Perhaps the most important motivation for this study is the calculation of the quantum mutual information $I(A, B)$ between two regions A and B. The mutual information is

$$I(A, B) = S_A + S_B - S_{A \cup B}, \tag{4.24}$$

and this definition requires knowledge of the entanglement entropy of disjoint regions to compute. We will see that the entropy of disjoint regions can be computed in a manner similar to that of convex regions via a more general formula that can handle arbitrary region geometry. The basic strategy remains the same: express all quantities in terms of sums over one dimensional modes on the Fermi surface. Because these one dimensional modes are conformal and, in fact, essentially free fermions, much can be calculated. In particular, the main information we need is the entanglement entropy of a one dimensional conformal field theory when the one dimensional subregion consists of multiple regions.

This quantity, the entanglement entropy of multiple regions in a conformal field theory, is not a simple quantity to compute in general. Despite some early claims in the literature it is not as universal as the single region entanglement entropy which depends only on the central charge of the conformal field theory. The multi-interval entanglement entropy depends on the entire operator content of the theory as it requires evaluating higher point correlation functions of twist fields. However, the
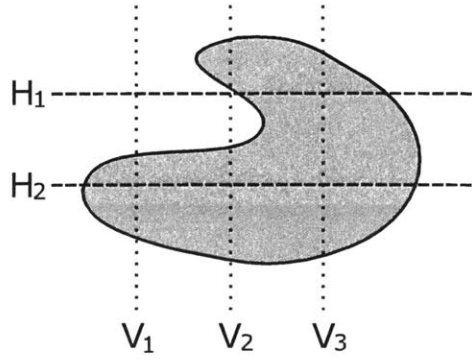
Figure 4-3: Geometry of the entanglement entropy for a non-convex real space region. The shaded grey region surrounded by the thick black line represents a particular non-convex real space region. Dotted lines labeled V_i ($i = 1, 2, 3$) represent particular one dimensional cuts experienced by a patch of the Fermi surface with vertical Fermi velocity. Similarly, dashed lines labeled H_i ($i = 1, 2$) represent particular one dimensional cuts experienced by a patch of the Fermi surface with horizontal Fermi velocity. Notice how the vertically moving fermion switches from an effectively single interval geometry in V_1 to a two interval geometry in V_2 and back to a single interval in V_3. On the other hand, H_1 and H_2 are both effectively single interval geometries.

relative simplicity of the Fermi liquid is a boon: the multiple interval result for a one dimensional free fermion is known. We will see shortly how this information permits calculation of the entanglement entropy of arbitrary regions in a Fermi liquid.

Let us briefly recall the one dimensional result. We consider a subsystem consisting of several disjoint intervals labeled $[a_i, b_i]$ $i = 1, ..., m$ with m the number of intervals. As we said before, the entanglement entropy of such a subregion is in general complicated, but for free fermions the answer is remarkably simple. The result is

$$S_{1+1} = \frac{c_L + c_R}{6} \left(\sum_{ij} \ln |a_i - b_j| - \sum_{i<j} \ln |a_i - a_j| - \sum_{i<j} \ln |b_i - b_j| \right), \qquad (4.25)$$

with the implicit presence of cutoffs in the logarithms is understood. This formula reduces to the usual result in 1 dimension in the case of a single interval. Note that when computing the mutual information, the number of logs being added and subtracted is equal giving a result independent of the cutoff.

How do we use this formula to compute the entanglement entropy of a Fermi liquid in an arbitrary geometry? The procedure is illustrated in Fig. 1 and goes as follows. First, we choose a point on the Fermi surface; this point defines a direction in space via the local Fermi velocity. Second, we choose a point on the real space boundary and draw a line through this point with direction determined by the Fermi velocity from step one. Third, we determine the intersections of this line with the boundary of the real space region; these intersection points are grouped into effectively one dimensional intervals. The contribution to the entropy of such a configuration is given by a slightly modified version of the one dimensional result above (4.25). To each logarithm in the one dimensional result we append geometrical "flux factors" $|n_x \cdot n_k|$ times a differential area element dA_x where n_k is the direction determined by the Fermi velocity and n_x is a real space normal vector. In detail, each logarithmic term of the form $\ln|x - y|$ is multiplied by a factor of $\frac{|n_x \cdot n_k| dA_x + |n_y \cdot n_k| dA_y}{2}$, where n_x and n_y are the local real space boundary normals. As illustrated in Fig. 2, the flux factors and differential area elements satisfy $|n_x \cdot n_k| dA_x = |n_y \cdot n_k| dA_y$. Finally, the contribution of this configuration of intervals must be divided by the number intersection points to avoid over-counting and integrated over all such points on the real space boundary and the Fermi surface. This geometrical calculation gives the leading boundary law violating contribution to the entanglement entropy of a Fermi liquid for arbitrary Fermi surface shape and real space geometry.

This formula is well defined but complex. There are a number of simple checks that can be performed. For two or more well separated convex regions, the formula above reduces to a sum of terms corresponding to the entanglement entropy of each region taken separately. For free fermions with a nested Fermi surface one immediately recovers the one dimensional result as all the flux factors become trivial. At finite temperature, all the logarithms $\ln L$ are replaced by crossover functions of the form $\ln\left(\sinh\left(\pi L T / v\right)\right)$ leading to a simple form at high temperature that is extensive in the total real space region size. This one dimensional crossover form is well known for single intervals in one dimensional conformal field theory, but it is nontrivial for the multiple interval case. It comes from evaluating higher point correlations functions of

70

twist fields on a Euclidean torus in the free fermion conformal field theory. As before, the simple form depends crucially on the fact that we are dealing with free fermions; this result does not hold in a general conformal field theory.

The absence of Landau parameters is reasonable given the fact that the entanglement entropy (at least for a single interval) doesn't depend on interaction strength even for a Luttinger liquid in one dimension. I cannot completely rule out the possibility that there is a prefactor f in the crossover function which is a function only of LT: $f = f(LT)$ with the limits $f(x \to \infty) \to 1$ and $f(x \to 0) \to$ constant, but such a prefactor seems unlikely. Given the absence of Landau parameters at high temperature and the large $U(1)^\infty$ symmetry, I believe the Fermi liquid entanglement entropy is universal as I have described.

There are also some subtleties in the evaluation of this formula. The most basic subtlety is that the number of intervals is subject to change depending on the point on the real space boundary chosen. These weak singularities are nevertheless completely harmless and do not render the integral ill defined. It is best to illustrate the formula by a simple example; further results of this nature will be presented elsewhere. Take a d dimensional spherically symmetric Fermi liquid, and consider a real space region consisting of two spheres A_1 and A_2 of radius R separated by a center-to-center distance ℓ. A very interesting quantity is the mutual information between the two spheres defined as $I(R, \ell) = S_{A_1} + S_{A_2} - S_{A_1 \cup A_2}$. This quantity is quite powerful as it bounds normalized connected correlation functions between operators localized in the two spheres. We now evaluate this quantity for the two sphere geometry in the limit $\ell \gg R$ thus bounding the long distance decay of correlations in the Fermi liquid.

Because we subtract the entropy of each region separately, the only contribution to the mutual information comes from configurations that involve both spheres. As shown in Fig. 2, each pair consisting of a Fermi surface point and a point on the real space boundary only contributes if the line drawn from the real space point parallel to the local Fermi velocity intersects both spheres. The fraction of pairs of points satisfying this constraint vanishes in the limit $\ell/R \to \infty$ which is the statement that the mutual information vanishes for infinite sphere separation. Our task is to estimate
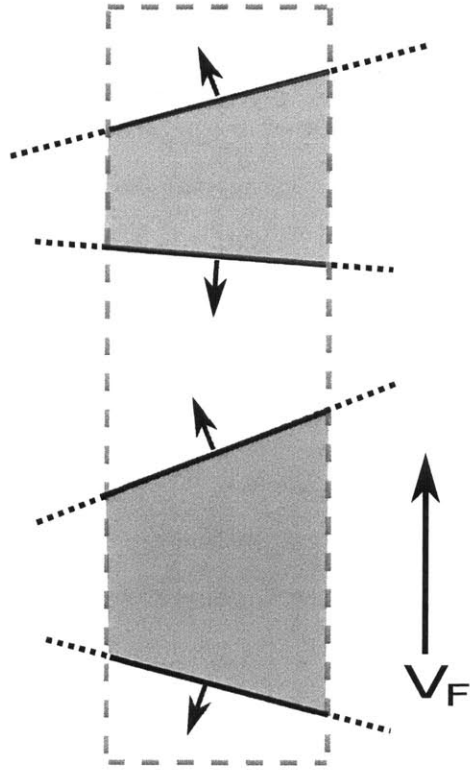
Figure 4-4: Multiple interval geometry and flux factors. A sequence of intervals similar to the situation shown in Fig. 1 V_2 with the local Fermi velocity vertical. The dashed grey line encloses the real space boundary segments of interest; the segments themselves are the black lines which continue into dotted lines outside the dashed grey enclosing line. The dark grey shaded regions are interior regions of the real space region, while arrows at the surfaces of the these regions indicate local normals to the real space boundary.

how this fraction vanishes in said limit. Let one sphere sit at $z = 0$ and the other sit at $z = \ell$; both spheres sit at $x_i = 0$ for $i = 1...d - 1$ with $x_d = z$. Since I have assumed spherical symmetry, the Fermi surface is sphere of radius k_F in momentum space with k_F fixed by density. Now the Fermi surface points with $\vec{v}_F = \pm v_F \hat{z}$ always gives lines connecting the two spheres, but as $\ell/R \to \infty$, only a small neighborhood around these points continue to generate lines connecting the two spheres. We can estimate the linear size δk of this neighborhood as $\delta k \sim k_F \left(\frac{\ell}{R}\right)$. For $\ell/R \to \infty$, the difference of logarithms appearing the mutual information nearly cancels with a residual $(R/\ell)^2$ falloff. Putting everything together, I find that roughly $(R\delta k)^{d-1}$ patches on the Fermi surface each contribute $(R/\ell)^2$ to the mutual information for a total mutual information going like

$$I(\ell, R) \sim (Rk_F)^{d-1} \left(\frac{R}{\ell}\right)^{d+1}. \tag{4.26}$$

As we have already indicated, the mutual information provides a bound on connected correlation functions. The precise statement is that the square of the connected correlation function of any two operators, normalized by the operator norms, is bounded by the mutual information. Thus we learn that connected correlation functions of local operators in a Fermi liquid must decay at least as $x^{-\frac{d+1}{2}}$ as $x \to \infty$. Calculations are trivially possible for free fermions, and one can directly verify that all two point functions of bosonic composite operators do indeed decay fast enough to satisfy the bound. The bound is saturated by the two point function of fermions which decays as $x^{-\frac{d+1}{2}}$ times an oscillating function of $k_F x$. This is not completely trivial since the fermion creation operator is not strictly speaking a local operator i.e. in the Jordan-Wigner representation, but this mild non-locality does not to spoil the utility of the mutual information. The exact coefficient is calculable by performing the geometrical integrals outlined above. On the other hand, nested Fermi surfaces give a mutual information that only decays as $1/\ell^2$ indicating the possible presence of slowly decaying correlations. Indeed, this bound is again saturated by the fermion two point function which decays as $1/x$ for a nested Fermi surface with x parallel to
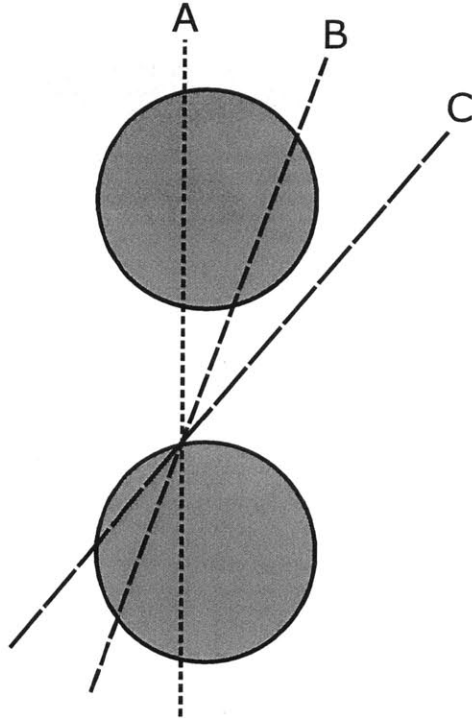
Figure 4-5: Geometry of the mutual information for disconnected real space regions. The three one dimensional cuts labeled A, B, and C represent three different patches on the Fermi surface for different angles of the Fermi velocity. Cut A comes from a mode with vertical Fermi velocity; it always cuts both spheres and hence always contributes to the mutual information in this geometry. Cut B also connects both spheres, at least for some choices of real space boundary point. However, cut C never intersects both spheres simultaneously and hence does not contribute to the mutual information. For the sphere geometry shown here, there is always a maximum angle from vertical such that cuts beyond that angle never intersect both spheres. As described in the text, this maximum angle approaches zero as the spheres are taken far apart relative to their size.

the nesting vector.

We can also numerically compute the mutual information between two rectangular blocks in a two dimensional free fermion system with a nearly spherical Fermi surface. The geometrical integrals can be done in the limit $R \gg W$ with the result

$$I \sim \frac{k_F R}{6\pi} \frac{W^2 R}{L^3} \tag{4.27}$$

where W is the box width, R is the box length, and L is the separation between the boxes. This expression agrees with the numerical result to within a few percent with the deviation due mostly to corrections in W/R and R/L; additionally, the qualitative $1/L^3$ dependence also agrees with the numerical results.

4.5.4 Number fluctuations

Finally, we turn to a description of the number fluctuations. Here at last Fermi liquid parameters will make an appearance. Recall that the basic result on the number fluctuations is that they scale as $L^{d-1} \ln L$ in a Fermi liquid for a real space region of linear size L. For free fermions the precise prefactor is known both from operator methods and from the conformal field theory approach advocated here. Unlike the result for entanglement entropy, the number fluctuations do depend on Landau parameters as interactions are turned on. To see this note that the same connected correlation function used to determine the number fluctuations is also related to the compressibility at finite temperature. This compressibility does depend on a Landau parameter in addition to the effective mass through the density of states. Thus we can already say that the number fluctuations $\Delta N_L^2(L, T)$ must depend on the Landau parameters in the limit $T \to \infty$ (always keeping $T \ll E_F$.) In fact, we can say much more because in Fermi liquid theory the interacting density-density correlation function is related to the free correlation function by a series of forward scatting diagrams that can be summed to give $1/(1 + F_0)$ where F_0 is the familiar $\ell = 0$ Landau parameter for spin-less fermions. The number fluctuations in a d dimensional Fermi

liquid at zero temperature take the asymptotic form

$$\Delta N_L^2 \sim \frac{1}{1 + F_0} \frac{1}{(2\pi)^{d-1}} \frac{\ln L}{4\pi^2} \int_x \int_k dA_x dA_k |n_x \cdot n_k|, \qquad (4.28)$$

with L the linear size of the convex region considered.

In the presence of interactions at finite temperature we find the familiar crossover form

$$\Delta N_L^2(L, T) = \frac{1}{1 + F_0} \frac{1}{(2\pi)^{d-1}} \frac{1}{4\pi^2} \int_k \int_x dA_k dA_x |n_x \cdot n_k| \ln \left(\frac{\beta v_F}{\pi \epsilon} \sinh \left(\frac{\pi L_{\text{eff}}}{\beta v_F} \right) \right), \qquad (4.29)$$

where the $\ln L$ term has been replaced by its finite T generalization $\ln (\sinh (\pi LT/v))$. As before, one can check that in the limit of high temperature one recovers the usual number fluctuations proportional to region size and depending on F_0 and the physical Fermi velocity v_F.

The generalization to non-convex regions or multiple regions is also possible in line with the generalization of the entanglement entropy discussed above. Indeed, the structure of logarithms in (4.25) also appears for the number fluctuations in a one dimensional Fermi liquid. The density-density correlation function is

$$\langle n(x)n(y) \rangle_c \sim \frac{1}{(x - y)^2}, \qquad (4.30)$$

and upon integrating x and y over different intervals we find exactly the structure of sums of logarithms appearing in (4.25). This means that the same geometrical integral that gave the multiregion entanglement entropy in the higher dimensional Fermi liquid also appears in the calculation of the number fluctuations. Indeed, these two quantities only differ in the prefactor of the geometrical integral describing the interplay of real space and Fermi surface geometries. To be precise, in the limit of large L with a fixed high energy cutoff, we find that $\Delta N_L^2/S_L = \frac{3}{\pi^2} \frac{1}{1+F_0}$. In fact, given the essentially identical forms of the postulated finite temperature scaling functions for entropy and number fluctuations, this ratio is actually valid even at finite temperature.

4.5.5 Discussion

We have described the calculation of Rényi entropy, mutual information, and number fluctuations in Fermi liquids in any dimension for arbitrary codimension one Fermi surface and sub-region geometry. These results give a very complete description of the low energy structure of quantum information in a Fermi liquid. This basic Fermi liquid state which underlies so many materials is a truly highly entangled quantum phase of matter. Remarkably, the entire structure of quantum information in these systems is controlled by a beautiful interplay between the geometry of the Fermi surface and the structure of one dimensional conformal field theory.

There is one subtlety which deserves a more careful discussion, namely the issue of singularities on the Fermi surface. The methods described above apply directly to smooth Fermi surfaces, but the formalism is strong enough to handle aspects of singular situations as well. To give a simple example, consider spinless fermions hopping on a square lattice at half filling. The Fermi surface consists of four straight lines running diagonally between the midpoints of the Brillouin zone boundary. There are singularities on the Fermi surface at $(\pm\pi, 0)$ and $(0, \pm\pi)$, points where the Fermi velocity vanishes leading to well known singularities in the density of states. As an example of the subtleties that may arise, consider the mutual information between two regions separated by a large distance compared to their size along the y-axis. A little thought reveals that the leading contribution to the mutual information from the Fermi surface, in the form presented above, vanishes in this geometry. In fact, the mutual information is not totally zero; indeed, it cannot be since the fermion correlation function doesn't vanish in the limit of large y. However, the fermion correlation function does decay faster $(1/y^2)$ than the result for a non-singular Fermi surface $(1/y^{3/2})$. In this sense, the vanishing of the leading "Fermi surface" part of the mutual information is physical, telling us that there are no extremely long ranged correlations such as would come from a non-singular Fermi surface. When the Fermi surface geometry does lead to extremely long ranged correlations, such as along the nesting vector (π, π) in the half filled example, then the mutual information

formalism above perfectly captures the requisite decay. The simple lesson is that there are always subleading terms in all quantities which can become visible if the Fermi surface contribution happens to vanish. We must simply always remember that the formalism developed in this paper captures only the leading Fermi surface contribution to the physics.

It should be clear by now that there are other quantities of interest that can be calculated for Fermi liquids using the one dimensional approach. Particularly interesting would be to study the behavior of entropy and other quantities in a non-equilibrium situation, following a quench of some type, for example. Powerful techniques from one dimensional conformal field should give a great deal of control over the non-equilibrium structure of entanglement in Fermi liquids. There is still the question of experimental observation of the effects described here. The number fluctuations are in principle easy to observe, we simply need to prepare a clean Fermi liquid, perhaps in an optical lattice, and repeatedly count the number of fermions in a given subsystem to evaluate ΔN^2. If the subregion can be made large enough we have a quite precise prediction for ΔN^2.

Given their experimental ubiquity, it is gratifying to have control of the quantum information content of Fermi liquids. Of course, in the case of Fermi liquids in the solid state, the logarithms will be cutoff by the mean free path in the presence of disorder. Still, any clean Fermi liquid system with a long mean free path will display the anomalous quantum information theoretic properties described here. In the larger framework of many-body entanglement, Fermi liquids have taught us how to produce one class of highly entangled quantum states. However, much remains to be understood about the role of entanglement in deeply quantum mechanical phases, especially gapless phases like those explored here [46, 45, 71, 72, 44]. Like Fermi liquids, these phases should violate the boundary law for entanglement entropy. And the search continues for other highly entangled phases of quantum matter.

4.6   Summary of results: Chapter 4

In Chapter 3 we argued that tensor network states may provide a useful starting point for local quantum systems that obey a boundary law for entanglement entropy. In this chapter we explored a variety of systems that weakly violate the boundary for entanglement entropy. In every case, we gave a simple heuristic picture of the violation in terms of many gapless one dimensional degrees of freedom [13, 14, ?]. The fact that gapless one dimensional systems violate the boundary law follows from the renormalization group argument in Chapter 2. We used holographic duality to show that this intuition is not restricted to weakly coupled theories and Fermi liquids, but also holds in a strongly coupled version of the Weyl fermion system [15]. Here again we see a valuable role for holographic duality in studying entanglement properties of generic local quantum systems. We also studied in much greater depth the physics of quantum information in Fermi liquids [16], including calculations of the Renyi entropy, mutual information, and number fluctuations.

Chapter 5

Entanglement Renormalization and Holography

5.1 Overview

In this chapter we develop a connection between the ideas of entanglement renormalization and holography. The phases of matter we will consider will typically obey the boundary so we seek instead to refine the crude characterization provided by the boundary law. We will devise a speculative framework for distinguishing between gapped and gapless phases of matter which both have a boundary law for entanglement in higher dimensions.

5.2 Basic idea

Entanglement renormalization [73] is a combination real space renormalization group techniques and ideas from quantum information theory that grew out of attempts to describe quantum critical points. The key message of entanglement renormalization is that the removal of local entanglement is essential for defining a proper real space renormalization group transformation for quantum states. This realization has permitted a compact description of some quantum critical points [74, 75]. Holographic duality [76, 77, 78] is the proposal that certain quantum field theories without grav-

ity are dual to theories of quantum gravity in a curved higher dimensional "bulk" geometry. We have already met holography in Chapter 4 when we computed the entanglement entropy a certain strongly coupled conformal field theory in a magnetic field. Holography provides a way to compute field theory observables from a completely different point of view using a small amount of information encoded geometrically. Real space renormalization is also important in the holographic framework [79, 80, 81, 82], thus hinting at a possible connection between holography and entanglement renormalization. We will begin with entanglement renormalization and build up to the full holographic picture.

Recall again the scaling argument from Chapter 2 for the entanglement entropy of a region A in the ground state. We partition the degrees of freedom by scale into groups labeled by a scale parameter r, and furthermore, we take these groups to be equally spaced in $\log r$. The appropriate measure for r is $d \log r = dr/r$ [83]. Degrees of freedom at each scale can be entangled with the region A, which we take to have linear size L in d spatial dimensions. Because the Hamiltonian is local, the contribution to the entropy of A from scale r should be proportional to the size of the boundary ∂A in units of the coarse grained scale r. This factor simply counts the degrees of freedom at scale r that are local to the boundary ∂A. The number of entangled degrees of freedom at scale r is also proportional to the measure dr/r and hence the entropy should scale as

$$dS \sim \frac{L^{d-1}}{r^{d-1}} \frac{dr}{r}.$$ (5.1)

The total entanglement entropy is obtained by integrating this formula from the ultraviolet cutoff ϵ to some larger length ξ_E. ξ_E is the length scale beyond which there is no entanglement in the quantum state, and at a quantum critical point this length will diverge. In one dimension the entropy also diverges with ξ_E, and cutting this divergence off with region size L naturally gives a weak violation of the boundary law. Here we ask if we can interpret this integral geometrically, that is can we find some geometrical space to that $dS^2 = ds^2$?

5.3 Lattice implementation

To obtain a more concrete formulation of entanglement as a function of scale, we will focus on a concrete lattice system where entanglement renormalization can be carried out numerically [74]. The quantum Ising model in one spatial dimension is a convenient model system, but the basic story applies to more general systems in higher dimensions. The quantum Ising model has a Hamiltonian

$$H = -J \sum_{<ij>} \sigma_i^z \sigma_j^z - gJ \sum_i \sigma_i^x, \tag{5.2}$$

where J sets the overall energy scale and g is a dimensionless parameter we can tune. The Hamiltonian consists of two competing pieces, and this competition gives rise to a quantum phase transition at $g = 1$ between an ordered ferromagnetic phase and a disordered paramagnetic phase.

Following the prescription of entanglement renormalization, one can implement a renormalization group transformation on the Ising ground state using unitary operators called disentanglers to remove local entanglement and isometries to coarse grain as shown in Figure 1. Note that information can be lost during the coarse graining steps since the isometries typically contain projectors. The resulting network of unitary and isometric tensors approximately encodes the ground state wavefunction using a multi-layered structure [84]. Each layer corresponds to a different scale in the full theory, and the quantum state is effectively extended into an emergent dimension representing scale. The network depends on g because the ground state does.

Inspired by holography and the connection between entropy and geometry encoded in the ordinary boundary law, we will define a geometry from the entanglement structure of the quantum state. Imagine drawing boxes or cells around all the sites in the tensor network representing the quantum state as in Figure 2. We view these cells as units filling out a higher dimensional "bulk" geometry where the size of each cell is defined to be proportional to the entanglement entropy S_{site} of the site in the cell. The connectivity of the geometry is determined by the wiring of the quantum

83
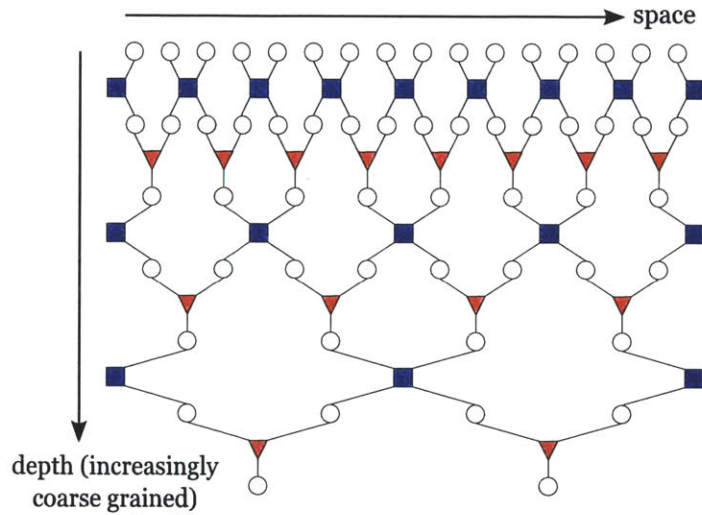
Figure 5-1: The tensor network structure of entanglement renormalization. Circles are lattice sites at various coarse grained scales. Squares with four lines are unitary disentaglers and triangles with three lines are isometric coarse graining transformations. The network shown here represents a $2 \to 1$ coarse graining scheme and has a characteristic fractal structure. In principle, each tensor can be different, but translation and scale invariance can provide strong constraints. This network implements a renormalization group transformation that is local in space and scale. This transformation has the important property that it coarse grains local operators into local operators.

Figure 5-2: Curved boxes represent primitive "cells" of the higher dimensional bulk geometry.
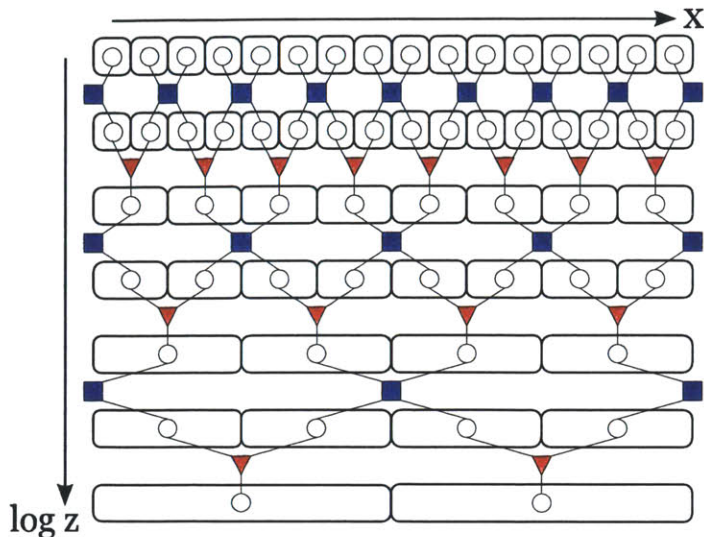
circuit represented by the tensor network in Figure 2. The geometry ends whenever the coarse grained state completely factorizes. Now why is such a definition useful from the point of view of entanglement?

To compute the entropy of a block of sites in the original ultraviolet lattice we must know the reduced density matrix of the block, but what determines this density matrix? The causal cone [84] of a block of sites in the ultraviolet is defined as the set of sites, disentanglers, and isometries that can affect the chosen block. The causal cone should not to be confused with ordinary causality in time. For the causal cone of a large block, the number of sites in a given layer shrinks exponentially, as in Figure 3, as we coarse grain. Note that for a small block, say two sites, the causal cone will actually grow slightly.

We start with the density matrix for a small number of sites deep in the causal cone of the block. The goal is to reach the ultraviolet by following the renormalization group flow backwards. This is possible because we have recorded the entire renormalization "history" of the state in the network, but subtleties remain because of the possible loss of information. In practice, the truncation error may be quite small with the proper use of disentanglers. More properly, the tensor network defines a
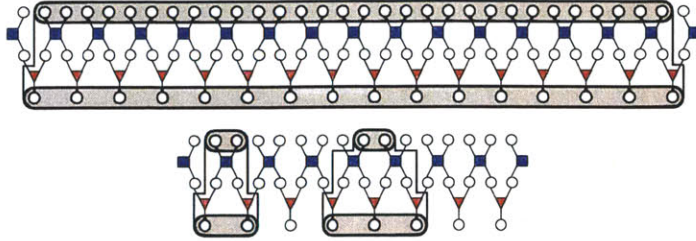
Figure 5-3: Causal cones of different blocks after a single layer of disentanglers and isometries. The causal cone of a large block decreases by roughly a factor of two in width (30 sites to 16 sites) after one coarse graining. On the other hand, causal cones for small blocks may grow slightly. Once the causal cone of a large block has reached a width of order one, it stops shrinking.

large variational class of states for which the entanglement entropy can be computed by reversing the flow [84].

Beginning with the density matrix for a small number of sites deep in the causal cone, we reverse the isometries and disentanglers to produce the density matrix of a larger number of sites at a less coarse grained scale. Any site at this new scale which is not in the causal cone of the block of interest can immediately be traced out as shown in Figure 4. Tracing out a site can increase the entropy of the remainder, but the increase is no more than the entropy of the traced out site. This procedure is repeated until the ultraviolet is reached. Looking at the whole process, sites that are traced out occur on the outside boundary of the causal cone and form a kind of curve in the bulk geometry. The length of this curve is by definition the sum of the entropies of all the traced out sites. Thus the length of a curve in the bulk, including a deep "cap" coming from the sites we began with, provides an upper bound for the entropy of a block in the ultraviolet.

This entropy calculation is a complicated process which depends on the details of the scheme, but we can extract at least two general lessons. First, the intuitive picture of distinct entropy contributions from each scale is realized concretely in the lattice framework. Second, subadditivity of the entropy permits us to give an upper bound for the entropy of a block of sites in the ultraviolet. From the cell model given above we can say that the entropy of a block of sites in the ultraviolet lattice
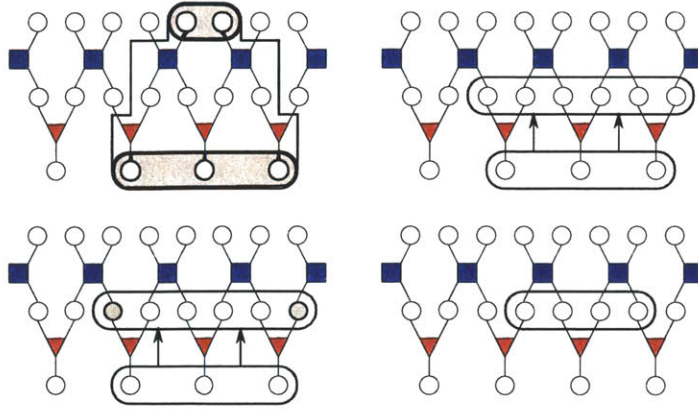
86

Figure 5-4: Upper left: a piece of the causal cone of a small block. Upper right: reversing the flow to proceed from three sites to six sites. Lower left: shaded sites are outside the causal cone of the two site block and can be traced out. Lower right: four sites remain and we can now apply the next layer of disentanglers to reach the two site block of interest.

is bounded by the length of a curve in a higher dimensional discrete geometry. This curve is precisely a holographic screen that hides information [85, 86]. It is natural to view the boundary of the causal cone as a minimal curve since it represents the minimal number of sites that must be traced out, and this agrees with the geometrical definition. As an aside, when the number of local degrees of freedom is large, similar to a thermodynamic limit, subadditivity is expected to be replaced by approximate additivity.

5.4 Geometry from entanglement

What geometries do these definitions give for the Ising model? In the large g limit, the Ising Hamiltonian is dominated by the transverse field, and the ground state is a product state. Each site is in a pure state and we find no geometry. Away from large g, the system possesses an energy gap to excited states and a finite correlation length. The size of cells is initially non-zero due to the presence of entanglement. However, as the quantum state is coarse grained using entanglement renormalization the correlation length should grow smaller. Similarly, after a finite number of coarse graining steps the entanglement will be completely removed. At this "factorization"

scale, which is the analog of ξ_E, the coarse grained quantum state factorizes, and we can conclude that the geometry ends. The entanglement entropy of a block in the ultraviolet lattice receives contributions from a finite range of scales corresponding to a minimal curve hanging down from the cutoff scale to the factorization scale. Note also that the length of this minimal curve isn't affected by the end of the geometry since the spatial length is zero there.

The geometrical picture becomes more interesting when the quantum Ising model is at its quantum critical point $g = 1$. Scale invariance forces each coarse grained layer to be identical, and the geometry continues forever. Coarse grained sites are equivalent and have the same size. It has been verified numerically that each coarse grained layer in the network gives an equivalent contribution to the entropy of a block, which means that the entropy is actually proportional to the length of a minimal curve [74]. Because of the fractal nature of the network and the equivalence of sites, the distance between points also shrinks after each coarse graining. Entanglement renormalization is crucial for this result. Without it we would have to keep many more states when coarse graining or otherwise settle for a poor approximation to the quantum state.

The discrete geometry that appears at the critical point is nothing but a discrete version of anti de Sitter space (AdS). The smooth version of two dimensional anti de Sitter space has the metric

$$ds^2 = R^2 \left(\frac{dz^2 + dx^2}{z^2} \right) = R^2 \left(dw^2 + \exp\left(-2w\right) dx^2 \right) \tag{5.3}$$

where R is some constant and $w = \log z$. The analog of $\log z$ in the lattice setup is simply the layer number or depth which counts how many coarse grainings have been performed. The second form of the metric makes explicit the change in proper length in the spatial direction as a function of depth in the tensor network. The appearance of AdS is perhaps not surprising from the point of view of holography, but it is gratifying to see it emerge from the definitions.

The entropy of a block in the ultraviolet is indeed bounded by the length of a

minimal curve in discrete AdS because this curve counts the minimal number of entangled sites over all scales that must be traced out. For example, we could also bound the entropy of the block by the sum of the entropies of the sites in the block, or in other words, by the length of a curve which doesn't dip into the bulk. The length of this curve is of order $n\,S_{site}$ where n is the number of sites in the block, but the length of the minimal curve is of order $\log n\,S_{site}$ giving a significantly better upper bound. These bounds are similar to holographic bounds in gauge/gravity duality coming from counting degrees of freedom [87]. It is also interesting to note that the minimal curve in an optimized network seems to directly control the entropy, rather than providing just an upper bound, as was confirmed in the critical case.

5.4.1 Finite temperature and correlation functions

Extending the picture above to finite temperature requires a shift in thinking due to the presence of classical correlations in addition to quantum entanglement at finite temperature. The entanglement entropy now has an extensive component due to thermal effects. However, the mutual information $I(A, B) = S(A) + S(B) - S(AB)$ between two regions A and B subtracts out this extensive piece and obeys a boundary law at finite temperature [26]. The appropriate generalization of entanglement renormalization, though it may not be as numerically tractable, is still be useful in removing local entanglement and correlations. The coarse grained Hilbert space will typically grow if we insist on keeping all eigenvalues of the reduced density matrix of a block up to some fixed cutoff.

Despite some peculiarities associated with hydrodynamics in quantum critical systems in one spatial dimension, we continue to focus on the quantum Ising model in one spatial dimension. At the quantum critical point we initially find a region of discrete AdS geometry corresponding to energy scales much greater than the temperature. However, the temperature grows as we renormalize since it represents a relevant perturbation to the quantum critical point. Thermal effects gradually become important, and the size of coarse grained sites must begin to grow to incorporate thermalized degrees of freedom.

Eventually we reach a scale where low energy modes live. Note that for the critical one dimensional Ising model, there is no hydrodynamic behavior for conserved currents, but the order parameter displays low energy "quantum relaxational" dynamics [88]. What would be the "hydrodynamic" scale is characterized by a renormalized temperature greater than the energy scale of interest but still less than the lattice scale. If the temperature continues to grow under further renormalization then it may exceed even the lattice scale, a result familiar from the real space renormalization group of the classical one dimensional Ising model.

At this final scale the reduced density matrix of any site is proportional to the identity and the coarse grained density matrix completely factorizes. I interpret this situation as corresponding to a black hole horizon for at least three reasons. First, the geometry ends from the point of view of an observer "hovering" at fixed scale. Second, the completely mixed state is like an infinite temperature state, and the local temperature measured by a hovering observer diverges at simple black hole horizons. Third, the final layer possesses finite entropy/size because the coarse grained sites are in mixed states. In particular, the entropy of a large block in the ultraviolet now consists of two pieces: the usual boundary contribution plus an extensive piece due to the horizon as shown in Figure 5.

Equal time correlation functions are also interesting when viewed geometrically. In the entanglement renormalization scheme, two operators can be correlated if the sites at which they are inserted have overlapping causal cones. The causal cone of a single site is a "thickened" line in the bulk geometry with a lattice scale width of a few sites. Consider a simple gapped system. Sites separated by less than a correlation length have overlapping causal cones, but distant sites have causal cones that end at the factorization scale before touching. Thus distant sites cannot be correlated, and this is precisely the exponential fall off in correlations characteristic of a gapped phase.

In the case of the critical geometry, the causal cones of distant sites always touch. For conformal primary operators, which have a simple scaling behavior under renormalization, the correlation functions have an additional geometrical interpretation.
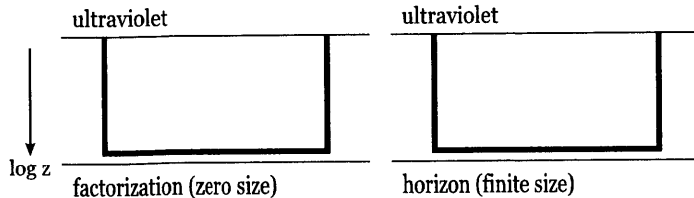
90

Figure 5-5: Sketch of minimal curves for the zero temperature gapped and finite temperature critical geometries. The curve, defined by the boundary of the causal cone of a large block, quickly falls to the factorization scale and then runs along it. In the gapped case, the length is zero at the factorization scale, and the entropy has only a boundary contribution which saturates for large blocks. However, in the finite temperature case, the horizon scale has finite size and gives an extensive contribution to the entropy of a large block in the ultraviolet.

The two point function, for example, is proportional to $\exp\left(-\Delta\,\ell\right)$ where Δ is the operator dimension and ℓ is the length of a minimal curve. This is identical to the holographic result in the conformal case. At finite temperature, the horizon is a source of decaying correlations because the causal cones of distant sites can end at the horizon before touching. This is nothing but thermal screening, with a screening length set by the temperature. In each case, the structure of correlation functions is determined by the basic geometry of the extra scale dimension.

5.4.2 Holographic duality

The appearance of higher dimensional black holes to describe thermal states of gauge theories is precisely the content of holographic gauge/gravity duality. The best known example of this correspondence is the duality between a certain supersymmetric quantum gauge theory in four dimensions, $\mathcal{N} = 4$ $SU(N)$ Yang-Mills theory, and a theory of quantum gravity, type IIB string theory, in a fluctuating spacetime that is asympotically five dimensional anti de Sitter space times a five sphere, $\mathrm{AdS}_5 \times \mathrm{S}^5$. This duality is simplest from the gravity point of view when the field theory is strongly coupled and when the number of "colors" tends to infinity, the large N limit. In this limit quantum gravity reduces to classical gravity in a weakly curved space.

The gauge theory in infinite volume is dual to anti de Sitter space in the Poincare

91

patch with metric

$$ds^2 = R^2 \left(\frac{dz^2}{z^2} + \frac{-dt^2 + dx_3^2}{z^2} \right), \qquad (5.4)$$

where again z represents something like length scale in the dual gauge theory. Finite temperature effects in the gauge theory map to black hole mechanics in AdS, and in particular, thermal screening has an interpretation in terms of geodesics falling into the horizon. In the classical gravity limit, the entanglement entropy of a region A in the field theory is given by the area in Planck units of a minimal three dimensional surface which hangs from the two dimensional boundary of A into the bulk [58, 59].

From the point of view advocated here that entanglement defines geometry, we are free to reverse this logic and define the higher dimensional geometry in terms of entanglement entropy in the field theory. This formulation exactly reproduces anti de Sitter space and makes the minimal surface prescription true by definition, but it may be more general since it applies to fairly generic local quantum systems. Further evidence for the connection between entanglement renormalization and holography comes from the holographic interpretation of the extra gravitational dimension in terms of energy scale in the gauge theory. However, this interpretation is heuristic and non-trivial because defining a real space quantum renormalization group is not straightforward. It is tempting to regard something like entanglement renormalization as an important ingredient for making precise the real space renormalization group structure in holography.

We have seen how a geometry can be defined from entanglement, but this scheme is ultimately too simple from the point of view of gauge/gravity duality. The dual gravitational theory typically contains other fields in addition to the metric which we must also in principle define from field theory quantities. Consistent with the interpretation of the extra dimension in terms of scale, we can attempt to define the higher dimensional bulk fields in terms of renormalized couplings in the dual field theory. The equations of motion for the bulk fields should be taken to be the renormalization group equations for the dual field theory [81]. These couplings are typically fixed at the ultraviolet cutoff and flow under the renormalization group, but

this running depends on which couplings are present and on the quantum state being renormalized [89]. One can check, for example, that relevant and irrelevant couplings in the Hamiltonian grow or decay as expected under entanglement renormalization [90].

Away from large N this definition is ambiguous since the bulk fields should fluctuate (the concept of a local field may even be ambiguous). The correct prescription may be that the renormalized couplings define the expectation values of fluctuating fields which are actually quantum mechanical, a kind of quantized renormalization group. Because entanglement renormalization permits us to address many kinds of states, it is natural to consider the renormalized couplings as dynamical variables. This point of view is also natural in string theory. For example, in the world sheet formulation, couplings on the string world sheet have a dual interpretation in terms of expectation values of quantum fields in the target space. The renormalization group equations expressing conformal invariance on the worldsheet are the equations of motion for the target space fields.

One further interesting feature of gauge/gravity duality at finite temperature is that the geometry is not always equivalent to a black hole. This understandable in our scheme because we are not guaranteed to reach a completely mixed state under a generic renormalization group flow at finite temperature. For example, the entanglement structure of gapped states should not change dramatically due to the presence of a small temperature. Alternatively, a conformal theory on a compact space can give at least two generic renormalization group behaviors based on whether one reaches zero spatial size or infinite temperature first. Something similar occurs in gauge/gravity duality in the form of the Hawking-Page transition for the $\mathcal{N} = 4$ theory on the space S^3 [91]. When a black hole does exist in the holographic geometry, the stretched horizon appears to be interpretable as the "hydrodynamic" scale in our construction, which is naturally distinct from the "true" (null surface) horizon.

5.5 Current status

We have described a framework for thinking about entanglement and correlation based on higher dimensional geometry. We can literally construct an emergent holographic space from the entanglement properties of a large class of many-body states including free bosons and fermions, quantum critical points, topological phases, frustrated quantum magnets, superconductors, and more. The gross features of entanglement and equal time correlation functions are encoded geometrically. This geometrical picture of entanglement is realized both in a concrete lattice setup based on entanglement renormalization and in the context of gauge/gravity duality, thus connecting these two beautiful ideas. The theory also incorporates black hole-like objects at finite temperature that seem to share many properties with more conventional black holes in semi-classical general relativity. What we have not done is give a detailed proposal for the gravity dual of, say, the Ising model, and if such a dual exists, it seems likely to be very complicated. Remarkably, much of this complexity seems irrelevant for the simple geometrical ideas explored here.

There are additional features as well as many open questions. For simplicity, we worked primarily with the quantum Ising model in one spatial dimension, but everything applies to more generic systems in higher dimensions with minor modifications. It is also possible to include time evolution within the geometrical framework. For example, one can determine the time component of the metric from the renormalization of the Hamiltonian. Other interesting geometries also exist, including situations where the effective spatial dimension changes as a function of scale or where the dynamical critical exponent flows. We are also not restricted to looking solely at ground states and thermal states, although the "geometry" of a highly entangled state may not be anything very simple. There are issues of non-uniqueness in the construction of the renormalization group and redundant descriptions should be interpretable in terms of bulk diffeomorphisms [92], but beyond identifying diffeomorphisms it must be possible to understand in what sense the geometry truly fluctuates away from large N.

We briefly comment on future directions and work in progress. Perhaps the most pressing issue for condensed matter applications is the need for a better understanding of what lies between gauge/gravity duality as inspiration and actually having the $\mathcal{N} = 4$ plasma in the lab. The general framework outlined here seems well suited to attacking this question. For example, our construction should certainly apply to quantum $O(N)$ vector models, which are known to show hints of a holographic description [93]. Perhaps one can make progress in understanding the dual gravitational theory.

The notion of a quantized renormalization group including gravity can be made more precise, particularly with regard to fluctuations in the bulk fields. A certain class of topological "string-net" phases realize exact versions of entanglement renormalization [36, 11] and provide a useful exactly solvable testing ground. More speculatively, it would be amusing to carry out this program for lattice systems defined on some nearly translation invariant fractal, perhaps realizing a holographic dual of the epsilon expansion and giving some kind of non-integer dimension version of anti de Sitter space. Finally, from the perspective of entanglement renormalization, variational principles for the higher dimensional geometry may help simplify the search for quantum circuits to describe interesting many-body states.

5.6   Summary of results: Chapter 5

In this chapter we presented a novel link between entangelement renormalization and tensor networks and holographic duality and quantum gravity. We also argued that both holography and entanglement renormalization realize in a very concrete way the renormalization group argument of Chapter 2. The material here is somewhat speculative. This is not surprising given the early stage of our search described in Chapter 1 for the basic principles and unifying themes of quantum many-body physics. Nevertheless, there is a concrete connection between entanglement renormalization and holography, a connection that has already born fruit in the form of the twist operator formalism to be developed in the next chapter. We believe this general area

is a rich source of intuition and suggestive physical pictures that should be developed further.

Chapter 6

Entanglement and Mutual Information

6.1   Overview

The connection between entanglement renormalization and holography is real but we do not yet know how far it will take us. It has inspired the more concrete investigations described below.   In this chapter we continue our attempt to formulate a general framework for the description of low energy universal entanglement properties of many-body phases. Thus we finally turn to the study of quantum field theories and investigate their entanglement properties. The mutual information will now play a crucial and we will use a novel operator technique to organize information about entanglement in quantum field theory.

6.2   Entanglement in field theory

6.2.1   Motivation

Entanglement entropy does suffer from at least one defect: it is a cutoff or high energy sensitive quantity [23]. In an unregulated quantum field theory, the entanglement entropy is formally divergent due to the presence of high energy singularities associated

with the boundary law behavior. To render the entropy finite, we must regulate the quantum field theory by providing a high energy completion such as a quantum lattice theory. In the context of quantum field theoretic studies, therefore, the focus has been on special contributions to the entanglement entropy that can be argued to be universal. Examples of such contributions include the logarithmic term in $1 + 1$ dimensional conformal field theories [27, 28] and the topological entanglement entropy in $2+1$ dimensional topological phases [94, 95]. This situation is unsatisfactory: while a great deal of intuition now exists for the behavior of the entanglement entropy, such intuition is often bound up with non-universal lattice scale physics. This is not to say that the lattice scale physics isn't of interest, only that a complete understanding of many-body entanglement should contain a clear separation between the physics of low and high energies to the extent possible.

There is a quantity, called the quantum mutual information, that shares some of the features of the entanglement entropy and remains finite in a quantum field theory. We already met this quantity in Chapter 4 in connection with our extended study of quantum information in Fermi liquids. To define the mutual information, we consider two spatial subsystems, A and B, of a larger many-body system. The mutual information is $\mathcal{I}(A, B) = S(A) + S(B) - S(AB)$, where $S(R)$ is the entanglement entropy of region R. The mutual information is positive and symmetric in A and B and, for separate regions, the subtraction insures that non-universal boundary law contributions cancel. On the other hand, if we take A and B to form the entire system (assumed to be in a pure state) then $S_{A \cup B} = 0$ and $\mathcal{I}(A, B) = 2S(A) = 2S(B)$. Note that this requires regions A and B to come together and touch, so new divergences may appear from this procedure. At the very least, the mutual information is interesting because it captures some of the physics of entanglement, because it bounds normalized correlation functions [?], and because it is well defined property of a quantum field theory. However, we also hasten to emphasize that the mutual information knows about more than just entanglement.

In field theoretic studies, the entanglement entropy is often computed using the replica trick: a partition function involving n copies of the field theory is developed

to compute the quantity $Z_R(n) = \text{tr}(\rho_R^n)$ from which the entanglement entropy of region R can be obtained. In $1 + 1$ dimensional conformal field theories this partition function may be computed with the help of interesting operators called twist operators [28, 27]. These operators turn out to be primary with conformal dimension related to the central charge of the conformal field theory. The mutual information is a finite quantity in the conformal field theory that accesses the properties of these interesting operators. In higher dimensions, the analog of twist operators are no longer point like, becoming instead line operators in $2 + 1$ dimensions and surface operators in $3 + 1$ dimensions. These line and surface operators are also twist operators of a sort, and the mutual information is a finite quantity which accesses the properties of these operators. Thus a careful study of the mutual information might reveal some information about these mysterious extended operators in higher dimensional quantum field theory.

One additional motivation for studying entanglement via the mutual information comes from the application of holographic duality to condensed matter systems [?, 77, 78, 96]. In the last chapter we made a connection between holographic duality and entanglement renormalization in condensed matter physics, but it remains unclear how general and useful this connection is. It is thus important to try to validate the new insights coming from holographic duality in the context of more ordinary quantum field theories. We want to establish as clearly as possible exactly what physical quantities are properly captured, at least in a qualitative sense, by holographic duality even in the large N and strong coupling limits. As a foundational element of all many-body quantum systems, the structure of entanglement seems an ideal place to begin such a systematic comparison. And there is growing evidence that holographic duality does indeed capture the structure of entanglement in generic quantum field theories.

6.2.2 Background

Before proceeding let us recall some background about the mutual information. The mutual information between two regions A and B is defined as $\mathcal{I}(A,B) = S(A) +$

$S(B) - S(AB)$. Subadditivity of the von Neumann entropy guarantees that the mutual information is a positive quantity, and the mutual information is manifestly symmetric in A and B. It measures in a uniform way the degree of correlation between regions A and B. If the density matrix ρ_{AB} factorizes into $\rho_A \otimes \rho_B$ then the mutual information vanishes. The converse is also true. The mutual information also gives more than just a yes/no answer to the question of correlations: it bounds the connected correlation functions of operators localized in A and B. In particular, we have $\langle \mathcal{O}_A \mathcal{O}_B \rangle_c^2 \leq ||\mathcal{O}_A||^2 ||\mathcal{O}_B||^2 \mathcal{I}(A, B)$ [26]. As an aside, we note that although the mutual information bounds connected correlations functions, it doesn't necessarily have to decay with separation, for example, the mutual information between distant regions doesn't decay at all in a "cat state" like $| \uparrow ... \uparrow \rangle + | \downarrow ... \downarrow \rangle$. Ultimately, the crucial property of the mutual information that makes it useful for our purposes is its cutoff independence. Indeed, the boundary law terms containing information about physics of the cutoff cancel in the subtraction that defines the mutual information. From another point of view, this independence from the cutoff can arise because we necessarily introduce additional length scales when considering multiple regions. We now turn to reformulating the scaling intuition for entanglement entropy described in Chapter 2 and 5 in terms of the mutual information.

We also wish to emphasize one final point. Mutual information measures both classical and quantum correlations. In principle, two regions can have no entanglement and still have finite mutual information due to purely classical correlations. We can say that if the state of AB is pure, then $\mathcal{I}(A, B)$ is simply $2S(A)$ and thus $\mathcal{I}(A, B)$ does measure entanglement. Despite this ambiguity, the short distance properties of the mutual information do reflect entanglement (essentially because these singularities mirror those in the entanglement entropy). Nevertheless, we must be cautious not to over-interpret results concerning mutual information in terms of quantum entanglement.

6.3 Universal singularities

6.3.1 1 + 1 dimensions

We begin with the case of one dimensional conformal field theory, in particular, the case of free fermions. In general, knowledge of the entanglement entropy for multiple regions, as required to compute $\mathcal{I}(A, B)$, is not trivially related to the single region result. The single region entanglement entropy in any conformal field theory in one dimension contains a universal logarithmic term depending only on the central charge. but the multi-region entanglement entropy is known to depend on the entire field content of the conformal field theory. However, for free fermions the result is actually known even for multiple intervals [97]. We will use only the result for two intervals specified by $[a_i, b_i]$ with $i = 1, 2$. The entanglement entropy is

$$S_{2 \text{ region}} = \frac{1}{3} \left(\sum_{ij} \log \left(\frac{|a_i - b_j|}{\epsilon} \right) - \log \left(\frac{|a_1 - a_2|}{\epsilon} \right) - \log \left(\frac{|b_1 - b_2|}{\epsilon} \right) \right). \quad (6.1)$$

For simplicity we consider the case of two intervals of equal size L separated by a distance x defined as the nearest distance between the two lines. The two interval entanglement entropy becomes

$$S_{2 \text{ region}} = \frac{1}{3} \left(2 \log \left(\frac{L}{\epsilon} \right) + \log \left(\frac{x}{\epsilon} \right) + \log \left(\frac{2L + x}{\epsilon} \right) - 2 \log \left(\frac{L + x}{\epsilon} \right) \right). \quad (6.2)$$

To obtain the mutual information between the two intervals, the two interval result is subtracted from the sum of the entanglement entropy of each region separately:

$$\mathcal{I}(L, x) = \frac{1}{3} \left(2 \log \left(\frac{L}{\epsilon} \right) \right) - S_{2 \text{ region}}. \quad (6.3)$$

There are many cancelations in this equation, and in particular, the cutoff dependence

completely disappears as promised. The final result is

$$\mathcal{I}(L, x) = \frac{1}{3} \log \left(\frac{(L + x)^2}{x(2L + x)} \right). \tag{6.4}$$

Something remarkable happens as as x goes to zero, that is, as the two regions approach each other: the mutual information contains a universal divergence going as $\log x$. Moreover, the coefficient of this divergence is precisely the central charge of the free fermion CFT that we wanted to interpret as the entanglement per scale in a conformal field theory. Now we recall a more general result: in any conformal field theory, the leading singularity in the mutual information as two regions approach each other is universal and given by the central charge of the conformal field theory [28]. Thus, despite the complicated nature of the mutual information in general, the singularity structure as regions collide is highly constrained. This result follows from the short distance properties of the twist operators that define the entanglement entropy in the replica version of the original CFT. These twist fields are primary with a dimension related to the central charge of the original CFT, and the leading term in their OPE is a fusion to the identity.

6.3.2 Higher dimensions

We will return to the subject of twist operators later, but for now, let us try to generalize this result to CFTs in higher dimensions. We will not try to directly compute the full mutual information in a conformal field theory in higher dimensions. Although this calculation may be possible in some cases, we are in this section only interested in certain universal divergences that appear as regions are brought together. Now, a natural question in higher dimensions, which does not arise in one dimension, is the precise nature of this collision process. There are several ways in which one can imagine performing this procedure. First, if regions A and B have a flat $d - 1$ dimensional surface, then we can bring the regions together along this surface. More generically, if the boundaries of the two regions are smooth, they will typically only touch at a single point with finite radius of curvature. A final interesting possibility

is the case of sharp corners approaching each other or another smooth interface. We will address all three situations below.

Consider first the case of a collision of flat $d-1$ dimensional surfaces. We want to know how the mutual information behaves as a function of x, the separation between the two flat sections of the boundary. The flat sections are taken to have equal $d-1$ dimensional size V_{d-1}. Based on the boundary law for entanglement entropy, and because we expect to recover part of the divergent entanglement entropy when the regions touch, the mutual information should diverge as $x \to 0$. By analogy with the boundary law, we find that

$$\mathcal{I}(x) = k \frac{V_{d-1}}{x^{d-1}} + ..., \tag{6.5}$$

where ... indicates subleading terms in $1/x$. The coefficient k in this expression should be a universal quantity that effectively counts the number of degrees of freedom in the conformal field theory (in terms of how much entanglement they contribute to the ground state). In a sense, this is the boundary law but with the non-universal cutoff ϵ replaced by a definite continuum quantity x, the separation between the $d-1$ dimensional surfaces. Indeed, if we assume that the divergence must be proportional to the size of the colliding regions then the dependence on x is fixed by dimensional analysis up to logarithmic corrections. Of course, such a logarithmic correction is realized in one dimension where we already found the result $\mathcal{I}(x) \sim \log x$, and there the constant k is proportional to the central charge.

But what happens in the more generic situation where the regions A and B collide only at a single point. The mutual information will still diverge, but with a weaker power of x. Suppose the two regions touch at a single point and that in the neighborhood of each point the boundary may be described as a parabolic surface rotationally invariant about the x axis with radius of curvature R. The mutual information should be a universal function of R/x. We will now give a scaling argument to determine this function. Consider two parabolic surfaces separated by a distance x parameterized by a radial coordinate ρ. The length of the line parallel to the x axis connecting the two surfaces at radial coordinate r is $x + \frac{\rho^2}{R}$. Let us now apply the form deduced

103

above for the scaling form of the mutual information in the case of flat regions to a small shell with inner radius r and outer radius $r + dr$. The approximate size V_{d-1} of this shell is $\rho^{d-2} d\rho$, and the distance between the shells along the x axis is $x + \frac{\rho^2}{R}$. We now integrate the mutual information obtained above from $\rho = 0$ to some cutoff value ρ_c:

$$\mathcal{I}(R, x) \sim \int_0^{\rho_c} d\rho \frac{\rho^{d-2}}{(x + \rho^2/R)^{d-1}}. \tag{6.6}$$

This formula is divergent as x goes to zero, and to determine the scaling form we simply $\rho = \sqrt{Rx}u$ to find

$$\mathcal{I} \sim \int_0^{u_c} \sqrt{Rx} du \frac{(Rx)^{d/2-1} u^{d-2}}{x^{d-1}(1 + u^2)^{d-1}}. \tag{6.7}$$

Collecting all the powers of x and R, we find that

$$\mathcal{I}(R, x) = k' \left(\frac{R}{x}\right)^{\frac{d-1}{2}} + ... \tag{6.8}$$

Thus, the mutual information still diverges but with a different power of x owing to the quadratic nature of the boundaries near the collision point.

Finally, one can consider the singular situation of a corner approaching a smooth surface. This case is similar to that of colliding quadratic surfaces except that the distance along the x axis between shells depends linearly on ρ. Carrying out the same integral as above with $x + \rho^2/R$ replaced by a linear function $x + m\rho$ (m is a function of the opening angle) gives a logarithmic divergence $\mathcal{I} = k'' \log x + ...$ in any dimension d. Not only do $d - 1$ dimensional flat surfaces replicate the boundary law, colliding corners also replicate the logarithmic term in the entanglement entropy associated with corners in any dimension.

We have argued on general grounds that the mutual information in a conformal field theory should contain certain universal divergent pieces when the regions involved collide. Depending on the geometry of the collision, one obtains different scaling forms with universal prefactors that measure the number of degrees of freedom contributing to ground state entanglement. However, it is desirable to check these
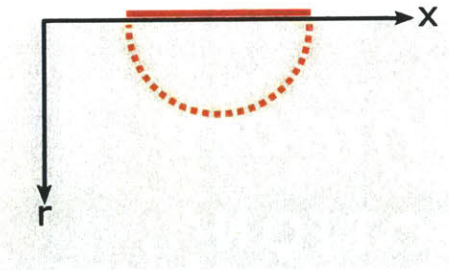
Figure 6-1: Sketch of the prescription for computing the entanglement entropy in a $1 + 1$ dimensional CFT via holographic duality. The horizontal axis is the spatial coordinate in the CFT while the $r-$axis is the bulk radial coordinate (the bulk is shown in gray). The time coordinate is suppressed. The region of interest in the field theory is shown as a thick red bar while the minimal surface of interest in the bulk is the red dotted line. The minimal surface is required to terminate at the boundary of the region in the field theory.

scaling relations in specific cases to explore the validity of the arguments just given. Thus, we now turn to class of theories for which the above conjectured scaling forms can be explicitly verified.

6.3.3   Holographic computation

The simplest setting in which these ideas can be tested is provided by holographic duality. Holographic duality relates quantum field theories in $d+1$ spacetime dimensions to theories of quantum gravity in curved higher dimensional spaces [?, 77, 78, 96]. The classic statement of the duality is between $\mathcal{N} = 4$ super Yang-Mills theory in four dimensions and type IIB string theory on asymptotically $\mathrm{AdS}_5 \times S^5$ spacetimes. The high energy limit of the field theory is in some sense located at the conformal boundary of AdS_5, and the extra radial dimension of AdS_5 is associated with energy scale in the field theory. The duality becomes particularly simple on the gravity side when we take the limit of large N and large $\lambda = g_{YM}^2 N$ in the field theory. In this limit, the string theory becomes well approximated by classical (coming from large N) supergravity (coming from large λ). Many interesting quantities in this strong coupling limit of the field theory become expressible as simple geometric objects in a higher dimensional spacetime with gravity.
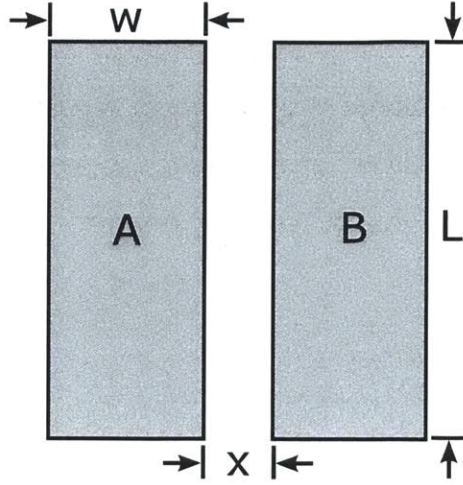
Figure 6-2: Strip geometry for the calculation of mutual information in the translation invariant case. We assume the $L \gg w \gg x$ so that the minimal surface problem reduces to a single variable problem. A singularity in the mutual information develops as x approaches zero.

In particular, the entanglement entropy in the field theory is related to minimal surfaces in the higher dimensional gravitational geometry [58, 59]. The detailed prescription is as follows. As we said, the high energy limit of the field theory lives at the conformal boundary of AdS. To compute the entanglement entropy holographically, we must study surfaces in the bulk gravitational geometry that asymptote at the conformal boundary of AdS to the boundary of the region in the field theory we are interested in. The entanglement entropy is then the area in units of the Planck length of the minimal area surface satisfying the boundary conditions. The prescription is illustrated in Fig. 1 for the case of a $1 + 1$ dimensional conformal field theory dual to an AdS$_3$ geometry. Using this prescription we can reduce the computation of the mutual information in holographic theories to a certain minimization problem in a curved higher dimensional geometry.

Let us first consider the case of colliding $d - 1$ dimensional surfaces in a $d + 1$ dimensional conformal field theory (d is the dimension of space). We will focus on the case of $d = 2$ for ease of presentation, but the results are quite general. The metric of AdS$_{3+1}$ is

$$ds^2 = \frac{L_\Lambda^2}{r^2} \left(-dt^2 + dr^2 + dx^2 + dy^2 \right), \tag{6.9}$$

106

where L_Λ is the AdS radius and r is the radial coordinate. Let the field theory regions A and B be strips of length L in the y direction with width w in the x direction. The strips are assumed to be separated by a distance x as illustrated in Fig. 2. Assuming $L \gg w$, we have translation invariance in the y direction. This greatly simplifies the minimal surface problem, allowing us to parameterize the minimal surface by $r(x)$ independent of y. Focusing first on a single strip, the area of the surface in the bulk is

$$L_\Lambda^2 L \int_{-w/2}^{w/2} dx \frac{\sqrt{1 + \left(\frac{dr}{dx}\right)^2}}{r^2}. \tag{6.10}$$

The result of the minimization procedure is an area of the form

$$L_\Lambda^2 \left(k_1 \frac{L}{\epsilon} - k_2 \frac{L}{w}\right), \tag{6.11}$$

where the constants k_1 and k_2 are calculable and ϵ is a high energy cutoff. The entanglement entropy of the single strip is simply this area multiplied by $1/(4G_N)$, that is, the area in Planck units.

As usual, the entanglement entropy is non-universal, depending on the high energy cutoff ϵ. To remove this defect we return now to the two strip geometry and compute the mutual information for the two strips. We need two quantities: the entropy of a single strip and the entropy of both strips together. We have already obtained the single strip entropy, so let us focus on the two strip problem. There are two cases that must be considered depending on the ratio of the strip width and the strip separation. These two cases correspond to two possible choices for the two strip minimal surface. The first choice corresponds to two disconnected surfaces, one for each strip, and each identical to the single strip minimal surface. This situation occurs when the strips are widely separated and gives zero mutual information. However, for the purposes of calculating universal divergences in the mutual information we are interested in the opposite limit of two very close strips. In this case, the minimal surface actually connects the two strips in the bulk. The near edges of the strips are connected by one component of the bulk minimal surface while the far edges are connected by another
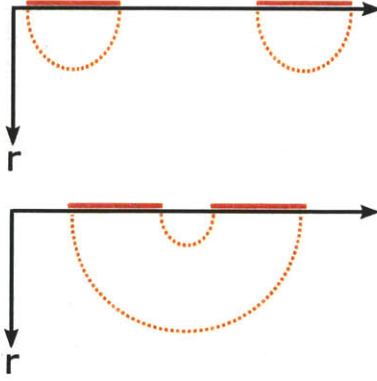
Figure 6-3: A sketch of the two bulk minimal surfaces relevant for the calculation of the mutual information. The translation invariant spatial coordinate is suppressed along with the time. In the top panel, the minimal surface for two widely separated strips is simply two copies of the minimal surface for a single strip. In the bottom panel, when the two regions come close, a new minimal surface appears which connects the inner and outer boundaries of the two regions. In this case, there is a non-zero holographic mutual information.

component. This geometry is illustrated in Fig. 3.

Repeating the analysis above for the minimal surface, we find that the entanglement entropy of the two strips taken together is

$$S_{2 \text{ strips}} = \frac{L_\Lambda^2}{4G_N} \left(\left(k_1 \frac{L}{\epsilon} - k_2 \frac{L}{2w + x} \right) + \left(k_1 \frac{L}{\epsilon} - k_2 \frac{L}{x} \right) \right). \qquad (6.12)$$

Now, the mutual information is $\mathcal{I} = 2S_{1 \text{ strip}} - S_{2 \text{ strips}}$ which gives

$$\mathcal{I}(L, w, x) = k_2 \frac{L_\Lambda^2}{4G_N} \left(\frac{L}{x} + \frac{L}{2w + x} - 2\frac{L}{w} \right). \qquad (6.13)$$

Note again that the mutual information is manifestly cutoff independent. The factor L_Λ^2/G_N is related to the total number of local degrees of freedom in the field theory, for example, it may be related to the dimension of the gauge group ($\sim N^2$ for SU(N)). As promised, the mutual information has a universal divergence as $x \to 0$, and this divergence is proportional to the size of the colliding region, here the length L, and to the total number of degrees of freedom.

We can also ask what happens when the colliding regions are not flat surfaces but

points with finite radius of curvature or corners. Of course, the minimal surfaces in this case which connect the two regions will be much more complicated, but we will argue that we do not need the full minimal surface to verify the scaling form proposed above. Consider first the case of two long strips, but now with the colliding side of each strip curved into a portion of a circle with a very large radius of curvature L as shown in Fig. 4. Now the two regions collide only at a single point, but nevertheless, the minimal surface will be approximately translation invariant in the y direction. Let us now parameterize the minimal surface as $r = r(x, y)$ but with the expectation that $\partial_y r \ll \partial_x r$ except possibly deep in the bulk, in other words, we suppose the surface varies slowly with y. The full expression for the minimal surface area is

$$L_\Lambda^2 \int dx\, dy \frac{\sqrt{1 + (\partial_x r)^2 + (\partial_y r)^2}}{r^2}, \tag{6.14}$$

and we want to be in a regime where $\partial_y r \ll \sqrt{1 + (\partial_x r)^2}$ for all x and y. In this regime, there is a separation of scales between the fast variable x and the slow variable y and we can approximately solve the fast problem treating the slow variable as fixed. This means we obtain the same sort of minimal surface as we found above for the infinite strip except that the strip width is a local quantity determine by the slow variable y. Only in the case where the strip width was independent of y were we able to perform the y integral exactly to yield L, the strip length.

Thus a segment y to $y + dy$ contributes an infinitesimal mutual information given approximately by

$$d\mathcal{I}(w(y), x(y)) = k_2 \frac{L_\Lambda^2}{4G_N} \left(\frac{dy}{x} + \frac{dy}{2w + x} - 2\frac{dy}{w} \right), \tag{6.15}$$

where $x(y)$ and $w(y)$ are the width and separation of the slightly curved strips as a function of y, the coordinate along the long length of the curved strips. In the limit of large radius of curvature L we may approximate the width as constant, $w(y) \approx w_0$, while the separation is approximated by a quadratic function, $x(y) \approx x_0 + y^2/L$, so that only the point $y = 0$ at the middle of the curved strip actually collides in the
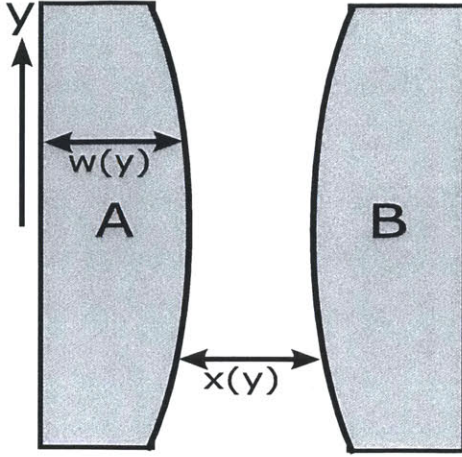
Figure 6-4: The analog of the strip geometry, but with one flat side of each strip replaced by an arc of a circle with large radius of curvature. The resulting regions are now nearly translation invariant in the y direction, but also only collide at a point as $x(y)$ approaches 0.

limit $x_0 \to 0$. Focusing now on the leading divergence in the mutual information, we find that we must determine the singularity in the integral $\int dy \frac{1}{x_0 + y^2/L}$ as x_0 goes to zero, but this is precisely the integral we considered above where we found that it diverges as $\sqrt{L/x_0}$ as x_0 goes to zero. Thus the holographic prescription for entanglement entropy reproduces the intuitive scaling we argued for above, at least in the nearly translation invariant limit. A completely analogous argument also shows that corners in the holographic case give a logarithmic singularity $\log x_0$ simply because the separation $x(y)$ is in that case a linear function of y.

All the explicit computations up to this point have been for a holographic field theory with 2 spatial dimensions. Of course, we can generalize these results to higher dimensions. The geometry is more complicated, but the results are unchanged, so we do not include the details here. Note also that we relied entirely on the spatial geometry of AdS for these computations, and this implies that the scaling we obtained for the universal divergences in the mutual information are identical in form for holographic $z \neq 1$ scale invariant theories with spatial AdS slices [98, 99]. There is also a connection between the minimal surface calculations described here and the structure of the multiscale entanglement renormalization ansatz (MERA), a class

110

of variation quantum states [10]. The minimal surfaces described here all have an interpretation on the MERA side in terms of the number of disentanglers cut by the tracing procedure, and in particular, the crossover between the short distance and long distance behavior of the mutual information is evident in terms of whether the regions entering the mutual information are renormalized to the lattice scale before or after they are merged together in the MERA.

6.3.4 Fermi liquids

So far we have considered mostly relativistic conformal field theories in any dimension, although the holographic results above also applied to non-relativistic scale invariant theories with dynamical exponent $z \neq 1$. However, once one is willing to consider non-relativistic situations, there are a number of interesting renormalization group fixed points to investigate. The simplest such fixed point (really fixed manifold) is the Fermi liquid fixed point in $d > 1$ spatial dimensions (in $d = 1$ we have the usual Luttinger liquid fixed line). This fixed point is applicable for fermions at finite density with short range interactions and is characterized by scaling towards a surface, the Fermi surface, in momentum space, rather than scaling towards a single point in momentum space [43, 42, 41]. The Fermi liquid fixed point is quite interesting for my purposes because its entanglement structure is controlled by the $1 + 1$ dimensional nature of the "radial" excitation near the Fermi surface [13, 14, 16].

Thus the result for two colliding $d - 1$ dimensional surfaces of size V_{d-1} in a Fermi liquid differs from the $d + 1$ dimensional conformal case. In fact, it resembles the $1 + 1$ dimensional conformal result because the Fermi surface can be thought of as a collection of $1 + 1$ dimensional conformal field theories, namely the local radial fermionic excitations which propogate with Fermi velocity normal to the Fermi surface. The result for the mutual information, using the prescription given in [16], is

$$I \sim k_F^{d-1} V_{d-1} \log x + ... \tag{6.16}$$

Note that this result must be interpreted somewhat carefully because of the presence

of the extra scale k_F. Indeed, if $x \ll k_F^{-1}$ then the mutual information will begin to probe the higher energy theory from which the Fermi liquid descends, perhaps a lattice theory or some relativistic conformal field theory perturbed by a finite chemical potential. Thus there is a scaling regime where x is small but not so small that $k_F x \sim 1$, and in this scaling regime the dominant term in the mutual information does behave like $\log x$. Note that if there are other gapped bosonic modes in the Fermi liquid then the mutual information will also contain contributions from these modes, and such a mode contributes a divergence of the type described above for ordinary scale invariant theories once the separation x becomes less than the correlation length ξ (or inverse mass, in the relativstic language) of the bosonic mode.

Of course, this is a relatively weak singularity. In fact, the entanglement structure is such that the mutual information only diverges if flat $d - 1$ dimensional segments collide. The case of a point with finite radius of curvature colliding produces only a non-divergent cusp-like behavior in the mutual information. This result follows from the prescription for the mutual information given in [16] upon taking into account the geometry of the colliding regions. We expect similar behavior for the mutual information in a critical Fermi surface [45], although there is a complication mentioned above of additional massless degrees of freedom, perhaps a gauge field, a particular angular momentum channel density fluctuation, or a $z = \infty$ low energy CFT [71, 72, 46].

6.4 Higher dimensional twist operators

6.4.1 Definition of twist operators

We have now described the basic scaling intuition for the mutual information and confirmed this intuition in the framework of holographic duality. Additionally, we have described how the story changes for other kinds of non-relativistic fixed points such as Fermi liquids. We are now ready to discuss the concept of higher dimensional operators, but first a review the situation in one dimension in appropriate. Twist

operators are often invoked in the calculation of entanglement entropy in one dimensional conformal field theory where the entanglement entropy is written as a path integral on a multi-sheeted Riemann surface via the replica trick:

$$S_R = \lim_{n \to 1} -\partial_n \text{tr}(\rho_R^n). \tag{6.17}$$

Let us first consider the case of a single interval. The path integral of the original $1+1$ dimensional conformal field theory on this multi-sheeted surface is traded for a path integral in a new conformal field theory, the symmetric product of n copies of the original conformal field theory. The relevant path integral in this symmetric product CFT is not quite the free path integral, however, as certain point-like fields called twist operators must be inserted at the two boundary points of the interval for which we are interested in the entanglement entropy [28]. These twist fields account for the conical singularity that was present in the original multi-sheeted surface formulation.

For a field Ψ in the original CFT, let Ψ_α denote the n copies of Ψ in the symmetric product theory. The role of the twist operators is to produce a shift $\Psi_\alpha \to \Psi_{\alpha \pm 1}$ as a field Ψ_α encircles the twist operator in spacetime. This shifting operation is the analog in the original multi-sheeted formulation of moving from one sheet Ψ_α to the next $\Psi_{\alpha+1}$. One may compute the entanglement entropy in the original conformal field theory in terms of correlation functions of these twist operators. Thus it is valuable to know the properties of these operators for the purposes of computing entanglement entropy, and vice versa, a knowledge of the entanglement entropy for general regions provides a handle on the properties of these operators.

Having argued that the quantum mutual information contains certain universal singularities, we would like to know how to translate this into the language of higher dimensional twist operators. The twist operators in $1+1$ dimensional conformal field theory are actually primary operators with dimension related to the central charge of the CFT and the number of replica fields n. What is the analog of this statement in higher dimensions? Before we investigate the properties of higher dimensional twist operators, we must attempt to give a clearer definition of these operators. As in the
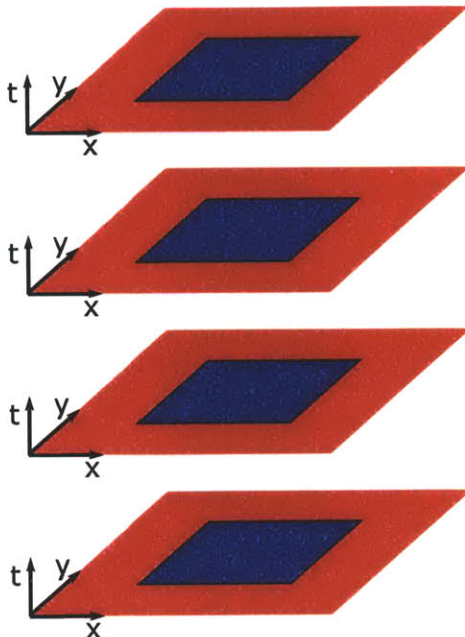
Figure 6-5: An example of the replica method with $n = 4$ copies. The region whose entanglement entropy we are calculating is in blue while the rest of the system is in red. The t axis is imaginary time. The copies are glued together so that one passes from copy α to copy $\alpha + 1$ when passing through $t = 0$ from below in a blue region, while in the red regions no such transition occurs. The blue region at $t = 0$ is thus a "branch surface" that terminates on a spacetime codimension 2 conical singularity given by the boundary between red and blue at $t = 0$. The twist operator lies along this 1 dimensional locus in spacetime.

$1 + 1$ dimensional case, the entanglement entropy is related to a path integral over a multi-sheeted higher dimensional spacetime as illustrated in Fig. 5. The spacetime looks locally unexceptional except at the boundary of the region for which one is computing the entropy, and on this boundary, there is a conical singularity in the spacetime associated with the joining of the n copies of the path integral. Like in the $1 + 1$ dimensional case, where the boundary of a set of intervals was a set of points having codimension 2 in spacetime, in higher dimensions the boundary also has codimension 2 in spacetime.

To formalize these notions, consider a region $\mathcal{R}$ with boundary $\partial \mathcal{R}$ in d spatial dimensions. We will focus on the case of a relativistic conformal field theory, but my considerations are generalizable, for example, to Fermi liquids. Following the usual replica trick methods, the entanglement entropy of this region is related to a multi-

114

sheeted path integral with a conical singularity along the boundary $\partial \mathcal{R}$. Alternatively, we may define an operator $K_n[\mathcal{R}]$ in the n-fold symmetric product theory by the equation $\langle K_n[\mathcal{R}]\rangle_n = \text{tr}(\rho_{\mathcal{R}}^n)$. It follows from the definition that in the limit $n \to 1$ and in the absence of other operator insertions, the operator K_n becomes trivial since $\text{tr}(\rho_{\mathcal{R}}) = 1$. We also assume that this operator is localized along the boundary $\partial \mathcal{R}$ of the region $\mathcal{R}$ at a fixed imaginary time.

6.4.2   Twist field ansatz

We want to make a guess as to the form this operator by analogy with the one dimensional conformal case. The key realization is that the twist field in $1 + 1$ dimensional CFT shares many properties with the exponential of a massless field, in other words, it behaves much like a vertex operator in a free boson CFT. Thus, let us assume that the twist field in higher dimensions can also be thought of as an exponential of a massless field of some type. Let us make the following ansatz for the form of the twist field:

$$K_n[\mathcal{R}] = \exp\left(i\alpha_n \int_{\partial \mathcal{R}} \phi^{(d-1)} \right), \tag{6.18}$$

where $\phi^{(d-1)}$ is taken to be a massless spatial $(d-1)$-form field of scaling dimension $d - 1$. Alternatively, one may trade this $(d-1)$-form for a spatial vector using the fixed background metric

$$K_n[\mathcal{R}] = \exp\left(i\alpha_n \int_{\partial \mathcal{R}} \hat{n} \cdot \vec{\phi} \right), \tag{6.19}$$

where $\hat{n}$ is the unit normal to the boundary $\partial \mathcal{R}$. A knowledge of the correlators of ϕ in a given conformal field theory would be sufficient to compute the entanglement entropy for any region.

Our ansatz for the twist fields can already reproduce all the scaling features discussed above under the particular assumption that ϕ has gaussian correlations. In fact, this assumption is equivalent to an assumption of "extensivity" of the mutual

information [100], and our results here provide another point of view on the nice ideas in [100]. Of course, this assumption cannot be correct in most cases, but it does capture the short distance singularity structure nicely. This is not so unreasonable, since the short distance structure in $1 + 1$ dimensions also depended on the two point function. What follows is a sketch of the structure of these twist operators, but it is certainly not the complete story and much remains to be understood. For example, possible complications due to phase transitions in the replicated theory as a function of n are not captured in the sketch below [101].

To begin, observe that the field ϕ^i ($i = 1$ to d is a spatial vector index) has a shift symmetry $\phi^i \rightarrow \phi^i + a^i$ for any constant vector a^i. The twist operators K_n are invariant under this symmetry because the boundary $\partial\mathcal{R}$ is closed so that $\int \hat{n} \cdot \vec{a} = 0$. This shift symmmetry is a specific example of a more general symmetry, namely the ability to shift ϕ^i by any vector field with zero divergence. In the form language, this is the statement that the form field $\phi^{(d-1)}$ has a "gauge symmetry" $\phi^{(d-1)} \rightarrow \phi^{(d-1)} + df^{(d-2)}$ with $f^{(d-2)}$ an arbitrary smooth spatial $d - 2$ form. There is clearly a strong analogy between these twist operators and the Wilson and 't Hooft lines of gauge theories, or more generally, between the twist operators and surface operators in p form gauge theories.

As Gaussian massless fields of dimension $d - 1$, the correlation functions of the ϕ^i are determined by the basic two point function

$$\langle \phi^i(x)\phi^j(0) \rangle = \frac{\delta^{ij} + \dots}{|x|^{2(d-1)}}, \tag{6.20}$$

where ... denotes additional terms like $\hat{x}^i \hat{x}^j$ which are not essential for our purposes. As a warmup, let me compute the entanglement entropy of a circular region in $d = 2$ spatial dimensions using the twist field. One must evaluate $\langle K_n \rangle$, but the assumption of Gaussian correlations for ϕ gives

$$\langle K_n \rangle = \exp\left(-\frac{\alpha_n^2}{2} \int_{\partial\mathcal{R}} \int_{\partial\mathcal{R}} \hat{n}^i \hat{n}^j \langle \phi_i \phi_j \rangle \right). \tag{6.21}$$

What is the meaning of this double integral over the circular boundary in $d = 2$?

First, it is certainly divergent and depends on the cutoff, but this is exactly what we expect for the bare entanglement entropy. Second, we must assume that while the limit of α_n as n goes to 1 is zero, the combination α_n^2 has a finite first derivative at $n = 1$. This is reasonable in light of one dimensional conformal field theory. In that case, α_n is roughly the square root of the dimension Δ_n of the twist field, and Δ_n does indeed have a non-zero derivative at $n = 1$.

From $\langle K_n \rangle$ one can compute the entanglement entropy via $S = -\partial_n \text{tr}(\rho^n)|_{n=1} = -\partial_n \langle K_n \rangle|_{n=1}$. We find

$$S = \frac{\partial_n(\alpha_n^2)|_{n=1}}{2} \int_{\partial \mathcal{R}} \int_{\partial \mathcal{R}} \hat{n}^i \hat{n}^j \langle \phi_i \phi_j \rangle. \tag{6.22}$$

To evaluate the divergent double integral over $\partial \mathcal{R}$ we use the fact that no special point is selected on the circle. Take the normal $\hat{n}_1$ of the first copy of the circle to point vertically and call θ the angle between the vertical and second normal $\hat{n}_2$. This gives the distance $|x| = 2R \sin \theta/2$ where R is the radius of the circle. The double integral may then be written

$$(2\pi R)2 \int_{\epsilon/R}^{\pi} R d\theta \frac{\cos \theta}{(2R \sin \theta/2)^2}, \tag{6.23}$$

where ϵ is the spatial cutoff (so that ϵ/R is the smallest angle available) and where we have kept only the δ^{ij} piece of the $\phi\phi$ correlator. This integral is divergent as $\epsilon \to 0$ as the entanglement entropy should be and for finite ϵ behaves like

$$S = c_1 \frac{R}{\epsilon} + c_2 + ... \tag{6.24}$$

with ... containing only positive powers of ϵ. Note that there is no logarithmic term.

Let us repeat the same calculation for a spherical region of radius R in $d = 3$ dimensions. Let us drop all unnecessary constant factors. The integral has a very similar structure with θ now a polar angle

$$S \sim R^2 \int_{\epsilon/R}^{\pi} R^2 d\theta \sin \theta \frac{\cos \theta}{(2R \sin \theta/2)^4}. \tag{6.25}$$

117

We still recover the divergent boundary law term going like R^2/ϵ^2, but now there is a pleasant surprise, namely the presence of a logarithmic term $\log R/\epsilon$. Precisely such a universal logarithmic correction has been found in conformal field theories in odd spatial dimensions. One can verify that our ansatz for the twist fields reproduces the pattern of logarithmic corrections for smooth regions in odd spatial dimensions [102, 103, 104]. Since the coefficient of this term is related to the derivative of α_n^2, we expect that this derivative at $n = 1$ is a universal quantity counting the number of degrees of freedom in the theory. Of course, in a more general formulation we would expect n dependence not just from α_n but also from the nontrivial higher point correlation functions of ϕ.

Along the same lines, one can check that the ansatz above predicts that regions with sharp corners in any dimension have universal logarithmic corrections in their entanglement entropy related to the deficit angle at the corner. The integral for a semi-infinite V shaped region of opening angle $\pi - \theta$ can be done exactly. If we keep only the δ^{ij} term in the correlation function (the other term doesn't change the qualitative structure), then the coefficient of the logarithmic term is given by

$$\left(1 - \frac{\theta \cos \theta}{\sin \theta} \right), \tag{6.26}$$

with $-\pi < \theta < \pi$ and where the overall coefficient is undetermined (it is related to $\partial_n \alpha_n^2|_{n=1}$). This result has a quadratic zero at $\theta = 0$ and a linear divergence at $\theta = \pi$ in agreement with previous results in a variety of systems [105]. In fact, this formula even does well in a semi-quantitative comparison with previous results provided the normalization is fixed appropriately. To understand the quadratic zero, consider the situation where the region A under study and its complement form a pure state. Then $S_A = S_{\bar{A}}$, but if A has a sharp corner with angle θ then $\bar{A}$ has a sharp corner with angle $-\theta$, and hence the coefficient of the logarithmic term must be even in θ in this case.

6.4.3 Mutual information from twist fields

Still, everything thus far is in some sense a warmup, especially since the entanglement entropy contains non-universal cutoff dependence. To study the mutual information in this twist operator formalism additional regions must be introduced. The mutual information between two regions $\mathcal{R}_1$ and $\mathcal{R}_2$ is related to the twist fields $K_n[\mathcal{R}_1]$ and $K_n[\mathcal{R}_2]$ via

$$\mathcal{I} = -\partial_n \left(\langle K_n[\mathcal{R}_1] \rangle \langle K_n[\mathcal{R}_2] \rangle - \langle K_n[\mathcal{R}_1] K_n[\mathcal{R}_2] \rangle \right)_{n=1}. \qquad (6.27)$$

In other words, one needs the n derivative of the connected correlation function between $K_n[\mathcal{R}_1]$ and $K_n[\mathcal{R}_2]$.

The connected correlation function ensures that after the n derivative the "self entanglement" terms $\partial \mathcal{R}_1 \partial \mathcal{R}_1$ and $\partial \mathcal{R}_2 \partial \mathcal{R}_2$ cancel. One is left only with an integral over $\partial \mathcal{R}_1 \partial \mathcal{R}_2$ that is not divergent so long as the two regions do not touch. Of course, we were originally interested in the singularities that develop in the mutual information precisely when the regions are brought close together. Let me first consider the standard case of two colliding flat strips in $d = 2$ dimensions. Following the calculations above, the mutual information takes the schematic form

$$\mathcal{I} \sim \int_{-L/2}^{L/2} dy_1 \int_{-L/2}^{L/2} dy_2 \frac{1}{(y_1 - y_2)^2 + x^2}, \qquad (6.28)$$

where as before the y coordinates run along the length of the strips and x is the separation between the strips with $L \gg x$. Note that in this case the product of the surface normals is independent of y_1 and y_2. The integral is done by switching to center of mass and relative coordinates with the now familiar result $\mathcal{I} \sim L/x$.

The cases of points with finite radius of curvature and corners can be treated in a similar manner, and we obtain the scaling forms described in detail above. Thus our ansatz for the twist fields reproduces the singularity structure of the mutual information in any dimension and in any of the collision scenarios considered above. It also naturally accounts for the divergent structure of the bare entanglement entropy including the presence of various kinds of universal logarithmic terms. Although we

have focused on the entanglement entropy and the mutual information, the ansatz above predicts very similar behavior for the more general Renyi entropy and Renyi mutual information. It is also possible, by introducing a length scale into the $\phi^i \phi^j$ correlator, to see the cross over structure of the entanglement entropy and mutual information in a theory with a finite correlation length. Of course, we have not derived this prescription from any particular conformal field theory, but this is a very tempting target for future calculation, especially in free conformal field theories such as the Lifshitz theory or free Dirac fermions.

We should note one unsatisfactory feature of the discussion above. The mutual information should bound the square of the connected correlation functions between any two local operators. Considering the limit where the regions $\mathcal{R}_1$ and $\mathcal{R}_1$ are far apart, the assumption of gaussian correlations gives a decay for the mutual information going like $1/x^{2d}$. For free Dirac fermions, for example, this does indeed exactly bound the square of the free fermion correlation function. However, for massless bosons, the square of the equal time correlation function decays as $1/x^{2(d-1)}$ and the bound appears to fail in our setup. This is not totally unexpected. In $1+1$ dimensions the boson correlation function actually grows logarithmically, a behavior clearly not in line with the decay of the mutual information.

One way out of this issue for lattice bosons is the observation that the operator norm of the lattice boson field $q_i \sim (a_i + a_i^+)$ actually diverges, or in other words, q_i is an unbounded operator. If the operator norm is infinite then the bound provided by the mutual information is vacuous. On the other hand, there do exist systems, for example certain magnetically ordered spin systems, where the relevant operators have bounded norm and the correlation function still decays like a free boson. What this appears to be telling us is that the long distance properties of the twist operators are considerably more variable than is captured in our assumption of Gaussian correlations. In particular, while the second cumulant may suffice for capturing short distance singularities, one must consider higher order cumulants when evaluating $\langle K_n \rangle$ in order to correctly capture the long distance behavior. Consider a simple example. The mutual information of free fermions in one dimension decays as $1/x^2$ precisely in

line with the fermion-fermion correlation function. However, this system is equivalent to an XX ferromagnetic spin chain via a Jordan-Wigner transformation. In the spin formalism we find that the spin-spin correlation function decays as $x^{-1/2}$. This decay does not violate the bound from mutual information in the fermion language since the spin operator is non-local in the fermion language.

6.4.4 A simple example: Dirac fermions

There remains the possibility that the story we have sketched above may be close to exact for a particular system, and a good candidate for that system seems to be Dirac fermions in any dimension. We can argue as follows. Consider a set of n replica fields ψ_n each corresponding to a free Dirac fermion. We work in $3+1$ dimensions for concreteness. These fields carry a representation of the symmetric group S_n and hence a representation of the Z_n subgroup generated by the twist $\mathcal{T}^\pm : \psi_n \to \psi_{n\pm1}$. One can make a unitary transformation to a new set of fields ψ_q that are eigenstates of $\mathcal{T}^\pm$ with eigenvalue λ_q. These fields will pick up a phase shift as they encircle the twist operators K_n in spacetime (remember, this makes sense because the twist fields live in a codimension 2 locus in spacetime) in a fashion reminiscent of the Aharonov-Bohm effect. Indeed, since λ_q satisfies $|\lambda_q| = 1$, one can introduce gauge fields A_q that couple to the ψ_q to implement the phase λ_q. These gauge fields are pure gauge everywhere except along the locus of definition of the twist operator. In $3+1$ dimensions, this locus is a closed two dimensional spatial surface that is a spatial analogue of the more familiar spacetime worldsheet of a flux tube or solenoid loop in $3+1$ dimensions. A similar approach has been used for Dirac fermions in $1+1$ dimensions [97].

Because the Z_n subgroup acts on the ψ_q just like the global $U(1)$ charge symmetry, we can use the $U(1)$ current to couple to the gauge fields A_q. Indeed, the Lagrangian in the terms of ψ_q is identical in form to the Lagrangian in terms of the ψ_n since the theory is free and the transformation from ψ_n to ψ_q is unitary. The twist operators

thus take the schematic form

$$K_n[\mathcal{R}] \sim \exp\left(i \sum_q \int A_q \cdot J_q\right),\tag{6.29}$$

where the A_q depend on $\partial\mathcal{R}$ and encode the flux needed to produce a phase shift of λ_q. Now introduce a new field by writing $J^\mu = \epsilon^{\mu\nu\lambda\sigma}\partial_\nu\phi_{\lambda\sigma}$ for each current J_q. Integrating by parts produces an integral of a 2-form field $\phi_{\mu\nu}$ over the surface $\partial\mathcal{R}$ exactly as above. Since the surface is purely spatial, the spacetime 2-form descends to a spatial 2-form and can be converted to a spatial vector using the spatial 3-metric. This is the setup described above. For example, the scaling dimension of J is 3 and thus the dimension of $\phi_{\mu\nu}$ is 2. Also, $\phi_{\mu\nu}$ by definition has the gauge freedom mentioned above. However, unlike in $1+1$ dimensions, the field $\phi_{\mu\nu}$ is not Gaussian, so the story is not as simple. There are also additional subtleties associated with fermion minus signs. We leave to future work more detailed calculations in this case.

6.4.5 Advantages of the twist field formalism

We have introduced the idea of twist fields as non-local operators used to compute the entanglement entropy in quantum field theory. Non-trivial information is available about these fields in $1+1$ dimensions because they can be identified as conformal primaries. Much less is known in higher dimensions, although we should point out that it is possible to study the operator produce expansion of local fields with the twist operators. One route to attacking this problem is provided by the identification, in higher dimensional conformal field theories, of the reduced density operator of a disk with the exponential of a certain special operator known as a modular Hamiltonian [25]. In the recent language of condensed matter physics, one has an exact expression for the "entanglement hamiltonian" K_A defined via $\rho_A = \exp\left(-K_A\right)$. In the above, we have made use of a mixture of general properties and the special approximation of gaussian correlations. As we have repeatedly stated, gaussian correlations are not sufficiently general. However, we argue that the twist field formalism, even in the gaussian approximation, already captures a great deal of useful information about

many-body entanglement.

The twist field formalism

- encodes the boundary law (and its violations) for entanglement entropy,

- guarantees the finiteness of the mutual information,

- gives a model of the special contributions of corners,

- makes sense of the pattern of logarithmic corrections to the entanglement entropy,

- can be easily generalized (by summing images around the imaginary time circle) to finite temperature,

- and in general seems to encode most of the generic behavior of entanglement entropy in quantum field theories.

For all these reasons, and because of the ease of calculation in the gaussian approximation, we believe the twist field formalism is a very powerful perspective on many-body entanglement. It will be very interesting to go beyond the gaussian approximation and explore the complete richness of many-body entanglement using this formalism.

6.5   Possibility of a generalized c-theorem

Having investigated in some detail the singularity structure of the mutual information in various settings, let us now turn to a concrete potential application of the results described above. There is the interesting possibility of identifying quantities in quantum field theory that are monotonic under a renormalization group flow. Of course, such quantities need not exist in general. However, the c-theorem of $1 + 1$ dimensional conformal field theory states that there is such a quantity in $1 + 1$ dimensions. The quantity is the central charge of the conformal field theory, which can be defined via the two point function of the stress-energy tensor. This quantity is guaranteed to be monotone under RG flow in any unitary conformal field theory in

$1 + 1$ dimensions. Remarkably, it is precisely this quantity which controls the size of the universal logarithmic divergence in the mutual information in $1 + 1$ dimensions. Thus we may phrase the $1 + 1$ c-theorem in the following way: for any two CFTs $\mathcal{C}_1$ and $\mathcal{C}_2$ such that $\mathcal{C}_1$ flows to $\mathcal{C}_2$ under some relevant deformation, the "entanglement per scale" k as encoded in the short distance divergence of the mutual information, satisfies $k_2 \leq k_1$. But now this opens the possibility that this result could be true for CFTs in any dimension.

There is some evidence for this claim beyond the $1 + 1$ dimensional setting. For example, it is known that holographic theories with a bulk consisting of Einstein gravity coupled to matter satisfying the null energy condition possess an analogous monotone quantity [106, 107, 108]. Moreover, this quantity is also interpretable as the number of degrees of freedom in the dual field theory, and it is, up to irrelevant numerical factors, precisely what appears in front of various universal divergences in the mutual information. Of course, this is not the first quantity that has been proposed to satisfy a higher dimensional c-theorem. Previous work has focused on the anomaly coefficients a and c in $3 + 1$ dimensions which control the trace of the stress-energy tensor in curved backgrounds. In the holographic setup, these quantities are known to be all related to my proposal in terms of mutual information, at least in $1 + 1$ and $3 + 1$ dimensions. One advantage of the mutual information based proposal is that it applies also in even spatial dimensions for which the usual anomalies are absent.

More generally there are counter-examples showing that c in $3+1$ dimensions is not monotone under RG flow, but the a anomaly coefficient is still a viable candidate. Indeed, precisely this coefficient has recently been shown to satisfy a holographic c-theorem in a more general class of holographic theories [109]. It is also related to a certain universal term in the entanglement entropy and hence to the mutual information. One can try to establish this relationship more directly by considering the operator product expansion of the stress tensor with the twist field we defined above. However, we must also be careful since it known that some random systems in one dimension do not satisfy the c-theorem, so it appears that a strictly quantum

information theoretic proof of the monotonicity of mutual information may not be possible.

There is an even more immediate objection to this proposal, namely the possibility of flowing outside the class of relativistic CFTs. For example, by perturbing the $3 + 1$ dimensional Dirac fermion CFT with a finite chemical potential, one flows to a new non-relativistic fixed point in the Fermi liquid class. Both such theories do have universal divergences in mutual information, but now even the most basic form of the scaling relation is different. It is true that the low energy theory has, in a sense, a much weaker singularity than the high energy theory. Perhaps this is the form of the mutual information c-theorem in this case, but we do not yet know if this can be made completely unambiguous. An interesting holographic version of this flow comes perturbing a holographic CFT_{3+1} by a finite chemical potential for some conserved U(1). This is described on the gravity side as an extremal black hole in AdS_{4+1} with a near horizon AdS_{1+1} region dual to a low energy $0 + 1$ dimensional conformal field theory. The low energy $0 + 1$ dimensional CFT has finite entropy due to a local ground state degeneracy but no entanglement as measured by the holographic mutual information. Thus the scaling form of the mutual information is also changed and again to a weaker sort of singularity (none at all).

Thus we conclude that in general the story is complicated, nevertheless, we suspect that quantum information ideas will be useful in finally elucidating the nature of higher dimensional c-theorems. As motivation, we prove a monotonicity theorem for the coefficient of the mutual information in $1 + 1$ dimensional theories possessing translation invariance and scale invariance (but not necessarily full conformal invariance). Another proof using different techniques and focusing on the entanglement entropy directly has been given in $1 + 1$ dimensions [110]. Our main advantage is fewer assumptions (we do not need full conformal invariance). Consider a CFT on a circle of circumference L. Let us study the mutual information $\mathcal{I}(x)$ between the regions $[x/2, L/2 - x/2]$ and $[L/2 + x/2, L - x/2]$ as a function of x. For $x \ll L$, the mutual information behaves as $\mathcal{I}(x) = \frac{2c}{3} \ln\left(\frac{L}{x}\right) + ...$ ($2c$ because of the two collisions) as we established above. Now suppose the same CFT is perturbed by a relevant oper-

ator so that it flows to another CFT in the infrared. Let the central charges of these two theories be c_{uv} (ultraviolet) and c_{ir} (infrared). The relevant operator determines a scale ξ so that the physics at length scales much less than ξ is controlled by the UV CFT and the physics at length scales much greater than ξ is controlled by the IR CFT. For the UV theory perturbed by the relevant operator, the mutual information is $\mathcal{I}(x) \sim \frac{2c_{uv}}{3} \ln\left(\frac{L}{x}\right)$ for $x \gg \xi$ and $\mathcal{I}(x) \sim \frac{2c_{ir}}{3} \ln\left(\frac{L}{x}\right)$ for $x \ll \xi$. Fix a number $M > 1$ so that $x = M\xi$ is deep inside the IR CFT and $x = 1/M\xi$ is deep inside the UV CFT. We do not detemine M explicitly except to say that it independent of system size. Now we are ready for the proof.

The mutual information is a monotone decreasing function of x because of the quantum data processing inequality. Thus we must have $\Delta\mathcal{I} = \mathcal{I}(1/M\xi) - \mathcal{I}(M\xi) \geq 0$. Using the results stated above we find $\Delta\mathcal{I} = (c_{uv} - c_{ir}) \ln\left(\frac{L}{\xi}\right) + (c_{uv} + c_{ir}) \ln M + \mathcal{O}(1)$. Since M and ξ are independent of system size, we can simply take $L \to \infty$ to conclude that $c_{uv} - c_{ir} \geq 0$. Although we used the properties of conformal field theory to write down the mutual information, the form we used actually follows from fewer assumptions. Using the scaling argument of Chapter 2, all we need is translation invariance, scale invariance, and a few technical assumptions. More generally, we can ask how this argument fails for random systems where it is known that the effective central as measured by the entanglement entropy can actually increase. An analogous argument in higher dimensions shows that the coefficient of the mutual information between two nearly touching hemispheres of a sphere cannot increase too much under RG flow. Extending these ideas to actually prove a c-theorem in higher dimensions is an ongoing work.

6.6 Summary of results: Chapter 6

In this chapter we have investigated the low energy structure of entanglement in quantum field theories. Viewed as effective field theories, these systems describe the low energy continuum limit of lattice models of many-body physics. Our goal in this chapter was to understand the universal aspects of entanglement in quantum

field theory. We argued that the mutual information in a quantum field theory is a cutoff independent quantity that probes the physics of entanglement and classical correlation in a unified way. We have computed the mutual information in a wide variety of models [16, 17] and seen how interesting physical quantities like the geometry of the Fermi surface geometry or trace anomalies are encoded in this quantity. We also developed the twist field approach to computing entanglement entropy in quantum field theory [17]. This approach offers a physical picture to underlie a wide variety of entanglement phenomena, including the contributions of corners, the area law, the presence or absence of subleading logarithmic terms, the crossover to finite temperature, and much more.

Chapter 7

The Big Picture

7.1 What have we learned?

In this thesis we developed many novel results pertaining to the physics of entanglement in local quantum systems. Although we freely blended background material with our own results for the sake of the narrative, much of the material presented here is original. In addition to the unique renormalization based perspective we have taken on the traditional aspects of many-body entanglement, our core results include:

- a tensor network description of non-chiral topological phases,

- a preliminary method to extract topological properties from tensor network states,

- an intuitive picture of entanglement in Fermi liquids for which no analytic calculation exists,

- a physical justification of the (mathematically unproven) Widom conjecture,

- a complete characterization of the leading contribution to mutual information in Fermi liquids,

- a proposal connecting "holographic" tensor network states to holographic models of quantum gravity,

- and an elucidation of the universal physics contained in the mutual information in quantum field theories.

We have seen how the area law for entanglement entropy naturally leads to variational states that can capture topological phases of matter, and we have explored the limits of the boundary law as we searched for highly entangled phases of matter. We have made a novel connection between holographic duality in string theory and entanglement and renormalization in field theory leading to the idea that entanglement is the fabric of spacetime. Finally, we have understood how to extract more detailed cutoff independent information about entanglement in many-body systems using the tool of mutual information. Taken together, we have provided a comprehensive picture of many-body including several exciting new points of view, like the idea of entanglement as geometry. This broad and intuitive framework should serve as a useful starting point for further investigations into many-body entanglement.

7.2 Connections

We have explored many-body entanglement primarily through the lens and language of theoretical condensed matter physics, but we have also emphasized the many connections to other areas of physics. The most important connection we might make is to experiments in solid state and cold atoms systems. However, the potential connections to ideas coming from quantum information science and string theory is also very interesting. We comment on all three of these points below.

7.2.1 Experiments

As we said at the beginning, there are very few direct experimental probes of many-body entanglement. We can relatively easily tell if entanglement is present, but quantifying and manipulating many-body entanglement experimentally is well beyond our current abilities. However, even if we cannot directly manipulate entanglement, the broad hope permeating this thesis is the idea that we can significantly enhance

our theoretical capabilities by thinking about entanglement. In our most optimistic moments we might dream of a powerful quantum simulator running on a classical computer that can answer otherwise intractable questions, for example, the ground state of the fermionic Hubbard model. We might even dream about classical simulation of quantum dynamics. While we are confident that a completely general classical simulator of quantum systems will not be found, we have very little understanding of where the boundary is. We can hope that many condensed matter systems of interest would be accessible. Of course, we will one day have the ultimate quantum simulator in the form of a quantum computer, and we will clearly have to understand the physics of entanglement to make sense of such a device.

So returning at last to experiments, what could we do with such a tool? We could imagine taking the parameters of a given Hamiltonian from measurements at high temperature and then predicting from scratch the ground state properties of the system. This ambitious goal is currently generally possible only for very weakly correlated materials and perhaps in one dimension. Thus while the content of this thesis has very little to do with immediate experimental realities, we do believe it is one small step towards realizing the dream outlined above.

More immediately, there is much to be done to try and make more direct contact between experimental probes and entanglement. Entanglement is a non-local thing, so to probe it we must learn to understand non-local probes of many-body systems. The earliest examples of such probes include large scale charge fluctuations [19] and behavior after quantum quenches [22], but there is much more to explore. For example, suppose we took a many-body system of cold atoms in an optical lattice and simply by hand suddenly removed half the degrees of freedom. Does anything in the subsequent non-equilibrium dynamics know about the entanglement entropy?

7.2.2 Holographic duality

It is very exciting from a theoretical point of view to imagine that ideas from string theory may have a use in condensed matter physics, or more broadly, in quantum many-body physics. Indeed, string theory is a kind of many-body physics, so perhaps

such a connection is not so surprising. However, the specific prospect that holographic duality has something profound to teach us about many-body physics in general is most exciting. Of course, this is by no means given. The connection between holographic systems and real world systems appears closest so far in the context of the quark-gluon plasma. Here perhaps the difference between supersymmetric Yang-Mills theory and QCD is not so great, but the relation to electronic or atomic condensed matter systems remains quite elusive. We speculate that the ultimate use of holographic duality in condensed matter physics will derive from its ability to suggest new physical pictures in general, rather than any particular calculation of properties in some mock theory. Certainly holographic duality has seriously impacted the physical picture we now have of many-body entanglement. Whether there is more to learn, about dynamics, for example, we do not know. But there is a great deal of room to explore.

7.2.3 Quantum information

There is also an exciting exchange developing between condensed matter physics and quantum information science. Of course, there is an obvious connection in the sense that many solid state systems are candidates for realizing the first scalable quantum computers. But more than this, we believe that the concepts, intuition, and questions arising from the abstract study of quantum information processing will be increasingly valuable as we explore more and more essentially quantum phases of matter. Given that quantum computers can serve as universal simulators for many-body dynamics, we would like to ask the conceptual question: how does a quantum computer see the world? Certainly such a computer would not "think" in terms of a wavefunction, instead states would be defined by their construction in terms of quantum circuits, that is in terms of quantum dynamics. Indeed, although it is exponentially hard to simulate quantum dynamics on a classical computer, we would obtain exponentially more information (the entire wavefunction) than a quantum computer could provide. Thus there is something profound to understand about the information that a quantum computer can manipulate, and whatever insights we gain

should help us better understand local quantum physics.

7.3   Where to go from here?

We want to end by describing some of the most interesting big questions that we are pursuing and that we believe are of fundamental importance. In addition to this list of big questions, there are many smaller open problems in the theory of many-body entanglement and room for a wide variety of approaches. We want to emphasize one last time that the framework we have described here should be seen as a beginning, not an end.

7.3.1   Big questions

- What does an approximate knowledge of the ground state tell us about a phase of matter? The ground state is only one state out of 2^N for an N spin Hamiltonian. If we do not require locality, then we obviously know nothing. Similarly, we may need to require that the Hamiltonian is generic. But if we grant these conditions, what can we say? From symmetry breaking and localization to topological entanglement entropy and the entanglement spectrum, the ground state seems to contain much dynamical information. How should we quantify this information without speaking about unphysical lists of 2^N complex numbers. How do we extract the "shape" or "pattern" that determines the physics from the ground state?

- We have considered almost exclusively entanglement in real space, but entanglement in momentum space should also play a profound role in the study of renormalization in local quantum systems. There are a few preliminary calculations in this case, but currently the field is wide open. What is the connection between entanglement and mutual information in momentum space and the renormalization group?

- Can we significantly elaborate the connection between entanglement renormal-

ization and holographic duality? Can we use the connection to make a heuristic proof of holographic duality in some special cases? We have already argued that entanglement renormalization captures well the renormalization group structure of real space entanglement in the ground state, but holographic duality also very naturally includes real time dynamics. Given the difficulty of extracting real time dynamics in complicated many-body systems, can holographic duality provide a clue to formulating dynamics in the context of holographic tensor networks?

- What can the structure of entanglement tell us about the physics of quantum gravity via holographic duality? Can we prove the various conjectures for holographic entanglement entropy in higher dimensions using field theory tools like twist operators by relating them to objects on the gravity side? Is entanglement the fabric of spacetime?

- How generic are tensor network states? In what sense can they capture the universal physics of phases of matter obeying a boundary law for entanglement entropy. What hidden structure distinguishes problems that are hard in the tensor network language? Is the gauge redundancy a curiosity or an important feature/limitation of the method? Can we capture the physics of chiral topological phases using tensor networks? What about gapless phases?

- Entanglement based methods of classification have been very successful in one dimension and for topological phases in higher dimensions. The idea of adiabatic transformations is very important. Can we use entanglement ideas to partially classify gapless phases? Are there analogs of adiabatic transformations in the gapless case? Can we use entanglement to give evidence for the stability of certain fractionalized gapless phases of matter? Does entanglement or quantum information decrease under RG flow?

- Geometry has repeatedly played a critical role in understand the physics of many-body entanglement, from the geometry of the Fermi surface to the geom-

etry of anti de Sitter space. Is this the best way to think about entanglement? We are also tempted to think of entanglement in terms of a fluid model, with the links of a tensor network providing "pipes" through which entanglement can flow. Does such a picture make sense, and if so, can we use it manipulate the "flow" of entanglement to design better algorithms? Is there a hydrodynamics of entanglement?

7.3.2 Final words

Our little story ends here, but the larger story is just beginning to unfold. As Hamlet remind us, "There are more things in heaven and earth, Horatio, Than are dreamt of in your philosophy." There are countless mysteries left to explore, fundamental principles to uncover, bizarre and delightful phases to discover, dynamical behaviors to unravel, and quantum computers to build. The future of entanglement and quantum many-body physics is wide open.

Bibliography

[1] J. Ziman. *Principles of the Theory of Solids*. Cambridge University Press, 1979.

[2] X.-G. Wen P. Lee, N. Nagaosa. Doping a mott insulator: Physics of high-temperature superconductivity. *Rev. Mod. Phys.*, 78(1):17–85, Jan 2006.

[3] D. C. Tsui, H. L. Stormer, and A. C. Gossard. Two-dimensional magnetotransport in the extreme quantum limit. *Phys. Rev. Lett.*, 48:1559, 1982.

[4] P. Braun-Munzinger and J. Stachel. The quest for the quark-gluon plasma. *Nature*, 448:302, 2007.

[5] Richard Feynman. Simulating physics with computers. *International Journal of Theoretical Physics*, 21:467–488, 1982. 10.1007/BF02650179.

[6] Seth Lloyd. Universal quantum simulators. *Science*, 273(5278):1073–1078, 1996.

[7] A. Kitaev, H. Shen, and M. Vyalyi. *Classical and Quantum Computation*. American Mathematical Society, 2002.

[8] Ulrich Schollwck. The density-matrix renormalization group in the age of matrix product states. *Annals of Physics*, 326(1):96 – 192, 2011. January 2011 Special Issue.

[9] Guifré Vidal. Efficient simulation of one-dimensional quantum many-body systems. *Phys. Rev. Lett.*, 93(4):040502, Jul 2004.

[10] B. Swingle. Entanglement renormalization and holography. arxiv:0905.1317. 2009.

[11] Z. C. Gu, M. Levin, B. Swingle, and X. G. Wen. Tensor-product representations for string-net condensed states. *Phys. Rev. B*, 79:085118, 2009.

[12] B. Swingle and X.-G. Wen. Topological Properties of Tensor Network States From Their Local Gauge and Local Symmetry Structures. arXiv:1001.4517. *ArXiv e-prints*, January 2010.

[13] Brian Swingle. Entanglement entropy and the fermi surface. *Phys. Rev. Lett.*, 105(5):050502, Jul 2010.

[14] B. Swingle. Conformal field theory on the fermi surface arxiv:1002.4635. 2010.

[15] B. Swingle. Highly entangled quantum systems in 3+1 dimensions. arxiv:1003.2434. 2010.

[16] B. Swingle. Renyi entropy, mutual information, and fluctuation properties of fermi liquids. arxiv:1007.4825. 2010.

[17] B. Swingle. Mutual information and the structure of entanglement in quantum field theory. *ArXiv e-prints*, October 2010.

[18] S. Popescu, A. J. Short, and A. Winter. Entanglement and the foundations of statistical mechanics. *Nature Physics*, 2:754, 2006.

[19] I. Klich and L. Levitov. Quantum noise as an entanglement meter. *Phys. Rev. Lett.*, 102:100502, 2009.

[20] Roger G. Melko, Ann B. Kallin, and Matthew B. Hastings. Finite-size scaling of mutual information in monte carlo simulations: Application to the spin-$\frac{1}{2}$ xxz model. *Phys. Rev. B*, 82(10):100409, Sep 2010.

[21] Roger G. Melko, Ann B. Kallin, and Matthew B. Hastings. Finite-size scaling of mutual information in monte carlo simulations: Application to the spin-$\frac{1}{2}$ xxz model. *Phys. Rev. B*, 82(10):100409, Sep 2010.

[22] John Cardy. Measuring entanglement using quantum quenches. *Phys. Rev. Lett.*, 106(15):150404, Apr 2011.

[23] J. Eisert, M. Cramer, and M. B. Plenio. Colloquium: Area laws for the entanglement entropy. *Rev. Mod. Phys.*, 82(1):277–306, Feb 2010.

[24] M B Hastings. An area law for one-dimensional quantum systems. *Journal of Statistical Mechanics: Theory and Experiment*, 2007(08):P08024, 2007.

[25] Horacio Casini, Marina Huerta, and Robert Myers. Towards a derivation of holographic entanglement entropy. *Journal of High Energy Physics*, 2011:1–41, 2011. 10.1007/JHEP05(2011)036.

[26] M. M. Wolf, F. Verstraete, M. B. Hastings, and J. Ignacio Cirac. Area laws in quantum systems: Mutual information and correlations. *Phys. Rev. Lett.*, 100(7):070502, 2008.

[27] C. Holzhey, F. Larsen, and F. Wilczek. Geometric and renormalized entropy in conformal field theory. *Nuc. Phys. B*, 424:443, 1994.

[28] P. Calabrese and J. Cardy. Entanglement entropy and quantum field theory. *J. Stat. Mech.*, 04:06002, 2004.

[29] M. Fannes, B. Nachtergaele, and R. Werner. Finitely correlated states on quantum spin chains. *Communications in Mathematical Physics*, 144:443–490, 1992. 10.1007/BF02099178.

[30] Xie Chen, Zheng-Cheng Gu, and Xiao-Gang Wen. Classification of gapped symmetric phases in one-dimensional spin systems. *Phys. Rev. B*, 83(3):035107, Jan 2011.

[31] Lukasz Fidkowski and Alexei Kitaev. Topological phases of fermions in one dimension. *Phys. Rev. B*, 83(7):075103, Feb 2011.

[32] X. G. Wen. Vacuum degeneracy of chiral spin states in compactified space. *Phys. Rev. B*, 40(10):7387–7390, Oct 1989.

[33] X. G. Wen and Q. Niu. Ground-state degeneracy of the fractional quantum hall states in the presence of a random potential and on high-genus riemann surfaces. *Phys. Rev. B*, 41(13):9377–9396, May 1990.

[34] A. Yu. Kitaev. Fault-tolerant quantum computation by anyons. *Annals of Physics*, 303(1):2 – 30, 2003.

[35] Chetan Nayak, Steven H. Simon, Ady Stern, Michael Freedman, and Sankar Das Sarma. Non-abelian anyons and topological quantum computation. *Rev. Mod. Phys.*, 80(3):1083–1159, Sep 2008.

[36] O. Buerschaper, M. Aguado, and G. Vidal. Explicit tensor network representation for the ground states of string-net models. *Phys. Rev. B*, 79:085119, 2009.

[37] Xie Chen, Bei Zeng, Zheng-Cheng Gu, Isaac L. Chuang, and Xiao-Gang Wen. Tensor product representation of a topological ordered phase: Necessary symmetry conditions. *Phys. Rev. B*, 82(16):165119, Oct 2010.

[38] D. Gioev and I. Klich. Entanglement entropy of fermions in any dimension and the widom conjecture. *Phys. Rev. Lett.*, 96:100503, 2006.

[39] T. Barthel, M.-C. Chung, and U. Schollwock. Entanglement scaling in critical two dimensional fermionic and bosonic systems. *Phys. Rev. A*, 74:022329, 2006.

[40] W. Li, L. Ding, R. Yu, and S. Haas. Scaling behavior of entanglement in two and three dimensional free fermion systems. *Phys. Rev. B*, 74:073103, 2006.

[41] G. Benfatto and G. Gallavotti. Perturbation theory of the fermi surface in a quantum liquid. *J. Stat. Phys.*, 59:541, 1989.

[42] J. Polchinski. Effective field theory and the fermi surface. hep-th/9210046. 1992.

[43] R. Shankar. Renormalization group approach to interacting fermions. *Rev. Mod. Phys.*, 66:129, 1994.

[44] O. Motrunich and M. Fisher. d-wave correlated critical bose liquids in two dimensions. *Phys. Rev. B*, 75:235116, 2007.

[45] T. Senthil. Critical fermi surfaces and non-fermi liquid metals. *Phys. Rev. B*, 78:035103, 2008.

[46] H. Liu, J. McGreevy, and D. Vegh. Non-fermi liquids from holography. arxiv:0903.2477. 2009.

[47] S.-S. Lee. Stability of the u(1) spin liquid with a spinon fermi surface in 2+1 dimensions. *Phys. Rev. B*, 78:085129, 2008.

[48] M. Wolf. Violation of the entropy area law for fermions. *Phys. Rev. Lett.*, 96:010404, 2006.

[49] L. Ding, N. Bray-Ali, R. Yu, and S. Haas. Subarea law of entanglement in nodal fermionic systems. *Phys. Rev. Lett.*, 100:215701, 2008.

[50] E. D'Hoker and P. Kraus. Magnetic brane solutions in ads. *J. High Energy Phys.*, 1009, 2009.

[51] C. Kane and E. Mele. Quantum spin hall effect in graphene. *Phys. Rev. Lett.*, 95:226801, 2005.

[52] B. Bernevig and S.-C. Zhang. Quantum spin hall effect. *Phys. Rev. Lett.*, 96:106802, 2006.

[53] L. Fu, C. Kane, and E. Mele. Topological insulators in three dimensions. *Phys. Rev. Lett.*, 98:106803, 2007.

[54] J. Moore and L. Balents. Topological invariants of time-reversal-invariant band structures. *Phys. Rev. B*, 75:121306, 2007.

[55] R. Roy. Topological phases and the quantum spin hall effect in three dimensions. *Phys. Rev. B*, 79:195322, 2006.

[56] B. Bernevig, T. Hughes, and S.-C. Zhang. Quantum spin hall effect and topological phase transition in hgte quantum wells. *Science*, 314:1757, 2006.

[57] C. Xu and J. Moore. Stability of the quantum spin hall effect: Effects of interactions, disorder, and z2 topology. *Phys. Rev. B*, 73:045322, 2006.

[58] S. Ryu and T. Takayanagi. Holographic derivation of entanglement entropy from ads/cft correspondence. *Phys. Rev. Lett.*, 96:181602, 2006.

[59] D. Fursaev. Proof of holographic formula for entanglement entropy. *J. High Energy Phys.*, 0609:018, 2006.

[60] Y. Ran, Y. Zhang, and A. Vishwanath. One-dimensional topologically protected modes in topological insulators with lattice dislocations. *Nature Physics*, 5:298, 2009.

[61] R. Helling, H. Leschke, and W. Spitzer. A special case of a conjecture by widom with implications to fermionic entanglement entropy. arxiv:0906.4946. 2009.

[62] A. Luther. Tomonaga fermions and the dirac equation in three dimensions. *Phys. Rev. B*, 19:320, 1979.

[63] F. D. M. Haldane. Luttinger's theorem and bosonization of the fermi surface. *Perspectives in Many-Particle Physics*, 1994.

[64] D. Gioev. Szego limit theorem for operators with discontinuous symbols and applications to entanglement entropy. 2002.

[65] H. Song, S. Rachel, and K. Le Hur. General relation between entanglement and fluctuations in one dimension. arxiv:1002.0825. 2010.

[66] M. Hastings, I. Gonzalez, A. Kallin, and R. Melko. Measuring renyi entanglement entropy with quantum monte carlo. arxiv:1001.2335. 2010.

[67] S. Flammia, A. Hamma, T. Hughes, and X-G Wen. Topological entanglement renyi entropy and reduced density matrix structure. arxiv:0909.3305. 2009.

[68] M. Headrick. Entanglement renyi entropies in holographic theories. arxiv:1006.0047. 2010.

[69] J. Eisert and M. Cramer. Single-copy entanglement in critical quantum spin chains. *Phys. Rev. A*, 72:042112, 2005.

[70] R. Ors, J. I. Latorre, J. Eisert, and M. Cramer. Half the entanglement in critical systems is distillable from a single specimen. *Phys. Rev. A*, 73:060303(R), 2006.

[71] S.-S. Lee. Low energy effective theory of fermi surface coupled with u(1) gauge field in 2+1 dimensions. *Phys. Rev. B*, 80:165102, 2009.

[72] M. Metlitski and S. Sachdev. Quantum phase transitions of metals in two spatial dimensions: I. ising-nematic order. arxiv:1001.1153. 2010.

[73] G. Vidal. Entanglement renormalization. *Phys. Rev. Lett.*, 99:220405, 2007.

[74] R. N. C. Pfeifer, G. Evenbly, and G. Vidal. Entanglement renormalization, scale invariance, and quantum criticality. *Phys. Rev. A*, 79:040301, 2009.

[75] S. Montangero, M. Rizzi, V. Giovannetti, and R. Fazio. Critical exponents of one-dimensional quantum critical models by means of mera tensor network. arxiv:0810.1414v1. 2008.

[76] Juan M. Maldecena. The large n limit of superconformal field theories and supergravity. *Adv. Theor. Math. Phys.*, 2:231, 1998.

[77] S. S. Gubser, I. R. Klebanov, and A. M. Polyakov. Guage theory correlators from non-critical string theory. *Phys. Lett. B*, 428:105, 1998.

[78] E. Witten. Anti de sitter space and holography. *Adv. Theor. Math. Phys.*, 2:253, 1998.

[79] E. Alvarez and C. Gomez. Geometric holography, the renormalization group and the c-theorem. *Nuc. Phys. B*, 541:441, 1999.

[80] V. Balasubramanian, P. Kraus, A. Lawrence, and S. Trivedi. Holographic probes of anti de sitter spacetimes. *Phys. Rev. D*, 59:104021, 1999.

[81] J. de Boer, E. Verlinde, and H. Verlinde. On the holographic renormalization group. *J. High Energy Physics*, 8:3, 1999.

[82] G. Horowitz and J. Polchinski. Gauge/gravity duality. arxiv:gr-qc/0602037v3. 2006.

[83] K. Wilson. The renormalization group: critical phenomena and the kondo problem. *Rev. Mod. Phys.*, 47:773, 1975.

[84] G. Vidal. Class of quantum many-dody states that can be efficiently simulated. *Phys. Rev. Lett.*, 101:110501, 2008.

[85] L. Susskind. The world as a hologram. *J. Math. Phys.*, 36:6377, 1995.

[86] T. Jacobson. Thermodynamics of spacetime: the einstein equation of state. *Phys. Rev. Lett.*, 75:1260, 1995.

[87] L. Susskind and E. Witten. The holographic bound in anti-de sitter space. 1998.

[88] S. Sachdev. *Quantum Phase Transitions*. Cambridge University Press, 1999.

[89] A. Lawrence and A. Sever. Holography and renormalization in lorentzian signature. *J. High Energy Phys.*, 0610:013, 2006.

[90] G. Evenbly and G. Vidal. Entanglement renormalization in free bosonic systems: real-space versus momentum-space renormalization group transforms. arxiv:0801.2449v1. 2008.

[91] E. Witten. Anti-sitter space, thermal phase transition and confinement in gauge theories. *Int. J. Mod. Phys. A*, 16:2747, 2001.

[92] V. Balasubramanian and P. Kraus. Spacetime and holographic renormalization group. *Phys. Rev. Lett.*, 83:3605, 1999.

[93] I. R. Klebanov and A. M. Polyakov. Ads dual of the critical o(n) vector model. *Phys. Lett. B*, 550:213, 2002.

[94] A. Kitaev and J. Preskill. Topological entanglement entropy. *Phys. Rev. Lett.*, 96:110404, 2006.

[95] M. Levin and X.-G. Wen. Detecting topological order in a ground state wave function. *Phys. Rev. Lett.*, 96:110405, 2006.

[96] J. McGreevy. Holographic duality with a view toward many-body physics. arxiv:0909.0518. 2009.

[97] H. Casini, C. Fosco, and M. Huerta. Entanglement and alpha entropies for a massive dirac field in two dimensions. *J. Stat. Mech.*, page P07007, 2005.

[98] K. Balasubramanian and J. McGreevy. Gravity duals for nonrelativistic conformal field theories. *Phys. Rev. Lett.*, 101:061601, 2008.

[99] D. Son. Toward an ads/cold atoms correspondence: A geometric realization of the schrdinger symmetry. *Phys. Rev. D*, 78:046003, 2008.

[100] H. Casini and M. Huerta. Remarks on the entanglement entropy for disconnected regions. *Journal of High Energy Physics*, 2009(03):048, 2009.

[101] M. Metlitski, C. Fuertes, and S. Sachdev. Entanglement entropy in the o(n) model. *Phys. Rev. B*, 80:115122, 2009.

[102] C. Robin Graham and Edward Witten. Conformal anomaly of submanifold observables in AdS/CFT correspondence. *Nucl. Phys.*, B546:52–64, 1999.

[103] S. Ryu and T. Takayanagi. Aspects of holographic entanglement entropy. *JHEP08*, 2006.

[104] S. Solodukhin. Aspects of holographic entanglement entropy. *Phys. Lett. B*, 665:305, 2008.

[105] H. Casini, M. Huerta, and L. Leitao. Entanglement entropy for a dirac fermion in three dimensions: Vertex contribution. *Nuc. Phys. B*, 814:509, 2009.

[106] D. Z. Freedman, S. S. Gubser, K. Pilch, and N. P. Warner. Renormalization group flows from holography supersymmetry and a c-theorem. *Adv. Theor. Math. Phys.*, 3:363–417, 1999.

[107] Robert C. Myers and Aninda Sinha. Seeing a c-theorem with holography. *Phys. Rev.*, D82:046006, 2010.

[108] A. Allais. Double-trace deformations, holography and the c-conjecture. arxiv:1007.2047. 2010.

[109] R. Myers and A. Sinha. Holographic c-theorems in arbitrary dimensions. *J. High Energy Phys.*, 2011:1, 2011.

[110] H Casini and M Huerta. A c -theorem for entanglement entropy. *Journal of Physics A: Mathematical and Theoretical*, 40(25):7031, 2007.